MASTERARBEIT | MASTER'S THESIS

Titel | Title

Application of real-time PCR and high resolution melting (HRM) analysis for authentication of honey

verfasst von | submitted by

Andrijana Marijan

angestrebter akademischer Grad | in partial fulfilment of the requirements for the degree of

Master of Science (MSc)

Wien | Vienna, 2026

Studienkennzahl lt. Studienblatt | Degree programme code as it appears on the student record sheet:	UA 066 862
Studienrichtung lt. Studienblatt | Degree programme as it appears on the student record sheet:	Masterstudium Chemie
Betreut von | Supervisor:	Univ.-Prof. Mag. Dr. Margit Cichna-Markl

Acknowledgement

I would like to sincerely thank my supervisor, Univ.-Prof. Mag. Dr. Margit Cichna-Markl for her support, constructive feedback and continuous encouragement throughout this research. It was a big pleasure working and learning in her group.

Many thanks to Katharina Pühringer, Youna Kim and Verena Wagner for the introduction and for showing me everything in the laboratory at the beginning of my experimental work and answering all my questions. I am also grateful to all other colleagues from WG Cichna, who assisted with laboratory work, shared their knowledge, provided support and made time in the laboratory and office more interesting.

I would also like to thank ao. Univ.-Prof. Mag. Dr. Mathea Sophia Galanski for performing the NMR analysis of my samples, processing the data, and interpreting the results.

I would like to thank cooperation partner "Institute of Food Safety Vienna Department of Molecular Biology and Microbiology" from AGES, Austria for providing honey and pollen samples.

I am deeply grateful to my husband Nikola for his encouragement, patience and unwavering support throughout the entire process of completing this thesis. His presence and confidence in me have played an essential role in the completion of this work and I feel incredibly fortunate to have him by my side.

I am especially grateful to my parents and sister for their constant love, support and encouragement throughout my studies and the completion of this thesis. Their belief in me and understanding during both challenging and rewarding moments has been a constant source of motivation.

I would also like to acknowledge the support and encouragement of everyone who, directly or indirectly, contributed to the successful completion of this thesis.

Abstract

Honey is considered a prized natural sweetener, valued for its flavor qualities and beneficial effects on health, influenced by the type of plants from which it originates. Its high market price makes honey an attractive target for fraud. Honey can be diluted with cheaper sugar syrups (rice, corn, beet or cane) without being easily detected. Honey is also particularly susceptible to mislabeling and falsification of its geographical and botanical origin. Therefore, reliable analytical methods for honey authentication are essential to ensure product quality and consumer protection.

The aim of this study was to investigate the potential of real-time PCR combined with high resolution melting (HRM) analysis for the authentication of honey available in Austria and other European countries. Our approach was based on amplifying polymorphic regions (16S rDNA and COI) of honeybee *Apis mellifera* and plant DNA (rbcL and ITS2) by real-time PCR, enabling the discrimination of *A. mellifera* subspecies and plant species through differences in the melting behavior of the amplicons.

DNA was extracted using the Dneasy mericon Food Kit (Qiagen), according to the manufacturer's instructions. As positive controls, DNA was also extracted from honeybee specimens collected in Austria, Bosnia & Herzegovina, Croatia, and North Macedonia, and plant seeds and leaves that may be present in honey. The extracted DNA was quantified using a Qubit fluorimeter.

Primer pairs for the DNA amplification of honeybee *A. mellifera* and plant DNA were taken from the literature and tested *in silico*. If required, primers were modified to achieve better similarity of annealing temperatures and HRM results.

Since different subspecies of the honeybee *A. mellifera* occur in different countries, PCR products amplified with the assay targeting COI were sequenced to detect SNPs in the amplified region. Pyrosequencing of these amplicons made it possible to assign specific melting profiles to the genotypes of different honeybees. This method has already been applied to 56 honey samples from Austria and other European countries.

In addition, physicochemical parameters were determined: water content by refractometry and electrical conductivity was also assessed. NMR analysis was also performed on 20 selected honey samples to better understand their chemical composition, and to identify possible characteristics of the NMR fingerprint of each honey type.

Zusammenfassung

Honig gilt als begehrter natürlicher Süßstoff, der wegen seiner geschmacklichen Eigenschaften und seiner positiven Auswirkungen auf die Gesundheit geschätzt wird, die von der Art der Pflanzen abhängen, aus denen er gewonnen wird. Sein hoher Marktpreis macht Honig zu einem attraktiven Ziel für Betrug. Honig kann mit billigeren Zuckersirupen (Reis, Mais, Rüben oder Zuckerrohr) verdünnt werden, ohne dass dies leicht zu erkennen ist. Honig ist auch besonders anfällig für falsche Kennzeichnung und Fälschung seiner geografischen und botanischen Herkunft. Daher sind zuverlässige Analysemethoden zur Honigauthentifizierung unerlässlich, um die Produktqualität und den Verbraucherschutz zu gewährleisten.

Das Ziel dieser Studie war es, das Potenzial der real-time PCR in Kombination mit einer hochauflösenden Schmelzkurvenanalyse (HRM) für die Authentifizierung von Honig zu untersuchen, der in Österreich und anderen europäischen Ländern erhältlich ist. Unser Ansatz basierte auf der Amplifikation polymorpher Regionen (16S rDNA und COI) der Honigbiene *Apis mellifera* und der Pflanzen-DNA (rbcL und ITS2) mittels real-time PCR und der Unterscheidung von *A. mellifera* Unterarten bzw. Arten bei Pflanzen anhand der Unterschiede im Schmelzverhalten der Amplikons.

Die DNA wurde unter Verwendung des Dneasy mericon Food Kit (Qiagen) gemäß den Anweisungen des Herstellers extrahiert. Als Positivkontrollen wurde auch DNA aus Honigbienenproben extrahiert, die in Österreich, Nordmazedonien, Bosnien und Herzegowina und Kroatien gesammelt wurden, sowie aus Pflanzensamen und -blättern, die in Honig vorkommen können, darunter Mais und Reis, da diese häufig als Sirup Zusätze verwendet werden. Die extrahierte DNA wurde mit einem Qubit-Fluorimeter quantifiziert.

Primer Paare für die Amplifikation von Honigbienen (*A. mellifera)* DNA und Pflanzen-DNA wurden der Literatur entnommen und *in silico* getestet. Bei Bedarf wurden die Primer modifiziert, um größere Ähnlichkeit der Annealing-Temperaturen und bessere HRM-Ergebnisse und zu erzielen.

Da in verschiedenen Ländern unterschiedliche Unterarten der Honigbiene *A. mellifera* vorkommen, wurden die mit dem COI Assay erhaltenen PCR Produkte sequenziert, um SNPs in der amplifizierten Region zu detektieren. Die Pyrosequenzierung dieser Amplikons ermöglichte es, den Genotyp verschiedener Honigbienen spezifischen Schmelzprofilen zuzuordnen. Diese Methode wurde bereits auf 56 Honigproben aus Österreich und anderen europäischen Ländern angewandt.

Zusätzlich wurden physikalisch-chemische Parameter bestimmt: der Wassergehalt wurde mittels Refraktometrie ermittelt und außerdem wurde die elektrische Leitfähigkeit gemessen. Darüber hinaus wurde eine NMR-Analyse von 20 ausgewählten Honigproben durchgeführt, um ihre chemische Zusammensetzung besser zu verstehen und mögliche Merkmale des NMR-Fingerabdrucks jeder Honigsorte zu identifizieren.

Table of content:

1 Introduction

Honey is produced by honeybees *Apis mellifera*, that collect sweet liquids from flowers or from plants that have been damaged by insects. The bees change this liquid and store it in the hive until it thickens. There are two main types of honey: blossom honey, which comes from flower nectar, and honeydew honey, which comes from substances left on plants by insects (1). Honey consists of sugars, mainly fructose and glucose. It also contains other substances such as organic acids, enzymes, proteins, and small particles from the collection process. The color of honey can be from almost colorless to dark brown and together with the taste and smell, it depends on the plants where the nectar or secretions come from (2). The labeling of honey must include the name of the food (for example "honey"), the name or company and address of the food business operator, the net quantity, the lot number, the best-before date, storage conditions, and the country of origin (3).

Since honey is rich in antioxidant compounds such as polyphenols and flavonoids, which give it antioxidant, anti-inflammatory and antibacterial properties, it has promising uses in medicine and has become a topic of interest in recent years (4). Research shows that honey can be a low-cost and effective treatment for diabetic foot ulcers because it can fight some multidrug-resistant bacteria and therefore reduce inflammation, support healing, and create conditions that help wounds close faster. This may also lower the need for hospital stays and amputations (5). These beneficial properties have made honey more popular and its price much higher.

According to the Food and Agriculture Organization (FAO), the biggest producer of honey in 2023 was China with 463,500 t of honey, followed by Turkey, Ethiopia, Iran, Argentina, and India (6). At the same time, the proportion of adulterated honey has increased in the last years and the detection of such adulteration remains challenging because honey is a complex mixture of various substances (7). Honey authentication comprises several dimensions, including the verification of botanical origin, geographical origin, entomological origin, and the detection of adulteration through the addition of exogenous sugars. While physicochemical techniques such as nuclear magnetic resonance (NMR) spectroscopy, Raman spectroscopy, near-infrared (NIR) spectroscopy, ultraviolet–visible (UV-VIS) spectroscopy are suitable for detecting sugar adulteration, molecular biological approaches primarily provide information about the biological origin of honey components (8). Food adulteration is typically economically motivated and performed in a way to reduce the likelihood of detection (9). The most common type of honey adulteration is the addition of less expensive syrups such as corn, rice or beet syrup. Another way to adulterate honey is feeding the bees with low-cost sugars such as syrups in the period of main nectar flow. This type of fraud is even more difficult to detect (10). In addition to these practices, honey may be adulterated through the misrepresentation of its origin. This includes falsely labeling the geographic origin, the honeybee subspecies involved, or the plant sources from which the honey was derived. Such fraudulent practices complicate authentication and highlight the need for analytical methods capable of assessing both chemical composition and biological origin, including plant and insect DNA (8,11).

According to the literature (12) there are many different honeybee subspecies depending on their origin. Beekeepers recognize mostly the subspecies based on their appearance, color and wings. In Central Europe, which was the region of interest for this research because of the origin of many honey samples, the most common honeybee is *A. m. carnica*, but it is also possible to find some other honeybee subspecies. In many parts of Austria, it is forbidden to use bee subspecies other than *A. m. carnica,* to protect this subspecies (13,14). Climate change is increasingly shaping the

availability of suitable habitats for bees, and the fate of bees is becoming inseparable from the ecosystem's ability to adapt to new environmental conditions (15). The presence of other bee subspecies may also be expected, as bees naturally disperse in search of climates to which they are adapted.

Consequently, different analytical strategies are required depending on the specific aspect of authenticity being investigated.

1.1 Analytical methods

A lot of recent studies have used different analytical methods in the analysis of honey, to obtain more information about its composition and the potential distinction between natural and adulterated honey. The most commonly used techniques are melissography, organoleptic analysis, isotope ratio mass spectrometry (IRMS), NMR, fourier transform infrared spectroscopy (FTIR), and liquid chromatography-mass spectrometry (LC-MS) (10). The European Commission started a coordinated EU action called “From the Beehives” in 2021 to address the problem of adulterated honey. The project took place from 2021 to 2022 and had three main steps: collecting honey samples at EU borders for testing; gathering information about where the shipments were going and which companies were involved; and carrying out investigations in EU and European Free Trade Association (EFTA) countries with the help of European Anti-Fraud Office (OLAF). The results confirmed the original concern: a large amount of honey imported into the EU does not follow the rules of the Honey Directive. Out of 320 samples, 46% raised suspicion. Most of the suspicious honey came from China (74%) and Turkey (93%) and 57% of the involved operators had sent honey likely mixed with foreign sugars. There are modern tests to check if honey is authentic, but many of them are not sensitive enough to detect small or medium amounts of added sugar. Because of this, fraudsters adjust how much foreign sugar they mix into the honey so it remains below the level these tests can detect (7). The revised Honey Directive (2001/110) must be adopted by EU countries until December 2025 and will apply from June 2026. After this, all honey sold in the EU must meet updated rules on quality and labeling. Blended honey will have to show the countries of origin, with percentages. The directive also introduces standard methods to detect sugar adulteration and updates composition rules to prevent overheating and pollen removal (16). Depending on the group of substances that are analyzed in honey, several different analytical methods can be used.

Honey is a natural product influenced by many factors. Its characteristics change depending on the flowers used by bees, the environment where it is produced, and how it is handled. Elements such as weather, soil type, bee variety, time of year and storage conditions all affect its final composition. Because plants develop different chemical substances under different environmental conditions, honey produced in different regions or countries can vary greatly. These differences mainly come from the types of nectar and pollen collected by the bees (17).

Pollen analysis is a key method for checking where honey comes from and what type it is, but because honey naturally varies, the main challenge is correctly identifying the pollen (18). The plant origin of honey is usually identified by studying the types and amounts of pollen it contains, but this method requires expert knowledge and good pollen references, so sometimes researchers instead rely on beekeeper information, sensory evaluation or the main flowers near the hives (17). The effect of adding different sugar syrups on the thermal properties of honey, especially the glass transition temperature (Tg), can also be detected (19). The major proteins present in honey serve as biochemical markers, and alterations in their protein profile can be used to detect honey

adulteration (20). In honey, the sugars we expect to find are the natural C-3 sugars that come from nectar, while C-4 sugars like corn or cane sugar should not be present because they indicate that the honey was mixed with cheap syrups. To check this, honey can be analyzed with stable isotope ratio analysis, which allows differentiation between natural C-3 sugars and added C-4 sugars. For this purpose, Association of Official Analytical Chemists (AOAC) Official Method 998.12 is used, because it can detect if any C-4 plant sugars were added to the honey (21).

In recent years, the use of NMR for honey analysis has increased. Many studies report successful results using NMR fingerprints of honey (22–24). By identifying reliable chemical biomarkers, NMR can offer a scientific approach to verify whether a honey originates from a specific plant species or geographic region, such as certain habitats on Corsica. This goes beyond traditional methods like pollen analysis or organoleptic analysis. In this way, NMR supports authenticity testing and improves traceability, which is important for consumers, producers and regulatory authorities (25). Unfortunately, many of these methods require advanced equipment and well-trained personnel, which makes them expensive and in some cases the analysis time is very long (19). Therefore, the need for new methods that are reliable but at the same time faster and less expensive is increasing.

Honey contains genetic material from many organisms involved in its production, including the bees themselves. Consequently, DNA extracted from honey can be used to analyze specific genetic markers to gain information about its botanical, geographical, or entomological origin. Such analyses are commonly based on DNA barcodes, which are short genomic regions that exhibit sufficient variability to distinguish between species. DNA barcoding refers to the amplification and analysis of these marker regions for species identification, whereas DNA metabarcoding enables the simultaneous detection of multiple species within complex mixtures such as honey (26,27). Numerous studies have successfully amplified DNA from bees, plants, and microorganisms in honey using barcode regions as targets (12,28,29). Recently usage of real-time polymerase chain reaction (PCR) coupled with high resolution melting analysis (HRM) methods for the authentication of honey is becoming more popular. In this context, PCR is used to amplify specific DNA barcode regions, while HRM analysis allows the differentiation of sequence variants based on their melting behavior. According to Al-Kahtani et. al real-time PCR can detect changes or contamination in food products more precisely and reliably than regular PCR (30). Because of this, quality control labs can use real-time PCR for food products that need careful testing. Real-time PCR can accurately also detect and measure small amounts of rice molasses added to honey, offering a cheaper and more sensitive method than others (31).

1.2 Honeybee

The subfamily of honeybee *Apinae* includes a small number of species (about four to six) and is mainly distinguished from other groups by a few physical traits (Figure 1) and important behavioral features (32). The foraging behavior of honeybees appears to be energy-efficient because they can remember the time of day and visit flowers when nectar is most abundant. This ability relies on their internal circadian clock, and they can retain this memory for several days. Worker bees show different strategies: some actively check known food sources and are known as persistent bees, while others known as reticent bees remain in the hive and respond based on the information returned by these persistent bees (33).

The western honey bee (*A. mellifera*) includes many different subspecies and a major taxonomic review published in 1999 listed 28 of these subspecies (34). Around the Karawanken mountains on the Austria-Slovenia border, traditional beekeeping uses different hives than in Northern Europe and the local bees belong to different subspecies: *A. m. carnica* in the Danube valley to the Carpathians, *A. m. ligustica* to the west, *A. m. mellifera* to the northwest and *A. m. macedonica* to the south and southeast as it can be seen in Figure 2 (35). Although honeybee subspecies are commonly associated with specific geographical regions, a strict geographic assignment is not possible. Modern beekeeping practices, such as moving hives and importing non-native subspecies, have increased interactions between honeybee subspecies, leading to hybridization and introgression-the mixing of genes between indigenous and imported subspecies, which can cause the loss of local genetic combinations, reduce resistance to local environmental conditions, and disrupt adaptations developed over time. Additionally, diseases, parasites, and other stressors further threaten honeybee populations (36). Historically, *A. m. mellifera* was widespread in Central and Northern Europe; however, during the 20th century it was largely displaced in many regions by *A. m. carnica* and *A. m. ligustica,* due to breeding preferences and management practices (37).

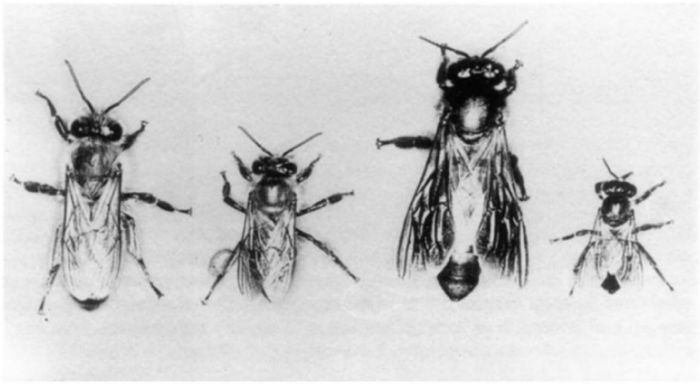

Figure 1 Four species of honeybees that differ in size and appearance: *Apis mellifera, Apis cerana, Apis dorsata and Apis florea* (from left to right), photo taken from (32)

There are two known types of *A. m. carnica*: Alpine and Pannonian type. Ruttner reported that honeybee populations from Slovakia (Little Carpathians, Tatra) cluster with the Alpine type of *A. m. carnica*, rather than with the Pannonian type, despite their geographic proximity to the Pannonian region. This also helps explain why, within Austria, there is no clear difference between the bees of the Alps and those of the Vienna Basin (35).

Figure 2 The distribution of certain honeybees subspecies across regions of Europe (35)

Using DNA extracted from honey, many studies have developed methods to distinguish between different honeybee species (38–40). By selecting suitable gene regions as DNA markers from honey, some studies have shown that it is also possible to distinguish honeybee subspecies of *A. mellifera*, allowing both the geographic origin and the entomological origin of honey to be identified (12,41,42). Advantage of real-time PCR is that it is more sensitive and reproducible than conventional PCR methods, that require post-amplification detection steps such as gel electrophoresis or blotting. Because real-time PCR monitors the accumulation of product during amplification in a closed reaction vessel, it also reduces the risk of contamination and shortens overall workflow times (43). DNA barcoding that uses the mitochondrial cytochrome c oxidase 1 (COI) gene is now widely used to identify and differentiate between animal species (44).

1.3 Plants

In addition to the presence of bee DNA, it is also possible to find plant DNA in honey, originating from the nectar and pollen of the plants used by the bees. As each region has its own characteristic flora, pollen DNA metabarcoding methods are highly valuable for determining the geographical and botanical origin of a particular honey. The floral DNA sequences in the honey act as a botanical signature and can be used to identify whether the honey is monofloral or polyfloral, as well as its region of origin (45).

Many studies have developed different assays using DNA markers that amplify the specific DNA barcode of the plants present in honey. However, it remains challenging to identify a method that can reliably determine the botanical origin of honey mixtures, such as polyfloral or forest honey (46). Today's studies mostly verify PCR-HRM by melissography as a method to confirm PCR-HRM results. The rbcL DNA barcode is the most used marker in plant DNA metabarcoding but other genes are also being tested to find the best marker for identifying the botanical origin of honey (47). ITS2 DNA barcode analysis in a study also showed that honey from different honeybees originates from different floral sources, which allows differentiation of honey samples. All identified plant sources in that study came from the Karangasem region in Bali, highlighting the importance of regional floral diversity in honey authentication (48).

2 Aims

Honey is highly valued for its taste and potential health benefits, so its price has been rising, which has led to an increase in fraudulent practices associated with its production. Verification of honey authenticity, particularly its botanical and geographical origin, is therefore essential for identifying mislabeling and other forms of fraud.

The aim of this master thesis was to investigate the potential of DNA barcoding for honey authentication using PCR-HRM and pyrosequencing (PSQ). Barcode regions targeting plants, insects and honeybee subspecies should be evaluated regarding their suitability for detecting botanical and geographical origin and potential inconsistencies in honey composition.

The first goal of this study was to establish a reliable DNA extraction protocol for honey samples as a prerequisite for PCR-HRM analysis. The extracted DNA should be used as template material for PCR-HRM analysis, allowing amplification of barcode regions and generation of melting profiles for sample discrimination. For this purpose, six primer pairs targeting plant, insect or honeybee DNA barcode regions should be selected from the literature, tested in silico, and modified where necessary to optimize amplification performance. In cooperation with AGES, 16 DNA extracts along with their corresponding sequencing results were provided, identifying the predominant pollen taxa present in each sample. These sequencing results should serve as a reference dataset to assess the discriminatory power and reliability of the PCR-HRM profiles generated with the plant-specific primers.

Additionally, the electrical conductivity of honey samples should be determined as a complementary physicochemical parameter. Prior to electrical conductivity measurement, the water content of each sample should be determined by refractometry, and the dry matter content should be calculated accordingly. Based on these values, the honey samples should be diluted with distilled water to a defined concentration to ensure standardized and comparable electrical conductivity measurements using a conductivity electrode

In cooperation with ao. Univ.-Prof. Mag. Dr. Mathea Sophia Galanski (NMR Centre, Faculty of Chemistry), a selected set of 20 honey samples should be prepared for nuclear magnetic resonance (NMR) analysis. The aim of this analysis was to obtain detailed NMR profiles of the samples and to evaluate whether these profiles correlate with the results obtained from DNA-based methods and electrical conductivity measurements, thereby providing complementary information for honey authentication.

3 Theory

3.1 DNA extraction

DNA extraction is the process of isolating DNA from tissues or cells. The DNeasy mericon Food Kit, which was used in this research, uses a modified cetyltrimethylammonium bromide (CTAB) method for DNA extraction. The CTAB method involves the cationic detergent CTAB in the lysis buffer to lyse the cells. CTAB forms complexes with proteins and carbohydrates, which facilitates the release of DNA. A high salt concentration in the lysis buffer keeps the DNA in solution (49). CTAB enhances the removal of proteins, polysaccharides and other inhibitors, especially when used together with Proteinase K, enabling the extraction of pure DNA from different food materials. During centrifugation, the inhibitors are removed as a pellet, while the DNA stays in the liquid phase. After that, a chloroform extraction removes the remaining CTAB complexes and other unwanted substances. The aqueous phase containing the cleaned DNA is then mixed with binding buffer and loaded onto the QIAquick spin column. The final DNA extract is ready for further use in real-time PCR (50). Eight main steps are usually involved in CTAB extraction protocols: tissue preparation, suspension, lysis, isolation, cleaning, elution, secondary cleanup, and quantification. However, many protocols do not include all eight steps, and the suspension and secondary cleanup steps are often omitted (51).

The concentration of extracted DNA is usually quantified using different methods: spectrophotometry, fluorometry, or gel electrophoresis. The preferred method for DNA quantification is fluorometry, which is frequently performed using the Qubit 4 system (Thermo Fisher Scientific) (51). The Qubit 4 Fluorometer is a device used to measure the amount of DNA, RNA, microRNA and protein with high sensitivity. In addition, it is often insufficiently sensitive for low DNA or RNA concentrations. Fluorometric DNA quantification relies on fluorescent dyes that selectively bind to DNA, since nucleic acids do not exhibit measurable fluorescence on their own. Instruments such as the Qubit fluorometer detect the fluorescence emitted by these dye-DNA complexes, enabling sensitive and specific concentration measurements (49,52).

3.2 Polymerase chain reaction

The polymerase chain reaction (PCR) represents one of the most influential techniques in molecular biology, significantly advancing research on the human genome and deepening our understanding of the molecular mechanisms underlying genetic diseases. A major advantage of PCR is its ability to amplify even very small amounts of nucleic acids obtained from a wide range of biological materials, generating sufficient copies for subsequent analysis. PCR is applied to address diverse research questions, typically following a standardized procedural framework (53).

In recent years, real-time PCR has established itself as a leading technique for the sensitive detection and precise quantification of nucleic acids. It is widely applied in gene expression studies and single nucleotide polymorphism (SNP) analysis, and it can also be adapted for protein detection through real-time immuno-PCR methods (54).

The progress of DNA amplification can be monitored in real-time, or the reaction can be stopped after a certain number of copies is reached. Real-time PCR is performed with a fluorescent dye, that becomes active only when it binds to double-stranded DNA. As a result, fluorescence increases during amplification. Since the fluorescence intensity is proportional to the number of DNA copies, PCR can be used to measure the amount of DNA quantitatively (55). These methods can basically be applied to all food products that are made from plant or animal material or with the help of microorganisms (56).

However, food samples often contain components that inhibit PCR. Substances such as polysaccharides, lipids, and polyphenols can interfere with amplification efficiency and may lead to false-negative results. Although inhibition can often be reduced by dilution of the DNA extracts, similar effects have been observed in complex food matrices as in clinical samples (56,57).

3.2.1 Primer design and *in silico* test

The design of suitable primers is a crucial prerequisite for the specific amplification of DNA targets in real-time PCR applications. Several fundamental guidelines should be considered when designing primer sequences for efficient PCR amplification. In general, primers are recommended to be 18–25 nucleotides in length, contain a balanced distribution of the four nucleotides, and possess a GC content of approximately 50–60%, which supports stable and specific binding to the target sequence (57). Sequences that are too short may compromise target specificity and complicate the selection of an optimal annealing temperature. At the same time, long oligonucleotides increase synthesis costs without improving performance. Longer primers also have a greater tendency to form secondary structures or promote primer dimer formation, which can reduce amplification efficiency, as primers themselves can interact through complementary regions (58).

There are numerous free and commercial software tools available for the computational evaluation of primer sequences prior to experimental use, a process referred to as *in silico* primer testing (e.g. Oligoanalyzer (59), OligoCalc (60), RNA fold (61), NCBI BLAST (62)). These programs can predict melting temperature, secondary structures such as hairpins and identify potential self-annealing interactions. These steps are essential for ensuring specificity, efficiency, and reliability in real-time PCR assays.

3.2.2 Principle of real-time PCR

PCR requires several essential components: two sequence-specific oligonucleotide primers (forward and reverse), four deoxynucleotide triphosphates (dNTPs), a thermostable DNA polymerase, and magnesium ions supplied in the reaction buffer, which are necessary for polymerase activity. Amplification is achieved through repeated temperature cycles. At the beginning of each cycle, the reaction mixture is heated to a high temperature (95 °C) to denature the double-stranded DNA, causing the two strands to separate and become accessible for primer binding. The temperature is then reduced to allow primers to anneal to their complementary sequences on the template DNA. Finally, the temperature is adjusted to approximately 72 °C, which is optimal for DNA polymerase activity, enabling elongation of the primers through incorporation of deoxynucleotide triphosphates (dNTPs) (54). The most frequently used enzyme in PCR is derived from the bacterium *Thermus aquaticus* and is known as Taq DNA polymerase. Native Taq polymerase functions as a DNA-dependent DNA polymerase with 5′→3′ polymerase activity and 5′→3′ nuclease activity. While the wild-type enzyme is commercially available, real-time PCR applications typically utilize recombinant

forms engineered to lack 3′→5′ proofreading activity, thereby improving performance in fluorescence-based detection systems (58).

The optimal annealing temperature is determined by the characteristics of the primers used. In principle, it should be set a few degrees below their melting temperature (Tm) to promote stable hybridization with the intended target sequence while minimizing nonspecific binding (54).

An amplification curve consists of background fluorescence, an exponential growth phase, a linear phase, and a plateau (Figure 3). The cycle threshold (Ct) is defined as the cycle at which the fluorescence signal crosses the threshold line. The plateau phase represents the stage where amplification reaches saturation. The fluorescence threshold is set based on the negative controls, which are essential for accurate interpretation. No template controls (NTCs) must be included in every run to confirm that detected signals originate from the sample rather than from contamination (58). Contamination of PCR reactions can originate from several sources. First, carryover contamination may occur when amplified products from previous PCR reactions are inadvertently introduced into new assays. Second, cross-contamination can arise between different samples during handling or preparation. As amplification progresses, the reaction ultimately enters a plateau phase, in which the fluorescence signal becomes constant due to reagent depletion or reduced enzyme activity (63). The optimal number of cycles depends on the initial concentration or copy number of the target DNA and typically ranges between 25 and 35 cycles. Excessive cycling can lead to the accumulation of nonspecific amplification products and reduced reaction specificity (57).

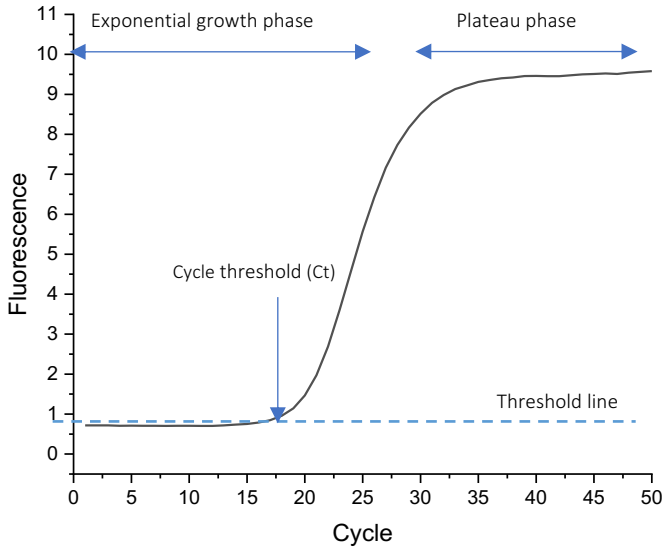

Figure 3 Schematic amplification curve illustrating intensity of fluorescence as a function of cycle number during real-time PCR. The exponential amplification phase, plateau phase, threshold line, and cycle threshold (Ct) value are indicated. Labeling on graphic adapted from (54).

3.2.3 Single nucleotide polymorphism (SNP)

Genetic variation at a single nucleotide position within the genome is defined as a single nucleotide polymorphism (SNP) when at least two allelic variants occur in a population with a frequency greater than 1% (64). For example, one organism may possess an adenine (A) at a specific genomic position, whereas another may carry a guanine (G) at the same locus. Such point variations contribute to genetic diversity among individuals (63). SNP are responsible for genetic differences between individuals (65).

SNPs located within genes can have diverse effects on protein function. When a SNP occurs within the coding region of a gene, it may alter the amino acid sequence of the encoded protein because codons differ between allelic variants. For instance, a point mutation affecting the third nucleotide of the codon TGC may produce the codons TGT, TGG, or TGA. The codon TGC encodes the amino acid cysteine. If the third nucleotide C, is replaced with T, the codon becomes TGT, which also encodes cysteine; therefore, this substitution represents a synonymous (silent) mutation. In contrast, TGG encodes tryptophan, resulting in an amino acid substitution, whereas TGA functions as a stop codon, leading to premature termination of protein synthesis (64). SNP analysis is a powerful molecular tool for distinguishing closely related species and subspecies. In honey studies, SNP markers enable the differentiation of plant species contributing to the botanical origin of honey (66), as well as the identification of honeybee subspecies through genetic traces present in honey (67).

In general, there is a high degree of allele sharing among honeybee populations, and approximately one million SNPs are polymorphic across the four major honeybee groups, highlighting both their genetic diversity and the resolution power of SNP markers for population and subspecies differentiation (67). SNP-based analysis therefore represents a valuable tool for verifying honey authenticity, determining its botanical and geographical origin, and detecting potential adulteration.

3.2.4 High resolution melting analysis

High resolution melting (HRM) analysis is a rapid and efficient method used for genotyping, mutation scanning, and sequence matching. Genotyping of many sequence variants can be achieved by analyzing the melting temperature (Tm) of PCR products. Mutation scanning and sequence comparison rely on sequence differences that promote heteroduplex formation, resulting in characteristic alterations in melting curve shape (68).

Double-stranded DNA remains stable under normal room-temperature conditions; however, as temperature increases, the hydrogen bonds holding the two strands together begin to break, leading to strand separation. The temperature at which half of the DNA molecules become single-stranded is defined as the melting temperature (Tm). This value is influenced by both fragment length and nucleotide composition, particularly guanine–cytosine (GC) content. Because GC base pairs are stabilized by three hydrogen bonds, compared with two in adenine-thymine (AT) pairs, DNA regions with higher GC content exhibit greater thermal stability and therefore melt at higher temperatures than AT rich sequences (69).

Single nucleotide polymorphisms (SNPs) do not produce uniform melting shifts: transitions that convert GC pairs to AT pairs typically produce larger melting temperature (Tm) differences, whereas certain SNP classes may cause only subtle changes in curve shape rather than measurable Tm shifts. Consequently, discrimination of variants may depend on detecting alterations in curve morphology

rather than absolute temperature differences. The position of a sequence variant within the amplicon also plays an important role. Variants located near the center of the amplicon generally produce more pronounced melting profile changes, while those near the ends may be more difficult to distinguish. In addition, uneven GC distribution within the fragment can influence melting domain behavior and reduce sensitivity (70).

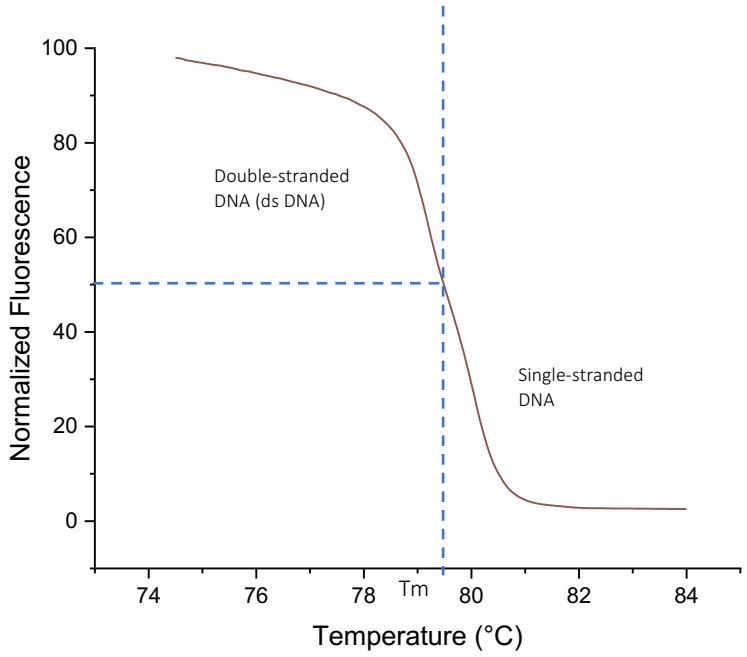

Figure 4 Melting curve obtained during real-time PCR analysis showing the decrease in normalized fluorescence as temperature increases. Interpretative markings and labeling on graphic adapted from (68).

Accurate interpretation of HRM data requires careful normalization and curve analysis. Software-generated normalized plots and difference curves improve discrimination between genotypes by highlighting subtle variations in melting behavior. HRM offers several advantages over alternative genotyping and mutation detection methods. It is performed in a closed-tube system, reducing contamination risk while providing a rapid, cost-effective, and highly reproducible analysis. When properly implemented, HRM can identify many sequence variants, thereby substantially reducing the need for routine sequencing. Because mutation scanning by HRM is nondestructive, samples showing abnormal melting profiles can be subsequently analyzed by sequencing if further characterization is required (68).

3.2.5 Melt curve analysis

Melting curve analysis is performed immediately after completion of the PCR amplification by gradually increasing the temperature of the reaction products. As double-stranded PCR products denature, the intercalating dye SYBR® Green dissociates from the DNA, resulting in a decrease in fluorescence intensity. The instrument software generates a negative first-derivative plot of fluorescence versus temperature (−dF/dT), in which the peak corresponds to the melting temperature of the amplified product (Figure 5) (58).

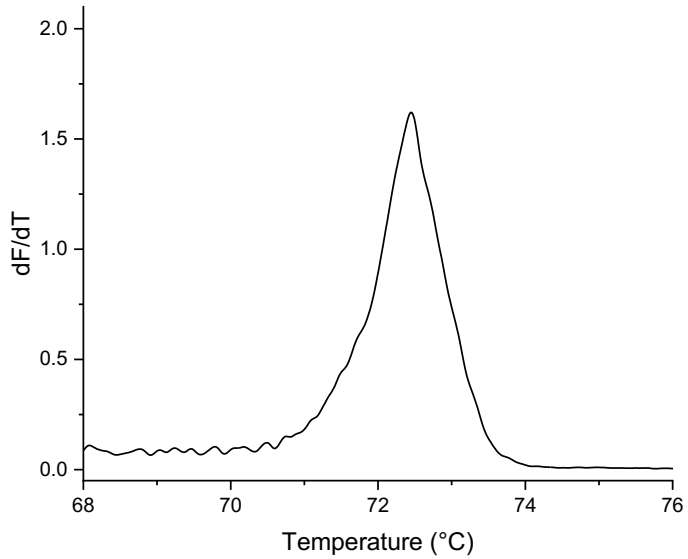

Figure 5 Representative melting curve derivative (dF/dT) of the PCR product showing a single sharp peak at approximately Tm=72.5 °C, indicating a specific amplification product.

The observed Tm should closely match the predicted melting temperature of the specific amplicon. This analysis enables verification of amplification specificity. A single, sharp peak indicates the presence of a specific PCR product, whereas additional peaks suggest nonspecific products or primer dimer formation. Primer dimers may occasionally be detected in negative controls and typically exhibit a lower melting temperature than the target amplicon. The melting temperatures of primer–dimers and specific products are often clearly distinguishable, frequently differing by approximately 10 °C (58).

3.3 Pyrosequencing

Pyrosequencing (PSQ) is a DNA sequencing method based on the detection of pyrophosphate (PPi) released during nucleotide incorporation in the process of DNA synthesis (71). The method relies on the coordinated activity of four enzymes (DNA polymerase, ATP sulfurylase, luciferase, and apyrase) while the addition of single-stranded DNA-binding protein (SSB) can improve sequence quality and extend read length. Owing to its accuracy and rapid signal detection, PSQ has been widely applied in areas such as SNP genotyping, detection of novel mutations, gene identification, and microbial typing (72).

3.3.1 Principle of PSQ

During DNA synthesis, successful nucleotide incorporation releases inorganic pyrophosphate (PPi), which is immediately converted into adenosine triphosphate (ATP) by ATP sulfurylase. The generated ATP drives a luciferase-mediated reaction that produces visible light proportional to the amount of nucleotide incorporated. Residual ATP and unincorporated nucleotides are subsequently degraded by the enzyme apyrase, allowing sequential nucleotide additions to be monitored. Because light emission occurs only when incorporation takes place, the presence or absence of photons directly indicates whether a nucleotide has been incorporated (71,73).

Prior to PSQ, the target region is amplified by PCR, typically using one primer labeled with biotin at the 5′ end. The resulting biotinylated PCR products are immobilized on a streptavidin-coated solid support and denatured to obtain single-stranded DNA, which serves as the sequencing template. After hybridization of a sequencing primer, DNA synthesis proceeds under PSQ conditions with iterative nucleotide dispensation and signal detection. The enzymatic cascade linking nucleotide incorporation to light emission occurs rapidly, typically within 3-4 s at room temperature. During a PSQ reaction, approximately 1 pmol of DNA template generates about 6×10^{11} ATP molecules, which subsequently produce more than 6×10^{9} photons at a wavelength of approximately 560 nm. This light output is readily detected using sensitive instruments such as photodiodes, photomultiplier tubes, or charge-coupled device (CCD) cameras (71) .

A key advantage of PSQ is its capacity to accurately read short DNA stretches of approximately 20 bases or more. This capability makes the method particularly useful for targeted sequencing and for identifying both known and previously uncharacterized polymorphic sites (72).

3.4 Measurement of electrical conductivity in honey

“The electrical conductivity of honey is defined as that of a 20% weight in volume solution in water at 20 °C, where the 20% refers to honey dry matter. The unit is expressed in milli Siemens per centimeter (mS.cm-1)” (74). Honey is called a secondary electrical conductor because, besides sugars and water, it contains electrolytes: substances that can form ions. In honey, these include mineral salts, organic acids (like amino acids and citric acids) and proteins. Measuring electrical conductivity shows the total effect of all these electrolytes. This makes electrical conductivity a simple way to check the electrical properties of honey (75).

Measuring honey’s electrical conductivity can help identify its botanical origin. This measurement is done using a 20% (w/v) solution of honey (based on its dry matter) at 20 °C. The electrical conductivity of honey varies widely, ranging from 0.6 to 17×10^{-4} S/cm. Honeydew honey samples have an electrical conductivity higher than 10×10^{-4} S/cm, while flower honey samples have lower values. Therefore, electrical conductivity reflects the type of plant the honey comes from (75).

4 Experimental part

4.1 Avoiding contamination in laboratory

To avoid cross-contamination, certain experimental steps were performed in separate laboratories. Lab1 was used for DNA extraction of samples. The samples, DNA extracts, primers, DNA-free water, master mix PCR and PSQ kit were stored in this laboratory in different places, separated from each other. While lab2 was used for the preparation of master mixes, in lab3, the DNA extracts were added to the master mix. In each of these laboratories, a different coat was worn. After every finished PCR, amplicons were stored in a freezer at -20 °C, until next analysis. Lab4 was used for PSQ analysis.

Before starting the experiment, the workstations, PCR station and fume hood were cleaned with DNA-Exitus. After cleaning, the gloves were changed to avoid contact between samples and DNA-Exitus. During the experiment, the laboratory book and other items that came from outside of the laboratory were not placed on the workspaces where the experiment took place. After contact with objects that were not from that laboratory, the gloves were changed. In lab2 and lab3, PCR stations were also equipped with UV disinfection systems that sterilized the workspace for 30 min after each use.

4.2 Samples

4.2.1 Honey samples

The honey samples (n=56) were purchased in supermarkets around Austria, at beekeepers or ordered online. Some honey samples were brought from Bosnia & Herzegovina, Croatia, Hungary and North Macedonia. Most honey samples originated from Austria, but also from other European countries and some honey samples were declared to originate from EU and non-EU countries. Honey samples were aliquoted from original package to 50 mL Falcon tubes (Figure 6) and so stored in lab1 at room temperature. Honey sample ID, type and origin are listed in Table 1.

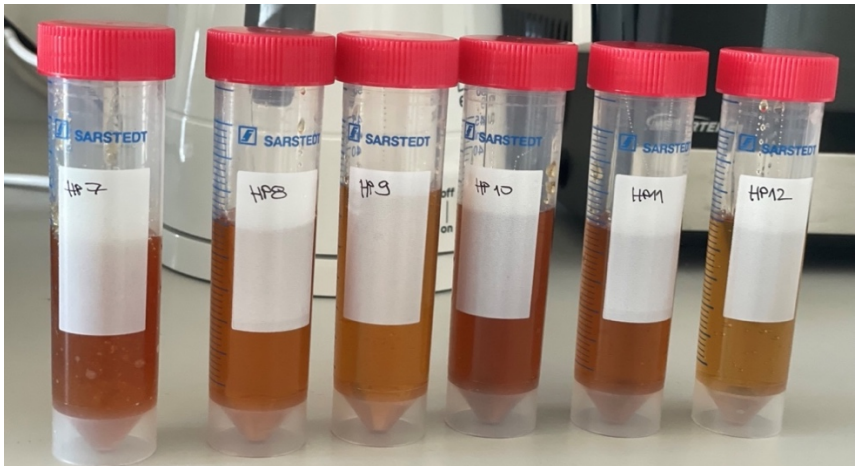

Figure 6 Selected honey samples stored in 50 mL Falcon tubes (HP7–HP12)

Table 1 Honey samples ID (HP1– HP56), honey type and origin

Sample ID	Honey type	Origin
HP1	Forest honey	EU and non-EU countries
HP2	Forest honey	EU and non-EU countries
HP3	Forest honey	Molln, Upper Austria
HP4	Forest honey	Styria, Austria
HP5	Forest honey	Spain and Greece
HP6	Forest honey	Aigen im Ennstal, Styria, Austria
HP7	Organic forest honey	Romania
HP8	Organic forest honey	Austria
HP9	Forest honey	Austria
HP10	Organic pine honey	Austria
HP11	Organic forest honey	Styria, Austria
HP12	Vegan honey - honey alternative	Austria
HP13	Organic forest honey	Germany
HP14	Forest honey	Austria
HP15	Forest honey	Austria
HP16	Organic forest honey	Lower Austria
HP17	Organic forest honey	EU and non-EU countries
HP18	Organic forest honey with organic blossom honey	EU and non-EU countries
HP19	Organic forest honey	EU and non-EU countries
HP20	Forest honey	Styria, Austria
HP21	Organic forest honey	Styria, Austria
HP22	Forest honey	EU and non-EU countries
HP23	Forest honey	EU and non-EU countries
HP24	Forest honey	EU and non-EU countries
HP25	Forest honey	Turkey
HP26	Forest honey with pine thyme	Greece
HP27	Forest honey with heather	Greece
HP28	Forest honey with sage	Greece
HP29	Mountain honey with white thyme	Greece
HP30	Forest honey	Germany
HP31	Blueberry honey	North Germany
HP32	Acacia honey	Brandenburg, Germany
HP33	Cornflower honey	Brandenburg, Germany
HP34	Honey with turmeric	n.d.*
HP35	North German early bloom honey	North Germany
HP36	Fennel in honey	n.d.*
HP37	Chestnut honey	Italy
HP38	Linden blossom	Germany
HP39	Blossom honey with acacia	Germany
HP40	Pine honey	n.d.*

HP41	Forest and blossom honey	n.d.*
HP42	Honey dew honey	Bulgaria
HP43	Organic honey dew honey	Bulgaria
HP44	Organic acacia honey	Bulgaria
HP45	Organic linden honey	Bulgaria
HP46	Raw forest honey	Estonia
HP47	Syrup (90%) + honey (10%)	n.d.*
HP48	Blossom honey	Hungary
HP49	Acacia honey	Hungary
HP50	Goldenrod honey	Hungary
HP51	Linden honey	Hungary
HP52	Forest honey	North Macedonia
HP53	Forest honey	North Macedonia
HP54	Field honey	North Macedonia
HP55	Mixed blossom honey	Bosnia & Herzegovina
HP56	Sage honey	Krk, Croatia

*n.d. no data

4.2.2 Plant and bee samples

Plant leaves and seeds used as positive controls were ordered online. These plants were selected because they are relevant for honey production and their DNA may be present in the analyzed samples. Bee samples (Figure 7) were provided by the beekeepers. Bee samples are marked with PBF or HPBF and plants with two or more letters contained in their German name. The plant and bee samples are listed in Table 2 and Table 3.

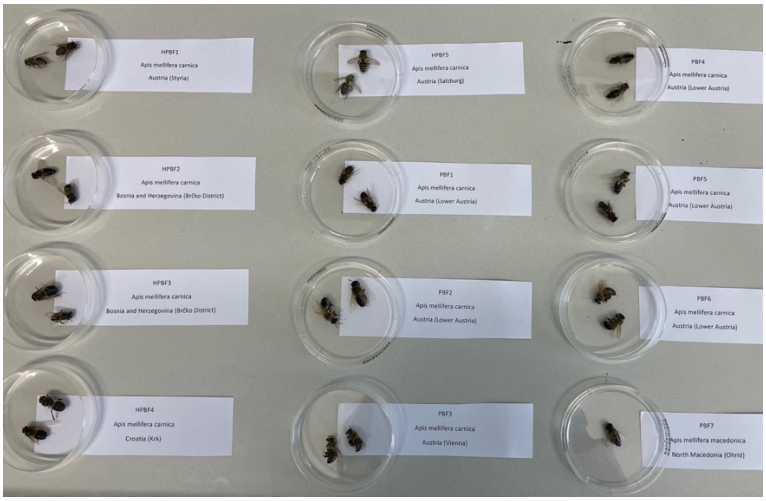

Figure 7 Samples of *A. m. carnica* from Austria, Bosnia & Herzegovina and Croatia and *A. m. macedonica* from North Macedonia.

Table 2 Selected plant species used as positive controls

Sample ID	Plant subspecies	Taxonomic classification (Genus)	Family, lat.
Reis	Rice	*Oryza sativa*	*Poaceae*
Mais	Corn	*Zea mays*	*Poaceae*
RK	Red clover	*Trifolium pratense*	*Fabaceae*
WK	White clover	*Trifolium repens*	*Fabaceae*
MSA	Clary sage	*Salvia sclarea*	*Lamiaceae*
RA	Black locust	*Robinia pseudoacacia*	*Fabaceae*
LB	Linden	*Tilia spp.*	*Malvaceae*
GE	Common ash	*Fraxinus excelsior*	*Oleaceae*
BM	Bee magnet	-	-
IK	Crimson clover	*Trifolium incarnatum*	*Fabaceae*
SWB	Plantain	*Plantago lanceolata*	*Plantaginaceae*
KA	Chamomile	*Matricaria chamomilla*	*Asteraceae*
BN	Nettle	*Urtica dioica*	*Urticaceae*
FE	Fennel	*Foeniculum vulgare*	*Apiaceae*
ANIS	Anise	*Pimpinella anisum*	*Apiaceae*
MM	Mallow bloom	*Malva sylvestris mauritiana*	*Malvaceae*
SFG	Yarrow	*Achillea millefolium*	*Asteraceae*
PF	Peppermint	*Mentha × piperita*	*Lamiaceae*
QR	Oak	*Quercus spp.*	*Fagaceae*
SLB1	Sage (leaves)	*Salvia officinalis*	*Lamiaceae*
SLB2	Sage (seed)	*Salvia officinalis*	*Lamiaceae*
Raps	Rape	*Brassica napus*	*Brassicaceae*
EK	Sweet chestnut	*Castanea sativa*	*Fagaceae*
PT	Lacy phacelia	*Phacelia tanacetifolia*	*Boraginaceae*

Table 3 Bee samples used as positive controls

Sample ID	Bee subspecies, lat.	Origin
HPBF1	*A. m. carnica*	Styria, Austria
HPBF2	*A. m. carnica*	Brcko, Bosnia & Herzegovina
HPBF3	*A. m. carnica*	Brcko, Bosnia & Herzegovina
HPBF4	*A. m. carnica*	Krk, Croatia
HPBF5.1	*A. m. carnica*	Salzburg, Austria
HPBF5.1.1	*A. m. carnica*	Salzburg, Austria
HPBF5.2	*A. m. carnica*	Salzburg, Austria
PBF1	*A. m. carnica*	Lower Austria
PBF2	*A. m. carnica*	Lower Austria
PBF3	*A. m. carnica*	Vienna, Austria
PBF4	*A. m. carnica*	Lower Austria
PBF5	*A. m. carnica*	Lower Austria
PBF6	*A. m. carnica*	Lower Austria
PBF7	*A. m. macedonica*	North Macedonia

4.2.3 Honey and pollen samples from AGES

The cooperation partner "Institute of Food Safety Vienna Department of Molecular Biology and Microbiology," AGES, Austria provided 16 honey-derived DNA extracts and 16 pollen-derived DNA extracts originating from the same set of sixteen honey samples. DNA concentration was not determined as it is generally below the limit of detection in such extracts, therefore, quantification was omitted to avoid unnecessary time and resource expenditure. Honey samples were marked with H1–H16, and pollen samples were marked with P1–P16 and are listed in Table 4.

Table 4 Honey and pollen extracts provided by AGES and their honey/pollen type

Sample ID	Honey/pollen type
H1/P1	Comb honey
H2/P2	Acacia honey
H3/P3	Herbal honey
H4/P4	Creamed honey
H5/P5	Forest honey
H6/P6	Alpine blossom honey
H7/P7	Pure natural honey-from Austrian beekeepers
H8/P8	Blossom honey
H9/P9	Sunflower blossom honey
H10/P10	Rape honey
H11/P11	Comb honey
H12/P12	Eucalyptus honey from Beira Litoral
H13/P13	Forest honey
H14/P14	Chestnut honey
H15/P15	Blossom honey
H16/P16	Linden blossom honey

4.3 DNA extraction

The steps of extraction process are schematically displayed in the Figure 8.

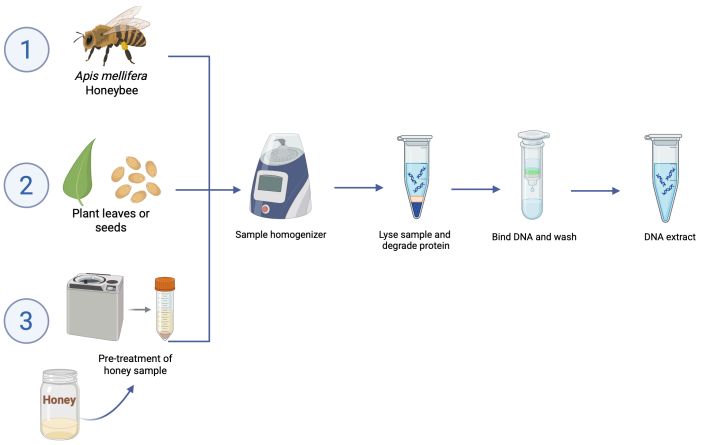

Figure 8 Workflow for DNA extraction from honeybees, plants, and honey, using the Food Kit, including honey sample pre-treatment. The schematic was created using Bio Render.

4.3.1 Sample pre-treatment

4.3.1.1 Honey samples

For the DNA extraction from honey, pre-treatment of the samples was done as described in (76) with minor modifications to achieve a higher concentration of DNA. Fifteen grams of each honey sample were weighed into a 50.0 mL Eppendorf tube and filled with ELGA water to the mark. The reaction mixture was heated for 10 min at 800 rpm at 50 °C then mixed briefly and then centrifuged for 10 min at 23 °C and 4500 rpm. After centrifugation, a pellet was visible, the supernatant was removed, and the pellet was re-suspended with 0.5 mL of ELGA water and transferred to a Lysing Matrix M tube. The samples were homogenized using a MP homogenizer, selecting 'Saved Programs' and 'Fixed museal tissues'. Homogenization was performed at a speed of 6 m/s for 40 s using Lysing Matrix M tubes containing two ¼ ceramic beads. The procedure consisted of three cycles with a 300 s pause between cycles. After completion of the homogenization process, the ceramic beads were removed from the tubes using a sterile needle.

4.3.1.2 Plant and bee samples

About 70 mg of bee or plant were chopped with a disposable knife in Petri dishes, and the exact mass was measured in MP tube using an analytical balance and then mixed with 1 mL of lysis buffer. Two ceramic ¼ beads were placed in each tube. The samples were processed in the MP homogenizer as described in section 4.3.1.1. After removing the ceramic beads with a needle, DNA extraction was carried out as described by the manufacturer and explained in section 4.3.2. DNA extracts from bees labeled PBF were prepared by colleague Andrea Bevilacqua from Cichna Group and used in this study to increase the number of honeybee positive controls and to enable comparisons between honeybee subspecies and honey samples.

4.3.2 DNA extraction with DNeasy mericon Food Kit

DNA extraction was carried out using the DNeasy mericon Food Kit. All steps were conducted as described by the manufacturer, following the Protocol: Small Fragment Protocol (200 mg) steps with minor modifications. 200 mg of the homogenized sample was transferred with a pipette into a 2.0 mL Eppendorf tube. Then, 1.0 mL of lysis buffer and 2.5 µL of Proteinase K were added to the sample, vortexed for 15 s, and incubated for 30 min at 60 °C and 1000 rpm.

After incubation, the samples were placed on ice for 5 min and then centrifuged for 5 min at 2500 rpm. A total of 700 µL of the clear supernatant was transferred into a new 2.0 mL Eppendorf tube, mixed with 500 µL of chloroform in fume hood, vortexed briefly, and centrifuged for 15 min at 14,000 rpm. Subsequently, 250 µL of the upper aqueous phase was added to 1.0 mL of binding buffer in a new 2.0 mL Eppendorf tube. The tubes were vortexed for 15 s, and 650 µL of the mixture was loaded onto a spin column.

The spin columns were centrifuged for 1 min at 17,900 rpm, the flow-through was discarded, and the columns were placed back into their respective collection tubes. This step was repeated to process the remaining part of the sample. In the following step, 500 µL of washing buffer was added, and the spin columns were centrifuged for 1 min at 17,900 rpm. The flow-through was discarded, and the collection tubes were replaced with clean 2.0 mL Eppendorf tubes.

Finally, 50 µL of pre-warmed elution buffer was added, the tubes were incubated for 5 min at 60 °C and then centrifuged for 1 min at 17,900 rpm. The DNA extracts were collected in Eppendorf tubes and were ready for concentration measurement using Qubit 4 device. After measuring the DNA extracts were stored at -20 °C.

4.3.3 Measurement of the DNA concentration

Fluorometric measurements of DNA concentrations were done using Qubit 4 Fluorimeter (Thermo Fisher Scientific). For the determination of DNA concentration, the Qubit HS DNA Assay Kit was used. The Qubit working solution was prepared using the Qubit reagent (red) and Qubit buffer. The exact volumes of reagent and buffer depended on the number of samples and standards. To calculate these volumes, the calculator function on the Qubit 4 Fluorimeter device was used. After entering the number of standards and samples, the required volumes of reagent and buffer were mixed.

Two standards were used for calibration. In each Qubit tube, 190 µL of the Qubit working solution was combined with 10 µL of Standard 1 or Standard 2, respectively. The tubes were vortexed and incubated for 2 min at room temperature. The same procedure was applied to the samples. For the measurement, the dsDNA High Sensitivity program on the instrument was selected, and the resulting DNA concentrations were given in ng/µL. Concentrations of DNA extracts are provided in Supplementary Table S1.

4.4 Primer design & *in silico* test

Together with master student Verena Wagner from WG Cichna, primers were selected from previous studies (12,29,39,77–79), tested *in silico* and purchased. All primer sequences used in this study are presented in Table 5.

Table 5 Primer sequences. Ins: insects; PL: plant; BEE: bee; fwd: forward; rev: reverse; seq: sequencing; Btn: biotinylated

Primer name	Sequence	Target species	Gene	Paper
BEE1 fwd	AGCTAATTAAAACAACAATACA	Bee	16S rRNA	(39)
BEE1 rev	AAGGTAGTAAATGTTGAATCATT			
BEE2 fwd	CAATGAGACTTATTATTCGAATAG	Bee	COI	(12)
BEE2 rev	GCCAATTTCCAAATCCTCCAA			
BEE2_1 fwd	GAATAGAATTAAGATCCCCAGG	Bee	COI	This work
BEE2_1 rev	[Btn]GCCAATTTCCAAATCCTCCAA			
BEE2_1 seq	CCAGGATCATGAAT			
Ins fwd	TWACGCTGTTATCCCTAAGG	Insects	COI	(77)
Ins rev	GACGAGAAGACCCTATAGA			
Ins_1 fwd	CTGTTATCCCTAAGGTAATTTAT	Bee	COI	This work
Ins_1 rev	[Btn]ATTAAATTTGATTGGGAGGATTG			
Ins_1 seq	ATTCTTTTAATTACAAT			
PL1 fwd	TCACGCGGGTACAGTAGTAG	Plant	rbcL	(29)
PL1 rev	ATGCCAAACGTGAATACCCC			

PL2_1 fwd	ATGCGATACTTGGTGTGAAT	Plant	ITS2	(78)
PL2_1 rev	(GA)CGCTTCTCCAGACTACAA(T)			Modified in this work
PL3_1 fwd	ATGTCACCACAAACAGAAAC	Plant	rbcL	(79)
PL3_1 rev	TCGCATGTACCTGCAGTA(GC)			Modified in this work

For primer pairs PL2 and PL3, the primer sequences reported in the literature (78,79) were modified by shortening (the deleted nucleotides are indicated in parentheses in Table 5) to obtain more similar annealing temperatures between forward and reverse primers. The modified versions were tested *in silico* and newly purchased.

For the BEE2 target region, the forward primer was repositioned using the NCBI BLAST tool to reduce the amplicon length, while the reverse primer sequence remained unchanged and was purchased in a biotinylated form for subsequent PSQ analysis. The primer pair BEE2_1 was redesigned to improve amplification efficiency, sensitivity, and suitability for real-time PCR. Due to the presence of four SNPs within the target region, a sequencing primer was additionally designed, tested in silico, and purchased.

The Ins primer was adopted from the literature (77) and initially tested on bee samples used as positive controls. To improve the amplification of the PCR product within the DNA COI region, both the forward and reverse primers were repositioned within the reference sequence obtained from the literature. The redesigned primers were subsequently evaluated in silico and then applied in the further analysis of honey samples and other available bee specimens.

4.4.1 *In silico* test

The theoretical melting temperature of the primers was calculated using online tool OligoCalc (“salt adjusted” temperatures were chosen). To check for possible secondary structures, the primers were analyzed using RNAfold WebServer at 37.5 °C and at 5 °C below the theoretical Tm. Finally, the primers were tested for potential self-dimer and hetero-dimer formation using OligoAnalyzer.

4.4.2 NCBI BLAST

To evaluate whether the forward and reverse primers specifically anneal to the target DNA sequence, National Center for Biotechnology Information (NCBI) Basic Local Alignment Search Tool (BLAST) was used. Using the NCBI BLAST database, it is possible to predict amplification with a specific primer. On the initial page, it is necessary to select nucleotide BLAST, then to enter the first primer and the species whose gene is intended to be amplified. When the whole sequence is obtained as a result, it is necessary to search for the second primer in its complementary reverse form. The website used for this purpose was Reverse complement from Bioinformatics. Research using BLAST is of great importance, as it enables the comparison of sequences among different species or subspecies. In this way, individual nucleotide variations, known as SNPs, can be identified by detecting differences at specific positions in the DNA sequences. It also allows checking whether a similar or identical sequence is already present in databases and provides insights into the organism or gene of an unknown sequence. In this work, special attention was given to sequences from bees and plants during BLAST research.

4.4.3 Primer resuspension

The primers were delivered in lyophilized form. In lab1, the primers were centrifuged using a Galaxy Mini Centrifuge. In lab2, at the PCR station, the primers were resuspended in RNA-free water using the volume provided by the manufacturer on the Sigma-Aldrich data sheet to obtain a 100 µM primer solution, followed by vortexing every 5 min for 20 min. Then, the primers were aliquoted (10×10 µL). Gloves were changed after each resuspension of a primer pair to avoid possible contamination. After resuspension and aliquotation, the primers were stored at -20 °C in lab1. When a specific primer was required, in lab2, 90 µL of DNA-free water was added to 10 µL of the 100 µM primer in an Eppendorf tube to obtain a 10 µM working concentration. The solution was vortexed thoroughly. These 10 µM primers were then used for PCR. For PSQ, the sequencing primer was further diluted from 10 µM to 4 µM.

4.5 PCR-HRM procedure

DNA amplification was performed using two instruments, Rotor Gene Q thermal cycler and Quantstudio 5. Quantstudio 5 was used to optimize the annealing temperature of each primer pair, as it allows multiple temperatures to be tested in a single run.

At this part of the experiment, three different annealing temperatures for each primer pair were tested: the theoretical melt temperature (Tm), Tm–1 °C, and Tm–3 °C. The amplification and melt curves were then evaluated, and the most suitable annealing temperature was chosen for the following studies (Table 6). The optimal annealing temperature was defined as the condition yielding the lowest Ct values indicating high amplification efficiency, a single sharp melt peak indicating specific product formation, and high repeatability across replicates. Additionally, the primer concentrations were optimized. For each PCR-HRM assay, specific primer concentrations were optimized to obtain sharp and well-defined melting peaks without primer-dimer formation; the selected conditions are presented in Table 6.

Table 6 The optimized PCR conditions for each assay, including the annealing temperature (°C) and primer concentration (µM).

Assay	BEE1	BEE2_1	Ins_1	PL1	PL2_1	PL3_1
Annealing temperature (°C)	50.1	55.6	55.0	57.4	53.3	53.3
Primer concentration (µM)	0.2	0.2	0.4	0.4	0.4	0.4

All other PCR reactions were done on Rotor-Gene Q, followed by evaluation of results using Rotor-Gene Software, where the melt profiles were obtained. First, the template was created using Excel and the Rotor Gene Q Software. The important information for each assay included annealing temperature, the number of samples and the primer concentration. Every sample was analyzed twice, to increase reliability and accuracy of the results and to detect possible pipetting errors or reaction failures. Once the template was created and saved on a USB stick, the work in the laboratory could be started. In lab1, the master mix, RNase-free water, and primers were placed with a metal plate and an ice bag in a styrofoam box. The DNA extracts were placed in a special red rack for lab3 and left on the bench in lab1, so that during the preparation of the master mix, the

samples could defrost. To prepare the master mix in lab2, the 2x TypeIt HRM PCR master mix was used. Depending on the primer concentration for each assay, the volumes of master mix, primer, and RNase-free water for one sample are shown in Table 7.

Table 7 Volumes required to prepare one reaction per assay with different primer concentrations

Assay 1 (0.2 µM assay)			Assay 2 (0.4 µM assay)		
RNase free water	7.20	µL	RNase free water	6.40	µL
2x TypeIt HRM PCR master mix	10.00	µL	2x TypeIt HRM PCR master mix	10.00	µL
10x CoralLoad concentrate	0.00	µL	10x CoralLoad concentrate	0.00	µL
Primer 10 µM fwd	0.40	µL	Primer 10 µM fwd	0.80	µL
Primer 10 µM rev	0.40	µL	Primer 10 µM rev	0.80	µL
Total	18	µL	Total	18	µL
Master mix per well	18	µL	Master mix per well	18	µL
DNA extract 2.5 ng/µL	2	µL	DNA extract 2.5 ng/µL	2	µL

As soon as the master mix was prepared, 18 µL of the master mix was pipetted into strip tubes, that were placed into metal plate. The tubes were not completely closed because the next step was adding 2 µL of sample in lab3. In lab3, after adding the sample, the tubes were closed and mixed so that no air bubbles were inside. The samples were transferred in the styrofoam box to the room belonging to lab2, where the Rotorgene Q thermal cycler is located, and the samples were then placed into the instrument.

In Table 8, the conditions of each step during PCR-HRM are shown. As amplification was carried out using the Rotorgene Q instrument, PCR cycling conditions were adjusted relative to those reported in the literature. The protocol began with an initial denaturation and polymerase activation step at 95 °C for 5 min. This was followed by 50 amplification cycles consisting of denaturation at 94 °C for 15 s, primer annealing at assay specific temperatures for 30 s, and elongation at 72 °C for 30 s. A final elongation step was performed at 72 °C for 10 min to ensure complete amplicon synthesis. Subsequently, HRM analysis was conducted across a temperature range of 65–95 °C, with temperature increments of 0.05 °C. A 90 s stabilization step was applied at the beginning prior to melting, followed by 2 s stabilization at each subsequent temperature step.

Table 8 The settings in HRM-PCR used during this research with variable annealing temperatures and final elongation

Step		Time	Temperature	Repeat
Hold 1	Denaturation, activation of polymerase	5 min	95 °C	
Cycling 1	Denaturation	15 s	94 °C	Number of cycles: 50
	Annealing	30 s	variable	
	Elongation	30 s	72 °C	
Hold 2	Final elongation	10 min	72 °C (65 °C; 68 °C)	
Hold 3	Denaturation	1 min	95 °C	
Hold 4	Strand pairing	1 min	40 °C	
HRM	HRM	-	65–95 °C	0.05 °C/step; 90 s; gain opt 70

After the run was completed, the melt curves were analyzed. To obtain more insights from multiple runs at the same time, the data from each run was exported into OriginLab. The melt curves from honey samples were then compared to positive controls depending on the assay; the positive controls were either plants or bees.

4.6 PSQ Sequencing

PSQ experiments were conducted using the PyroMark Q24 Advanced CpG Reagents Kit (Qiagen) according to the manufacturer's instructions. First, the assay was designed using PyroMark Q48 Autoprep software, selecting New SNP assay. The assay name, reference sequence, and SNP position(s) were entered, with SNP positions indicated by a slash. A new run file template was then created and saved, and the disc layout was then prepared by assigning the required assays to the selected wells and entering the corresponding sample information. The assays were added by dragging them from the browser and the wells were automatically color-coded based on the assay type. After designing, the template was transferred to a USB stick.

The reagent kit was taken from lab1. PCR amplicons from the selected PCR run were placed in a styrofoam box together with an ice pack and the reagent kit, and transported to lab4, where the PSQ PyroMark Q48 (Qiagen) machine is located. After turning on the instrument, all reagent cartridges were washed twice with 200 mL ELGA water. The USB stick, containing the template was inserted into device, and the steps displayed on the machine were followed, including changing the absorber strip and adding different volumes of dNTPs, sequencing primer, buffer solutions, enzyme, and substrate to the channels. Then, the sample disc was inserted and 3 µL of PyroMark Q48 Magnetic Beads were added to each well. Because of their high density, the beads settle quickly after vortexing, so special precautions were taken during pipetting. Subsequently, 10 µL of biotinylated PCR product (amplicon) were added into the correct well position for each sample. Blank dispensations were automatically created by the software and served as internal quality controls for the assay.

After the run, data are automatically saved to the USB stick. If the USB stick was removed during the run, the data can be manually recovered directly from the instrument. After completed run, the reagent cartridges were washed again twice with ELGA water, and the sample disc and absorber strip were removed from the machine. Results were interpreted by opening the run file. The disc layout overview (Figure 9) provides a general summary of the quality evaluation. The color bar indicates the assessment status for all variable positions within a well: blue: passed; yellow: check; red: failed. The PyroMark software is designed for biological samples, where SNPs are either homozygous or heterozygous (approximately 50:50). Because the honey samples are mixtures, any ratio of wild type to SNP is theoretically possible. If the ratio deviates significantly from 50:50, the software marks the well red, even though the measurement may be correct.

For each selected well, the pyrogram and histogram are displayed. The pyrogram (upper panel) (Figure 9A), represents the actual nucleotide sequence in peak heights. The histogram, shown in the lower section (Figure 9B) represents a theoretical peak pattern expected for that sequence. This makes it possible to identify SNPs as heterozygous (e.g. A/G) and homozygous (e.g. A/A) SNPs. The quality of the result is reflected by the background color displayed behind the analysis outcome (80).

Figure 9 Disc layout overview of PSQ run file demonstrating SNP analysis for selected honey samples and *A. m. carnica (HPBF)* from Styria, Austria. The pyrogram (top) and histogram (bottom) were obtained with the assay BEE2_1.

4.6.1 Quantification of SNP allele frequencies

In the PSQ assay, the signal of each nucleotide is measured as a peak in the pyrogram. The peak height is proportional to the number of incorporated bases and is used for the calculation of allele frequencies at SNP positions. However, raw peak heights can be influenced not only by background noise and neighboring peaks but also by the incorporation of the same nucleotide multiple times in a row. In such cases, the measured peak height does not scale linearly with the number of incorporated nucleotides. To obtain reliable results, a correction step was applied. In this step, specific peak heights were adjusted by subtracting background contributions before calculating the allele percentages. A correction factor was applied to adjust A-peak intensities, since A-peaks are typically higher than other nucleotide peaks. The default setting for this factor was 0.90. The correction for each SNP was calculated according to Equation 1.

Equation 1 To minimize the influence of background noise as well as signal contributions from neighboring peaks in the pyrogram, correction formulas were applied for each SNP.

$$\text{SNP1} = \frac{\text{Position3 (A)} \times 0.9 - \text{Position2 (T)}}{\text{Position4 (G)}}$$

$$\text{SNP2} = \frac{\text{Position5 (C)}}{\text{Position6 (T)}}$$

$$\text{SNP3} = \frac{\text{Position32 (C)} - \text{Position30 (G)}}{\text{Position31 (T)}}$$

$$\text{SNP4} = \frac{\text{Position40 (C)} - \text{Position36 (C)}}{\text{Position39 (T)} - 2 \times \text{Position36 (C)}}$$

4.7 Measurement of water content and electrical conductivity

The experimental part of measuring electrical conductivity in honey samples started with the determination of water content (%) in the samples using refractometry. The water content of the honey samples was determined using an HHTEC beekeeper refractometer (measuring range 12–35% water). Prior to measurement, the instrument was calibrated with a colorless, non-toxic calibration solution according to the manufacturer's instructions. The prism surface was cleaned and dried before analysis. A small amount of honey was placed onto the main prism, and the cover plate was closed to ensure even distribution of the sample. The water content was then read directly from the scale through the viewing window. In relation to the standard DIN 10753:2021, the electrical conductivity of honey is determined in a solution containing a defined amount of dry matter. Therefore, the exact mass of honey required to obtain the specified dry matter content was calculated based on the previously determined water content using Equation 2. The calculated amount of honey was weighed into a 50 mL flat-bottom flask, and distilled water was added up to the mark. The solution was thoroughly mixed until complete dissolution, and electrical conductivity was measured using a calibrated pH meter equipped with a conductivity electrode. Prior to measurement, the instrument was calibrated using a standard electrical conductivity solution (1413 µS/cm) according to the manufacturer's instructions. The electrical conductivity values were recorded in mS/cm.

Equation 2 Dry mass in grams equals desired concentration in grams per 100 milliliters, multiplied by 100, divided by 100 minus the water content percentage in the sample.

$$\text{Dry mass (g)} = \frac{\textbf{Desired concentration}\left(\frac{\text{g}}{\text{100 mL}}\right) \times \textbf{100}}{\textbf{100}-\textbf{\% Water in sample}}$$

4.8 NMR

In cooperation with ao. Univ.-Prof. Mag. Dr. Mathea Sophia Galanski, some honey samples were selected and analyzed using NMR spectroscopy. Selected honey samples were prepared in lab1. NMR spectroscopy analyses were always performed in deuterium oxide (D_2O). Trimethylsilylpropanoic acid (TSP) was used as a reference standard, with its signal set to 0. A 0.05% w/v TSP solution was prepared in D_2O. For the measurement, 120 mg of honey was dissolved in 0.8 mL of 0.05% TSP in D_2O, vortexed and transferred to the NMR tube. NMR tubes with samples were then transferred to NMR Center and directly positioned in the device.

The pH value was measured in a subset of honey samples to preliminarily evaluate a possible influence of pH on the NMR spectral profiles. To obtain the same sample to solvent ratio as used for NMR analysis, 7.5 g of selected honey was weighed into a 50 mL flat-bottom flask and diluted to the mark with distilled water. The solution was thoroughly mixed until complete dissolution, and the pH was measured using a pH meter (Metrohm, Model 691). Prior to measurement, the pH meter was calibrated with three standard buffer solutions according to the manufacturer's instructions.

5 Results and Discussion

To assess the potential of the DNA barcoding method for honey authentication, this study analyzed selected DNA barcode regions for honeybee subspecies and plant species. Primer sequences were obtained from previously published studies and were first tested *in silico* to evaluate their specificity, coverage of the target regions, and potential amplification efficiency. Subsequently, the selected primers were also tested experimentally to assess their practical applicability for the amplification of targeted DNA regions from honey samples.

This chapter presents the results of the *in silico* analyses as well as the outcomes of the laboratory experiments, including amplification success and the quality of the obtained sequences, using PCR-HRM and PSQ techniques.

5.1 DNA extraction results

DNA extraction results were assessed for plants species, honeybee subspecies and honey samples. The measured DNA concentrations are presented in Table S1–Table S3, respectively. Overall, DNA extracts obtained from plants and honeybee samples consistently showed higher concentrations compared to those isolated from honey samples. Among the different honey types, forest honey samples exhibited higher DNA concentrations than floral and acacia honeys. Prior to PCR-HRM analysis, DNA concentrations were standardized. Samples with concentrations exceeding 2.5 ng/µL were diluted to 2.5 ng/µL, while samples with lower concentrations were used without further dilution. This normalization step was performed to ensure comparable template input across all reactions.

5.2 DNA barcoding assays for distinguishing between honeybee subspecies

5.2.1 BEE1 assay

The primer pair BEE1 was taken from (39) without any modifications and was first tested *in silico* prior to its application in PCR-HRM analysis. The primer sequences are summarized in Table 5. According to Soares et. al (39), this primer pair seemed promising for differentiating between two types of honeybees, *A. mellifera* (European) and *A. cerana* (Asian). The data from this paper show that all European honeybee subspecies amplified with this primer clustered together, and separated from another cluster, which consists of positive control *A. cerana*, honeybee from Asia (39). Primer pair BEE1 targets the 16S rRNA gene region. An overview of in *silico tests* of primer pair BEE1 is presented in Figure 10.

BEE1		
Amplicon length: 111bp	Forward (fwd)	Reverse (rev)
Sequence	AGCTAATTAAAACAACAATACA	AAGGTAGTAAATGTTGAATCATT
Length (bp)	22	23
GC content (%)	23	26

Tm (°C)	51.9	53.9
Sec (T=37 °C)	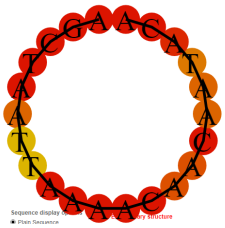	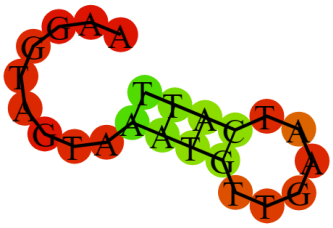
Sec (T=Tm-5 °C)	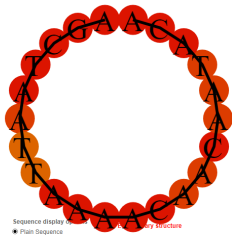	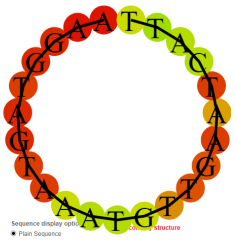

Figure 10 Summary of the *in silico* analysis of the BEE1 primer pair, including amplicon length; primer sequences; GC content (%); melting temperature (Tm); and predicted secondary structures (Sec).

5.2.1.1 BEE1 PCR-HRM assay

The BEE1 assay was evaluated to determine its ability to detect honeybee DNA in honey samples and to assess its specificity across different *A. mellifera* subspecies. Amplification results demonstrated that honey samples (HP1–HP25) exhibited higher Ct values (Ct > 35) compared to the positive control DNA extract of *A. m. carnica* (HPBF1), which showed Ct values of around 20 (Figure 11). Despite differences in Ct values, no significant variation in melting temperature or melting curves was observed between honey samples and the subspecies *A. m. carnica* and *A. m. macedonica*. The differences in melt peak height are related to the amount of amplified DNA, which depends on DNA concentration or quality of the sample (Figure 12). However, the BEE1 assay demonstrated that the primer pair BEE1 was able to detect the presence of honeybee DNA in honey samples.

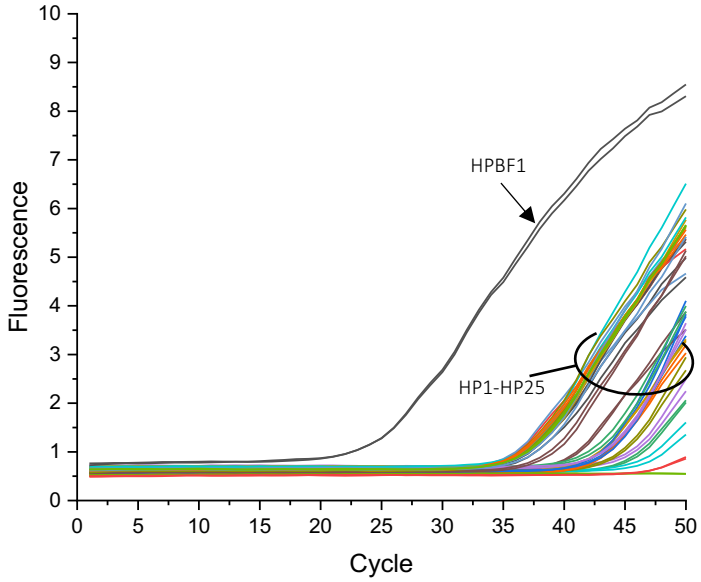

Figure 11 Amplification curve of honey samples (HP1–HP25) and the honeybee *A. m. carnica* from Styria, Austria (HPBF1) with primer pair BEE1.

However, the results confirmed findings from (39), as it was not possible to distinguish between honeybee subspecies. Additionally, all honey samples showed similar melting profiles, since most are from European-based countries.

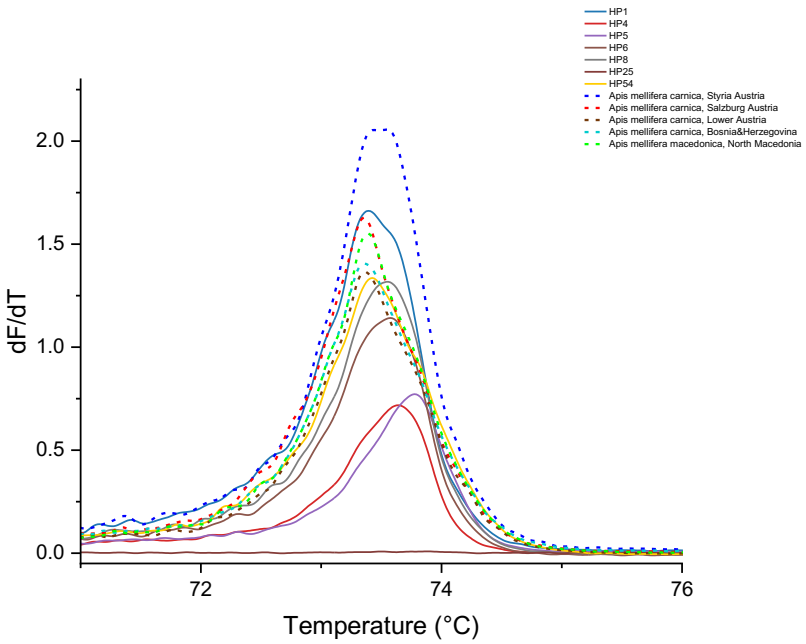

Figure 12 Melting curves of the PCR products from seven honey samples HP1, HP4, HP5, HP6, HP8, HP25, HP54 (solid curves) of different origins and honeybee samples *A. m. carnica* and *A. m. macedonica* (dashed curves) obtained with primer pair BEE1. All PCR products of honey samples and honeybee samples melt at similar temperatures.

Since the primer pair BEE1 did not appear suitable for distinguishing between honeybee subspecies, no further experiments were conducted using this primer pair.

5.2.2. BEE2_1 assay

According to the literature, the COI region, located in the mitochondrial genome, is a region of interest in animal DNA barcoding studies (44). The BEE2 primer targeted this COI gene region, and the melt curves showed differences between honey samples and different bee subspecies, due to the presence of four SNPs in the amplified sequence. Previous studies have demonstrated that this primer pair is suitable for differentiating honeybee subspecies (12).

The BEE2 primer pair was originally taken from the literature, tested *in silico*, and applied in the initial PCR-HRM analyses. To improve the clarity of PCR-HRM results, a new primer, BEE2_1, was designed and tested *in silico*; from that point, only BEE2_1 was used in further PCR-HRM analyses. The overview of *in silico* tests of primer pairs BEE2 and BEE2_1 are presented in Figure 13. Additionally, a sequencing primer (BEE2_1 seq) was also designed. Because four SNPs are present within the BEE2_1 amplicon (Figure 15), this primer was intended to enable sequencing of the PCR products. The amplicon was shortened by 18 base pairs, while the reverse primer sequence remained unchanged. Due to the shorter sequence, the melting curves shifted to the left, into the region of lower melting temperature. The reverse primer was ordered in a biotinylated form to allow subsequent pyrosequencing of the PCR product. Newly designed primers (fwd, rev and seq) and a complete BEE2_1 amplicon are shown in Figure 14.

BEE2		
	Forward (fwd)	Reverse (rev)
Sequence	CAATGAGACTTATTATTCGAATAG	GCCAATTTCCAAATC CTCCAA
Length (bp)	24	21
GC content (%)	29	43
Tm (°C)	56.6	57.5
Sec (T=37 °C)	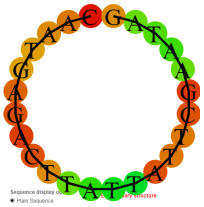	
Sec (T=Tm-5 °C)	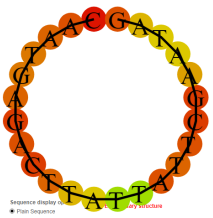	
BEE2 amplicon (150 bp): CAATGAGACTTATTATTCGAATAGAATTAAGATCCCCAGGATCATGAATTAGCAATGATCAAATTTATAATACAATTGTTACTAGTCATGCATTCCTAATAATTTTTTTTATAGTTATACCATTTTTAATTGGAGGATTTGGAAATTGGC		
BEE2_1 (Amplicon length: 132bp)		
Sequence:	GAATAGAATTAAGATCCCCAGG	
Tm (°C)	58.0	

Sec (T=37 °C)	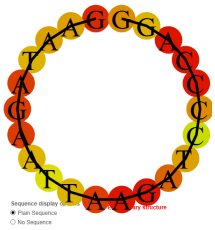	
Sec (T=Tm-5 °C)	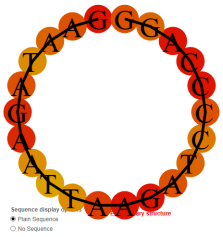	

Figure 13 *In silico* analysis of the primer pairs BEE2 (forward and reverse, top) and BEE2_1 (forward only, bottom), showing amplicon length and sequence, GC content (%), primer sequences, melting temperature (Tm), and predicted secondary structures (Sec).

Amplicon length: 132 bp	Sequence	Tm (°C)
fwd	GAATAGAATTAAGATCCCCAGG	58.0
seq	CCAGGATCATGAAT	38.0
rev	TGGAGGATTTGGAAATTGGC	57.5

BEE2_ 1 amplicon (132 bp):

GAATAGAATTAAGATCCCCAGGATCATGAATTAATAATGATCAAATTTATAATACAATTGTTACTAGCCATGC
ATTTCTAATAATTTTTTTTATAGTTATACCATTTTTAATTGGAGGATTTGGAAATTGGC

Figure 14 *In silico* characteristics of the primers used in this study. The table shows amplicon length, primer sequence, and melting temperature (Tm); blue: the forward (fwd), orange: sequencing (seq), and yellow: reverse (rev) primers. The full sequence of the BEE2_1 amplicon is provided at the bottom.

Figure 15 Some subspecies of honeybees, characteristic of the European region, were selected and their sequences amplified with BEE2_1 were found in NCBI database. Nucleotides marked in red indicate single nucleotide polymorphisms (SNPs).

5.2.2.1 BEE2_1 PCR-HRM assay

The following section presents the PCR-HRM results obtained with the BEE2_1 assay and their interpretation. As it can be seen in Figure 16, Ct values of PCR products of selected honey and honeybee samples (HP56, HPBF1, HPBF4, HPBF5.1, HPBF5.1.1) ranged between 10 and 20. By changing the elongation temperature during real-time PCR from 72 °C to 65 °C, the amplification curves were improved, from a "zig-zag" (Figure 16A) shape to the normal expected amplification curve (Figure 16B).

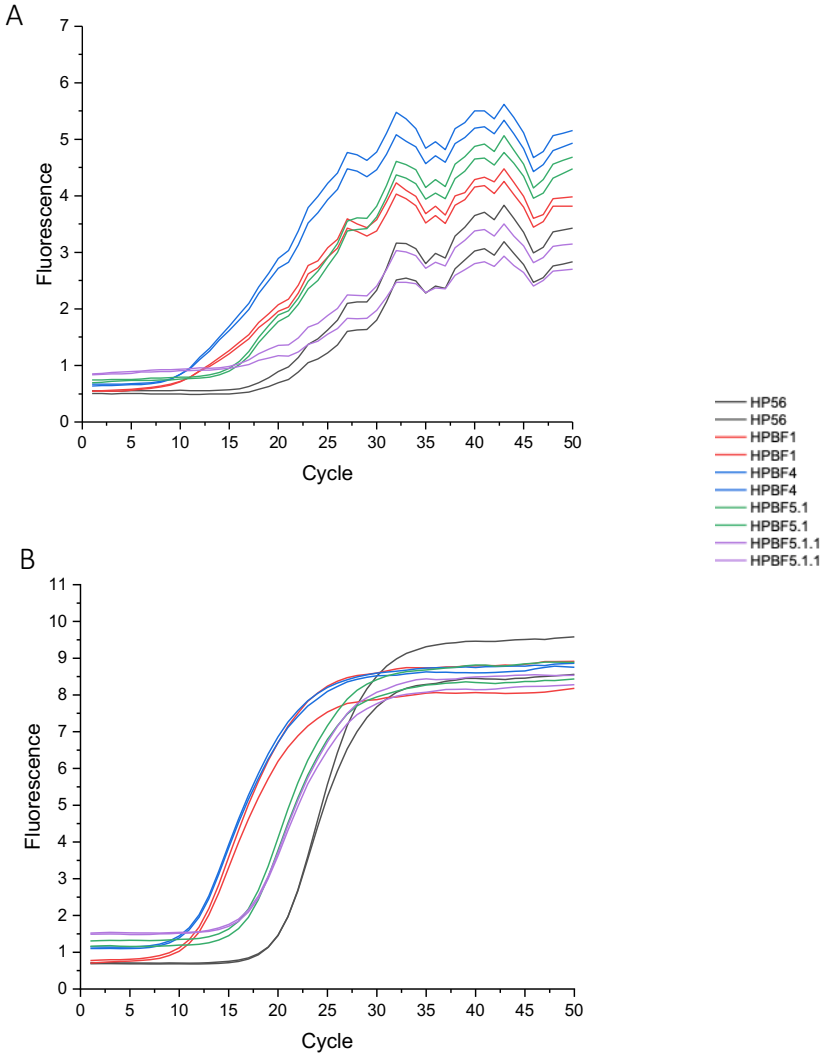

Figure 16 Amplification curves of PCR products from honey and honeybee samples (HP56, HPBF1, HPBF4, HPBF5.1, HPBF5.1.1) using the primer pair BEE2_1 at different elongation temperatures. Top: elongation at 72 °C, showing an unusual zig-zag curve. Bottom: elongation at 65 °C, producing the expected amplification curve.

The melting curves generated with primer pair BEE2_1 showed differences between various honeybee subspecies and honey samples, which was later confirmed by the PSQ results. These differences can be explained by biological origin. In honeybee subspecies, the mtDNA comes from individual bees, so that only one allele is present and the curve shows a single peak (homozygous). In contrast, honey samples contain DNA from many bees from different subspecies, resulting in a mixture of alleles that can produce additional peaks or changes in the melting curve. In addition, honey matrix effects can slightly shift the position of the peaks. Since the origin of many honey samples was diverse, different melt peaks were also observed (Figure 17–Figure 18). DNA extracts of honeybees *A. m. carnica* from Austria showed differences compared to honey samples from Austria, as the honey samples had an additional peak on the left (Figure 17), indicating a difference in DNA sequence. This pattern suggests the presence of multiple genetic subspecies in Austria.

In Figure 18A, a honey sample from Bosnia & Herzegovina (HP55) and a honeybee from the same region were compared. The melt peaks show similarity in both peak profile and melting temperature. The melting peaks of the honeybee from Bosnia were slightly shifted to the left compared to those of the honeybees from Austria, even though they belong to the same honeybee subspecies, *A. m. carnica*. This confirms that there are different genetic lines within the subspecies. In the case of Croatian honey (Figure 18B) and the honeybee from the same beekeeper, differences in melting curves were observed. The melting peaks (Figure 18C) of honey samples from Bulgaria and North Macedonia were comparable to those of *A. m. macedonica*. However, slight shifts were observed, likely due to matrix effects.

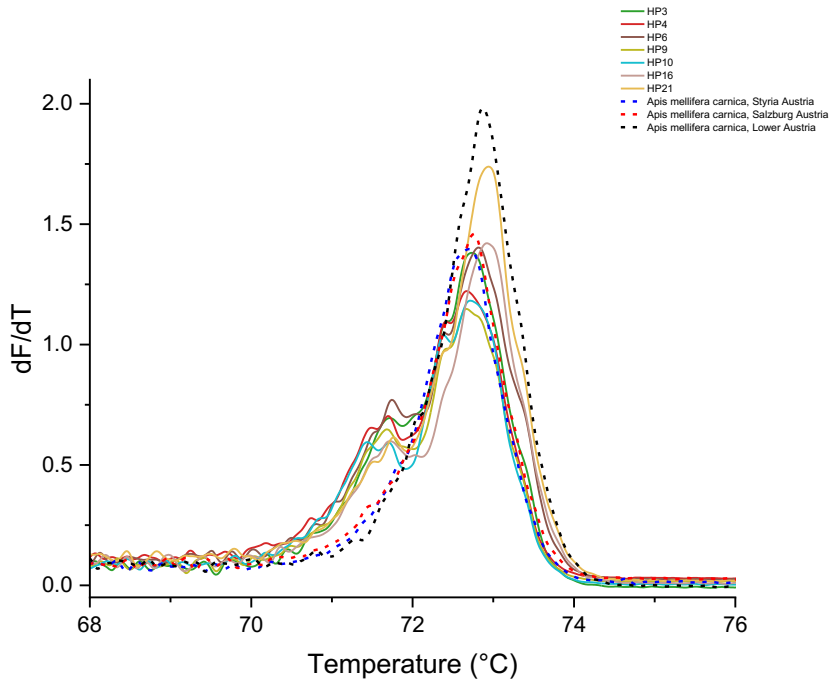

Figure 17 Melt curves of PCR products of honey samples HP3, HP4, HP6, HP9, HP10, HP16, HP21 (solid curves) from Austria and honeybee samples *A. m. carnica* (dashed curves) from different parts of Austria, obtained with primer pair BEE2_1.

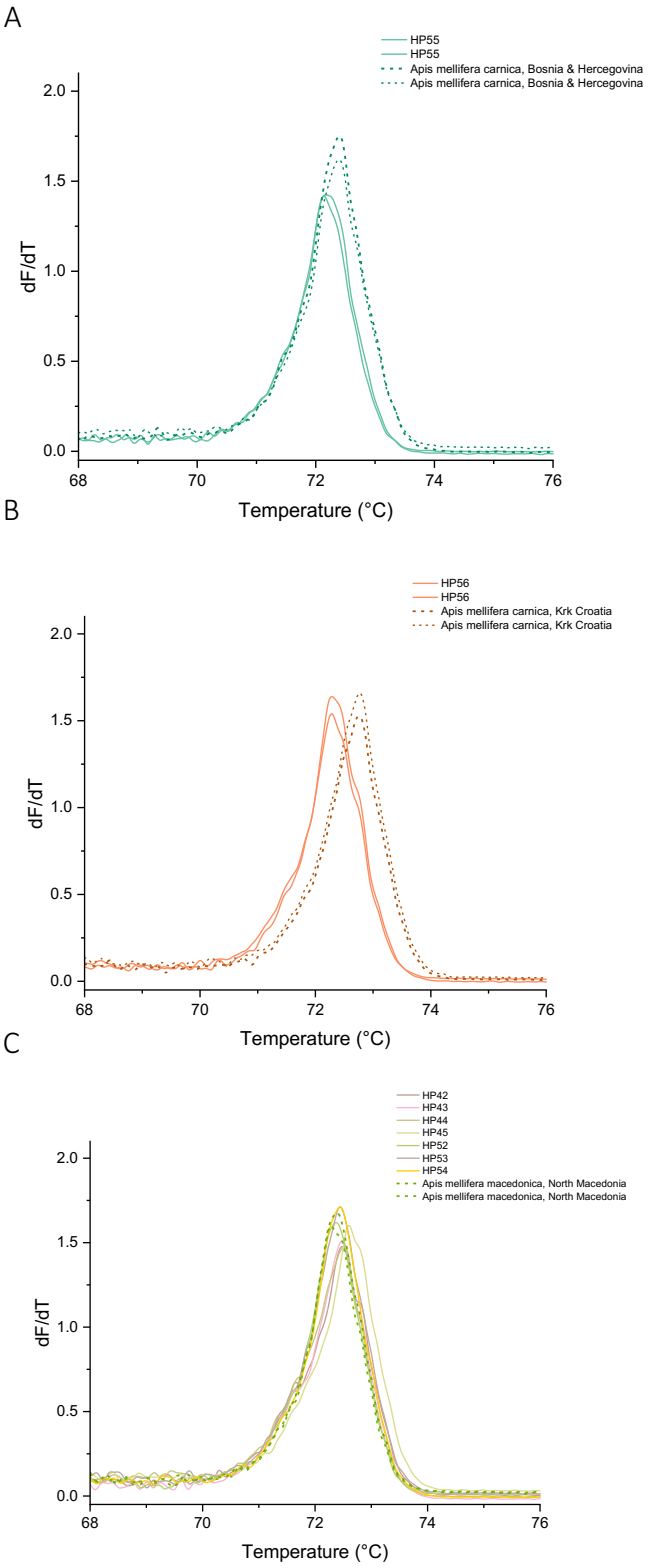

Figure 18 Melting curves of PCR products of selected honey samples (solid curves) compared to honeybee samples (dashed curves) from the same origin: (A) Honey sample (HP55) and *A. m. carnica* from the same beekeeper from Bosnia & Herzegovina, (B) Honey sample (HP56) and *A. m. carnica* from the same beekeeper from Krk, Croatia, (C) Honey samples (HP42, HP43, HP44, HP45, HP52, HP53, HP54) from North Macedonia and Bulgaria and *A. m. macedonica* from North Macedonia.

5.2.2.2 BEE2_1 PSQ assay

To better understand the variations in the melting curves, the PCR amplicons were analyzed by PSQ sequencing. In BEE2_1 amplicon there are four SNPs, and each of them can have two possible nucleotides. Considering all four SNPs together, there are several possible allele combinations. For example, one possible combination is A/G, C/T, C/T, C/T (Figure 15). Since there were no data about *A. m. macedonica* in NCBI BLAST, this honeybee subspecies from North Macedonia was included in analysis. PSQ results showed that *A. m. macedonica* has A C T C, same as *A. m. carnica,* which limited applicability of the assay. When obtaining bee samples from beekeepers in Austria, Croatia, and Bosnia & Herzegovina, the beekeepers, who were familiar with the subspecies, confirmed that it was *A. m. carnica*. By contrast, not all honeybee subspecies showed the expected sequence in PSQ and melting curves. After completing the analyses, results could lead to conclusion that some of the honeybee samples represented different types of *A. m. carnica*: the Alpine and the Pannonian *carnica*. For example, the first SNP shows variation between A and G, where the Alpine *carnica* carries the A allele, while the Pannonian *carnica* carries the G allele. Some other subspecies, however, share the same nucleotide combination across the four SNPs, which represents a limitation of this assay (Figure 15).

When comparing the PSQ results with the melting curves of PCR products generated using the primer pair BEE2_1, it became evident that distinct DNA sequences corresponded to distinct melting profiles. The findings reveal that *A. m. carnica* from different geographic origins differed at the first SNP (Figure 19). This variation was sufficient to produce a shift in the melting curve, explaining the observed differences in peak position between samples. Consequently, this may explain why honey samples from Austria showed an additional peak (Figure 17). In Austria, different types of *A. m. carnica* (PBF 1–6, HPBF1, HPBF5.1, HPBF5.2) exhibit variation at the first SNP, with either an A or G present (Figure 19). As honey contains DNA from multiple honeybee individuals, both nucleotide variants may be present, resulting in additional melting peak.

Honey samples from EU and non-EU countries were also analyzed in this study. These samples are mixtures of honey from different origins, resulting in the presence of DNA from multiple honeybee sources. The exact origin and proportion of each source are not yet required to be indicated on the label. The observed nucleotide differences at each SNP were confirmed by sequencing, which caused the PSQ device to display mostly yellow or red (Figure 21), as differences in nucleotides at each SNP caused the PSQ device to show mostly yellow or red signals. These color bars indicate the software limitations, as it is designed for the analysis of homogeneous biological samples and not for mixed DNA samples such as honey. Calculated nucleotide percentages at each SNP show a consistent mixture of nucleotide variants at each SNP.

Honey samples originating from Bulgaria and North Macedonia are expected to contain *A. m. macedonica*, and the sequencing results confirmed this (Figure 22) (35). The analysis showed that the first SNP in these samples contained only the nucleotide A. A limitation of this study is that honey samples from Bosnia & Herzegovina and Krk, Croatia showed the same results as those from Bulgaria and North Macedonia, although another honeybee subspecies should be present. It is important to note that the honey sample from Croatia (HP56) did not show the same DNA sequence as the positive control *A. m. carnica* from the same beekeeper. This may be attributed to differences in the honeybee population at the beekeeper's location or different origin of honey.

The following figures (Figure 19–Figure 22) present the sequencing results and the calculated nucleotide percentages by applying Equation 1 at each SNP in selected honey samples and honeybee amplicons generated using the primer pair BEE2_1. The heatmaps are displayed as a heat map with conditional formatting. Color intensity reflects the relative percentage of each nucleotide at a given SNP position. Darker shades indicate a higher proportion of the displayed nucleotide, while lighter shades indicate a lower proportion. Specifically, darker red corresponds to a greater percentage of that nucleotide among the samples, allowing for quick visual comparison of nucleotide abundance across SNP positions.

	SNP 1		SNP 2		SNP 3		SNP 4			
Sample ID	A (%)	G (%)	C (%)	T (%)	C (%)	T (%)	C (%)	T (%)	Subspecies	Origin
PBF 1	12.83	87.17	97.89	2.11	0.00	100.00	93.19	6.81	*Apis mellifera carnica*	Lower Austria
PBF 2	5.93	94.07	97.82	2.18	0.00	100.00	90.37	9.63	*Apis mellifera carnica*	Lower Austria
PBF 3	6.73	93.27	98.38	1.62	0.00	100.00	94.28	5.72	*Apis mellifera carnica*	Vienna, Austria
PBF 4	10.97	89.03	98.23	1.77	0.00	100.00	94.47	5.53	*Apis mellifera carnica*	Lower Austria
PBF 5	6.85	93.15	97.67	2.33	0.00	100.00	98.93	1.07	*Apis mellifera carnica*	Lower Austria
PBF 6	6.73	93.27	97.67	2.33	0.00	100.00	93.58	6.42	*Apis mellifera carnica*	Lower Austria
PBF 7	98.53	1.47	97.82	2.18	0.00	100.00	83.13	16.87	*Apis mellifera macedonica*	North Macedonia
HPBF 1	9.72	90.28	98.33	1.67	0.00	100.00	91.22	8.78	*Apis mellifera carnica*	Styria, Austria
HPBF 2	98.46	1.54	98.26	1.74	0.00	100.00	77.69	22.31	*Apis mellifera carnica*	Bosnia & Hercegovina
HPBF 3	98.78	1.22	97.84	2.16	0.00	100.00	81.55	18.45	*Apis mellifera carnica*	Bosnia & Hercegovina
HPBF 4	12.44	87.56	96.73	3.27	0.00	100.00	95.44	4.56	*Apis mellifera carnica*	Krk, Croatia
HPBF 5.1	7.13	92.87	97.82	2.18	0.00	100.00	91.78	8.22	*Apis mellifera carnica*	Salzburg, Austria
HPBF 5.2	98.67	1.33	97.87	2.13	0.00	100.00	86.95	13.05	*Apis mellifera carnica*	Salzburg, Austria

Figure 19 Sequencing results of honeybee samples amplified with primer BEE2_1. The percentage of each nucleotide at each SNP was calculated. According to the PSQ machine, the sequencing results were shown in blue, indicating that they are reliable.

	SNP 1		SNP 2		SNP 3		SNP 4			
Sample ID	A (%)	G (%)	C (%)	T (%)	C (%)	T (%)	C (%)	T (%)	Honeytype	Origin
HP3	72.18	27.82	98.23	1.77	0.00	100.00	91.82	8.18	Forest honey	Austria
HP4	54.93	45.07	97.82	2.18	0.00	100.00	97.09	2.91	Forest honey	Austria
HP6	64.47	35.53	97.93	2.07	0.00	100.00	94.62	5.38	Forest honey	Austria
HP9	54.81	45.19	97.99	2.01	0.00	100.00	90.35	9.65	Forest honey	Austria
HP10	40.14	59.86	97.61	2.39	0.00	100.00	90.19	9.81	Organic pine honey	Austria
HP16	33.52	66.48	98.23	1.77	0.00	100.00	97.15	2.85	Organic forest honey	Austria
HP21	16.57	83.43	97.64	2.36	0.00	100.00	95.04	4.96	Forest honey	Austria

Figure 20 Sequencing results of selected honey samples declared to originate from Austria.

	SNP1		SNP2		SNP3		SNP4			
Sample ID	%(A)	%(G)	%C	%(T)	%C	%(T)	%C	%(T)	Honey type	Origin
HP1	54.44	45.56	63.82	36.18	29.30	70.70	70.02	29.98	Forest honey	EU and non-EU countries
HP2	66.96	33.04	68.02	31.98	22.38	77.62	82.52	17.48	Forest honey	EU and non-EU countries
HP7	65.84	34.16	80.43	19.57	13.19	86.81	71.66	28.34	Organic forest honey	Romania
HP13	49.36	50.64	64.10	35.90	29.91	70.09	64.85	35.15	Organic forest honey	Germany
HP18	79.04	20.96	46.10	53.90	44.62	55.38	83.46	16.54	Forest- and flower honey	EU and non-EU countries
HP22	46.80	53.20	74.31	25.69	17.83	82.17	80.06	19.94	Forest honey	EU and non-EU countries
HP23	40.91	59.09	76.33	23.67	14.71	85.29	69.21	30.79	Forest honey	EU and non-EU countries
HP24	45.59	54.41	63.97	36.03	28.32	71.68	62.24	37.76	Forest honey	EU and non-EU countries
HP30	84.48	15.52	72.73	27.27	19.79	80.21	65.63	34.37	Forest honey	Germany

Figure 21 Sequencing results of selected honey samples, which are mostly declared as mixtures from different countries (EU and non-EU countries).

	SNP 1		SNP 2		SNP 3		SNP 4			
Sample ID	A (%)	G (%)	C (%)	T (%)	C (%)	T (%)	C (%)	T (%)	Honeytype	Origin
HP42	88.76	11.24	98.02	1.98	0.00	100.00	86.59	13.41	Honey dew honey	Bulgaria
HP43	89.16	10.84	97.24	2.76	0.00	100.00	80.69	19.31	Organic honey dew honey	Bulgaria
HP44	93.12	6.88	92.03	7.97	3.40	96.60	79.94	20.06	Organic acacia honey	Bulgaria
HP45	94.73	5.27	97.58	2.42	0.00	100.00	83.92	16.08	Organic linden honey	Bulgaria
HP52	97.37	2.63	98.05	1.95	0.00	100.00	78.37	21.63	Forest honey	North Macedonia
HP53	98.56	1.44	98.10	1.90	0.00	100.00	84.43	15.57	Forest honey	North Macedonia
HP54	98.93	1.07	98.25	1.75	0.00	100.00	81.58	18.42	Field honey	North Macedonia
HP55	99.07	0.93	97.01	2.99	0.00	100.00	74.16	25.84	Mixed blossom honey	Bosnia & Hercegovina
HP56	98.56	1.44	96.21	3.79	0.00	100.00	94.16	5.84	Sage honey	Krk, Croatia

Figure 22 Sequencing results of selected honey samples declared to originate from Bulgaria, North Macedonia, Bosnia and Herzegovina, and Croatia.

The presence of different SNPs within the amplified sequence can be distinguished by distinct melting profiles and melting temperatures, which is shown in Figure 23. PSQ results support the interpretation of the HRM data by confirming the nucleotide composition of the analyzed region. All SNPs in samples HP42 and HP55 show a single distinct melting peak, indicating the presence of one predominant allele. In contrast, HP6 and HP24 display additional peaks, suggesting the presence of multiple alleles. For HP6, this pattern is consistent with the presence of two alleles at SNP1 (A and G), whereas HP24 shows evidence of multiple alleles across all analyzed SNPs, likely reflecting the mixed origin of EU and non-EU honeys (Figure 20,Figure 21). A detailed examination of the PSQ results reveals that HP42 exhibits a higher proportion of G at SNP1 compared to HP55, which may account for the slightly higher melting temperature of the HP42 product (Figure 22).

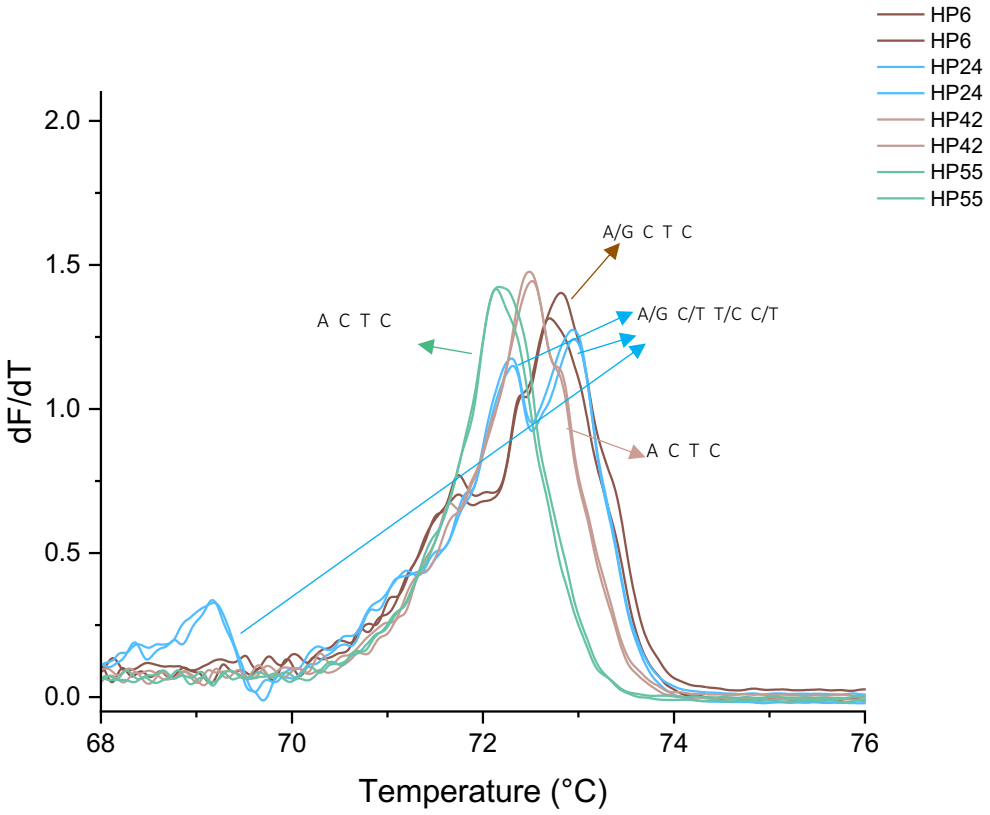

Figure 23 Melting curves of PCR products of four honey samples (HP6, HP24, HP42, HP55) obtained with the primer pair BEE2_1. All four SNPs of honey samples HP42 and HP55 show a single distinct peak, indicating the presence of one predominant allele, although the melting temperatures differ slightly. In contrast, samples HP6 and HP24 display additional peaks, suggesting the presence of multiple alleles.

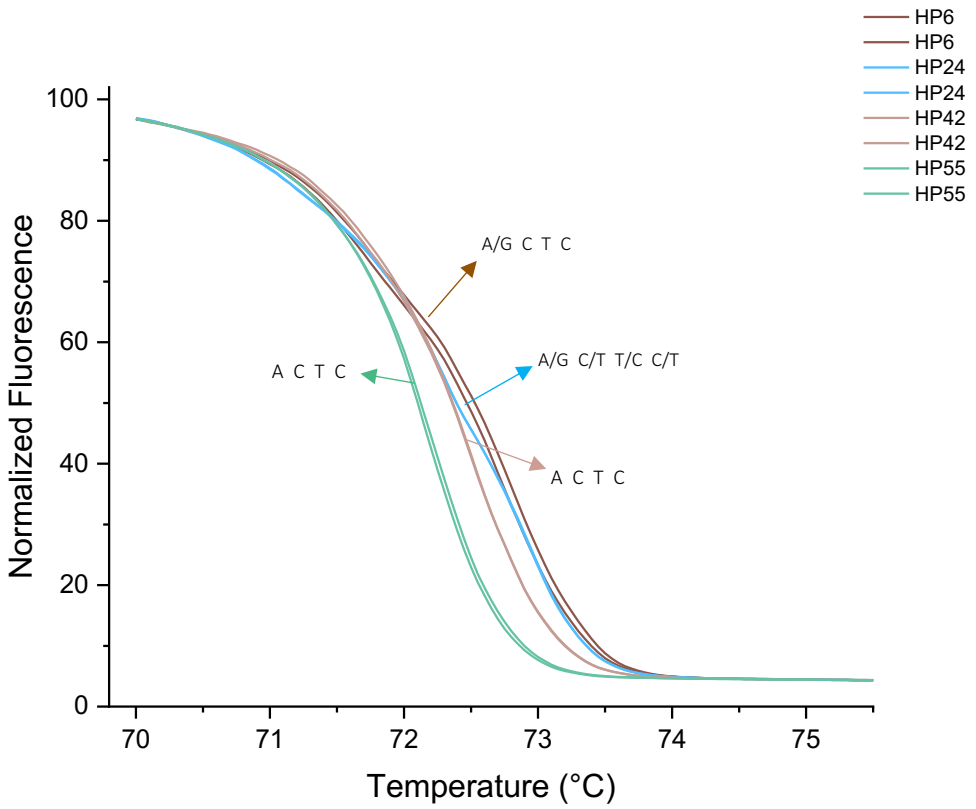

Figure 24 Normalized melting curves of PCR products obtained from four honey samples (HP6, HP24, HP42, and HP55) with assay BEE2_1, demonstrating slight differences in melting curves indicative of sequence variation among samples.

The BEE2_1 assay proved to be a suitable tool for distinguishing honeybee subspecies based on SNP-specific melting profiles. The combination of HRM analysis and PSQ sequencing demonstrated that single nucleotide variations directly correspond to distinct melting profiles. Therefore, the assay enables the discrimination between various honeybee subspecies, but at the same time allows the identification of mixed patterns in honey samples. However, the assay also has limitations. Some honeybee subspecies (e.g. Alpine *carnica* and *A.m. macedonica*) share same SNP combinations and therefore cannot be differentiated using this marker.

5.2.3 Ins_1 assay

Austrian Agency for Health and Food Safety (AGES) designed the primer Ins for DNA metabarcoding of insects (77). In master thesis of Michaela Wildbacher from WG Cichna, this primer pair was applied for the HRM analysis of different insects in food (81). Primer pair Ins targets the COI gene region. To further investigate the variability of the DNA barcode in honeybee subspecies, the target sequence was analyzed using the NCBI BLAST tool, and a new primer pair Ins_1 was designed within the same region, reducing the amplicon length by 74 bp (Figure 25). The newly designed primer pair Ins_1 was tested *in silico* and subsequently applied in PCR-HRM analysis. Because the newly designed amplicon contained two SNPs, relevant for the discrimination of honeybee subspecies, a sequencing primer was also designed and tested *in silico*, and the reverse primer was ordered in a biotinylated form to enable PSQ analysis of the PCR products.

Ins amplicon (198 bp) (77)

TWACGCTGTTATCCCTAAGGTAATTTATTCTTTTAATTACAATTTATAATTCAAAAAATTATCTTTAT
ATCAAAATTAAATCTTAAATAAAGTTTATTAAATTTACCAATCCTCCCAATCAAATTTAATCTTAAAT
ATATTTATTAAAATTATAAATAAATTTAAAAATTAAATTAAATTCTATAGGGTCTTATCGTC

Ins_1	Sequence	Tm (°C)
Ins_1 fwd	CTGTTATCCCTAAGGTAATTTAT	56.0
Ins_1 biorev	ATTAAATTTGATTGGGAGGATTG	56.0
Ins_1 seq	ATTCTTTTAATTACAATT	36.0

Ins_1 amplicon (124 bp)

CTGTTATCCCTAAGGTAATTTATTCTTTTAATTACAATTTATAATTCAAAAAATTATCTTTATATCAAA
ATTAAATCTTAAATAAAGTTTATTAAATTTACCAATCCTCCCAATCAAATTTAAT

Figure 25 *In silico* characteristics of the modified primer pair Ins_1 for *A. mellifera*. The table shows primer sequences and their melting temperature (Tm); The full sequences of Ins (top) and modified Ins_1 amplicon (bottom) are presented: blue: the forward (fwd), orange: sequencing (seq), and yellow: reverse (rev) primer. W indicates a degenerate nucleotide position representing A or T.

5.2.3.1 Ins_1 PCR-HRM assay

A universal insect primer pair, Ins, was initially applied to honeybee samples (HPBF1, PBF1.1, PBF5.1, PBF7.1) and selected honey samples (HP1, HP5, HP6, HP7). The resulting PCR products were analyzed using melting curve analysis, which revealed distinct melting peaks for different samples. Three different elongation temperatures were also tested to evaluate how the melt curves of PCR products varied among the honey and honeybee samples. This was done because, at an elongation temperature of 72 °C, the PCR products produced melting peaks around 70 °C, and we wanted to assess how the amplification and corresponding melt curves would behave at lower elongation temperatures. At the higher elongation temperature (72 °C), some non-specific products were amplified in samples HP1, HP6, and HP7, indicated by an additional peak at a higher temperature

(Figure 26A). At lower elongation temperatures, the PCR product melt peaks of HP1 and HP7 (Figure 26C) corresponded to the region expected for *A. m. carnica*. In contrast, HP6 still displayed a second peak even at lower elongation temperatures, suggesting that this honey contains DNA from other insect species, as expected, since this method was designed for metabarcoding of insects in food. For comparison, four honey samples *A. m. carnica* from Austria were also included and their PCR product melt peaks matched the same temperature region.

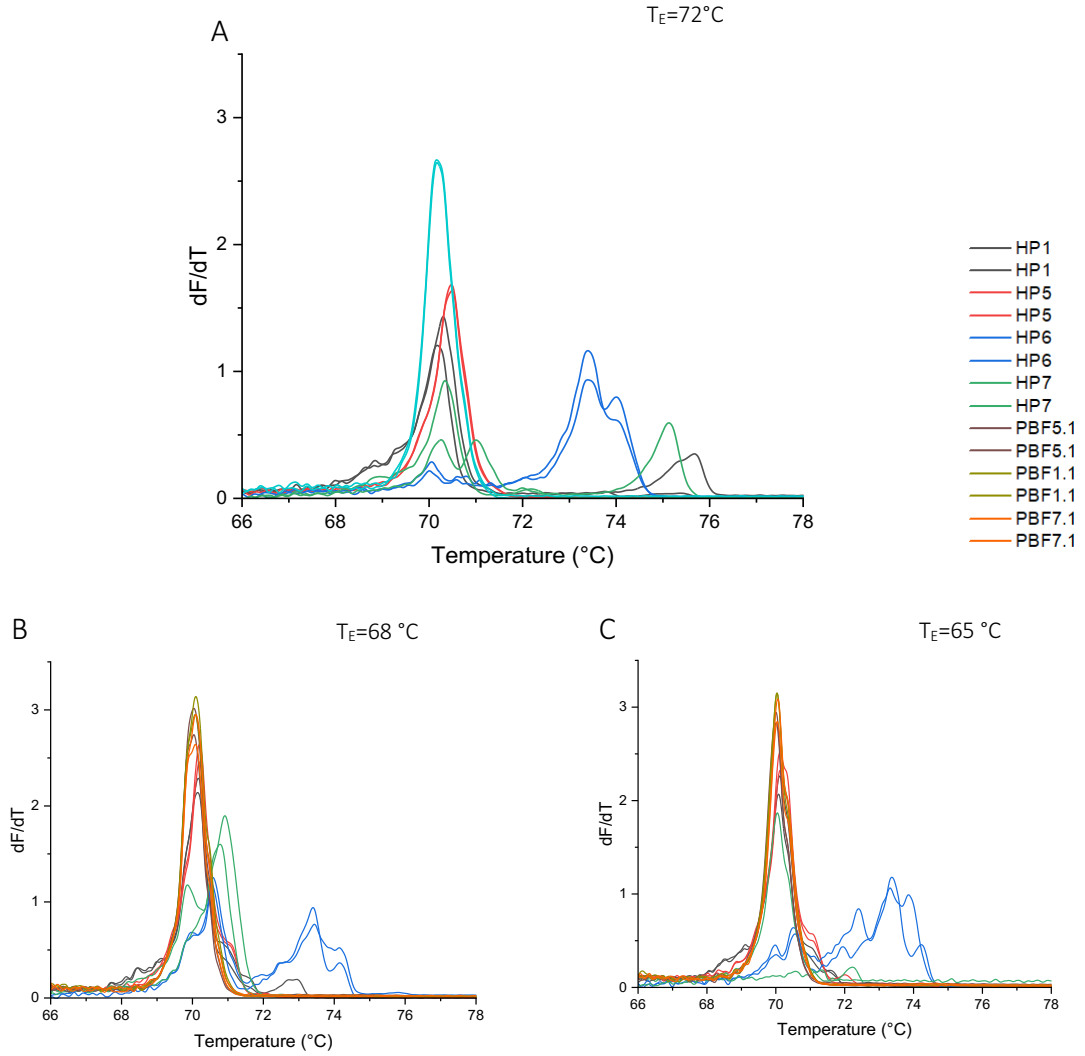

Figure 26 Melting curves of PCR products obtained with the universal insect primer pair Ins from selected honey samples (HP1, HP5, HP6, HP7) and honeybee samples (HPBF1, PBF1.1, PBF5.1, and PBF7.1) at different elongation temperatures (T_E).

Using the modified primer pair Ins_1, the PCR product melt curves of the honey sample HP6 did not show the additional peak observed with the original primer pair Ins, indicating that this modification improved specificity and minimized amplification of non-target DNA. Melting curves of PCR products of honeybee subspecies and selected honey samples in Figure 27–29 are shown as a single representative curve per sample to improve clarity and facilitate interpretation, although all samples were analyzed in duplicate and showed good reproducibility.

The HRM analysis using the Ins_1 primer assay showed that the melting curves of PCR products of all honeybee subspecies *A. m. carnica* and *A. m. macedonica* were identical (Figure 27), despite analyzing different honeybee subspecies, confirmed by BEE2_1 assay. Some honey samples originating from EU and non-EU countries (HP1, HP17, HP22); Austria (HP15, HP20); Turkey (HP25); and Greece (HP29) and therefore likely from different honeybee subspecies, exhibited slightly different melting curves (Figure 28) compared to *A. m. carnica* from Styria, Austria (HPBF1).

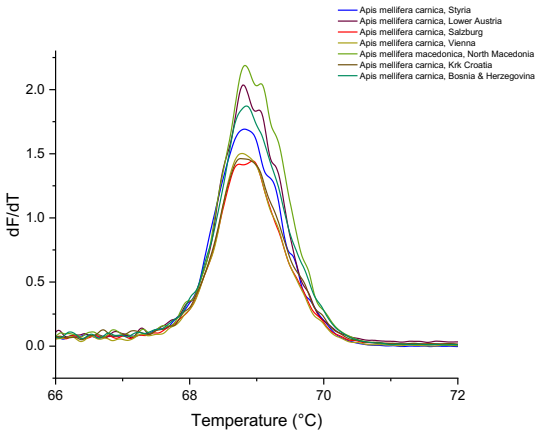

Figure 27 Melting curves of PCR products of honeybee subspecies *A. m. carnica* and *A. m. macedonica* obtained with the primer pair Ins_1. The melting profiles are very similar for all honeybee samples.

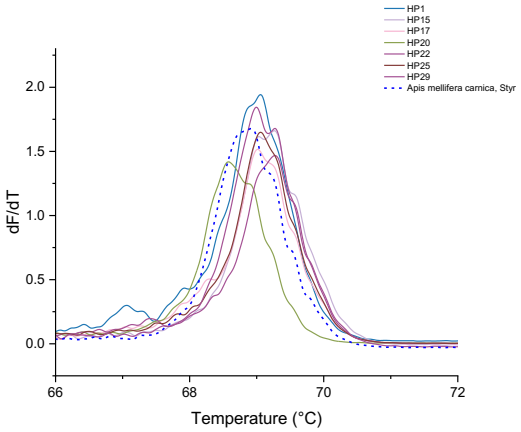

Figure 28 Melting curves of PCR products of honey samples HP1, HP15, HP17, HP20, HP22, HP25, HP29 (solid curve) obtained with the primer pair Ins_1. Some honey samples show differences in melting temperature and melting curve shape compared to *A. m. carnica* from Styria, Austria (dashed curve).

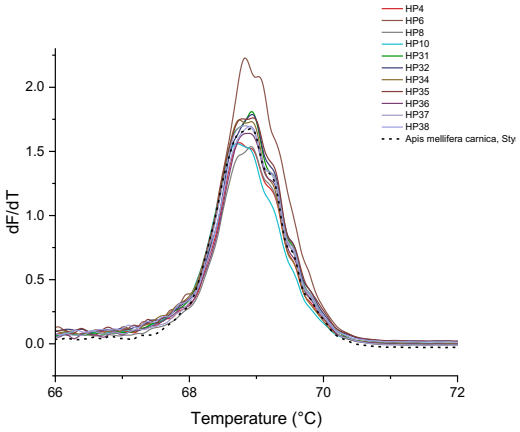

Figure 29 Melting curves of PCR products of honey samples HP4, HP6, HP8, HP10, HP31, HP32, HP34, HP35, HP36, HP37, HP38 (solid curve) obtained with the primer pair Ins_1. All samples have a similar melting profile and temperature compared to *A. m. carnica* from Styria, Austria (dashed curve).

5.2.3.2 Ins_1 PSQ assay

To facilitate interpretation of the melting curves, selected amplicons from honey and honeybee samples (HP1, HP5, HP6, HP7, PBF1.1, PBF7.1) were sequenced using PSQ technique. The presence of two SNPs in the amplified sequence appeared promising for distinguishing between honeybee subspecies. However, at the second SNP position, three different nucleotides were detected in honey samples due to the mixture of DNA from multiple honeybees (Table 9). This mixed signal caused a challenge for the PSQ software, causing the presence of red warning boxes in the results, and was observed not only in honey samples but also in individual bee samples (Figure 30).

Table 9 The variation of nucleotides of two SNPs in DNA sequence from honeybee amplified with the primer pair Ins_1, using NCBI Blast.

SNP	*A. m. carnica / carpatica/ligustica/caucasica*	*A. m. iberiensis/ mellifera*	*A. m.anatoliaca*	*A. m. intermissa*
1	A	G	A	A
2	C	T	A	T

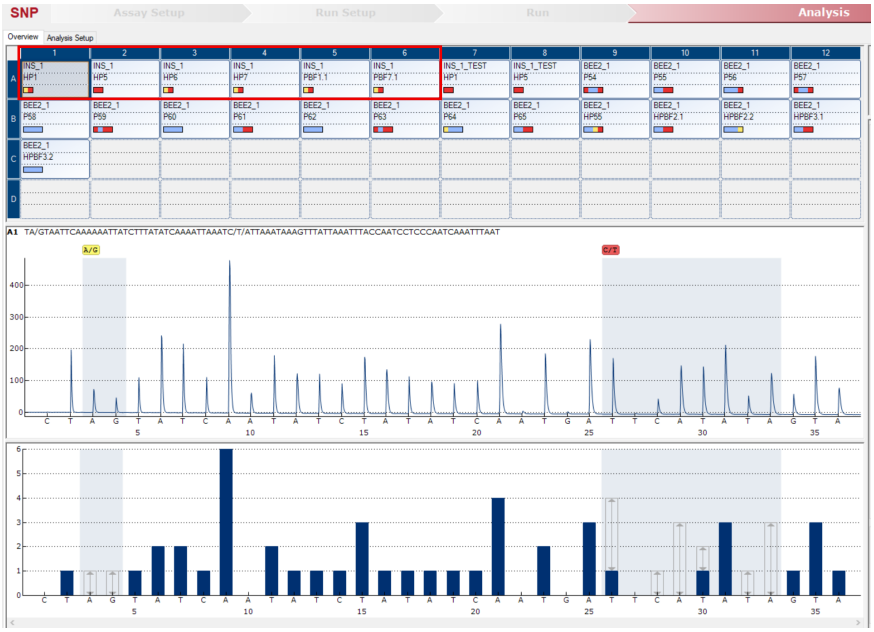

Figure 30 Screenshot of a PSQ run file demonstrating SNP analysis for selected honey samples and *A. m. carnica* amplified with primer Ins_1. The presence of red boxes indicates unreliable results.

The redesigned primer pair Ins_1 seemed promising, since amplicon contained two SNPs, which increased the potential of the HRM assay and suggested that the method could enable differentiation of certain honeybee subspecies. However, a limitation was observed, as specific SNP combinations were shared among some subspecies (e.g. *A. m. carnica* and *A. m. ligustica*), preventing their clear discrimination. This represents a limitation of the present study, particularly because the available bee and honey samples originated from these closely related subspecies. Additionally, three possible nucleotides at the second SNP produced mixed signals, leading to red warning boxes in the PSQ software for both honey and honeybee samples.

5.2 Plant DNA barcoding assays for distinguishing between plants

A set of plant species (n = 20) that could be included in the composition of the honey samples was selected and ordered online as leaves or seeds and used as positive controls. DNA from these plants was extracted. The concentrations of DNA extracts from positive controls are presented in Table S1. Due to the relatively high DNA concentrations in the positive controls, all extracts were diluted to a final concentration of 2.5 ng/µL. For honey samples, extracts with concentrations above 2.5 ng/µL were similarly diluted to 2.5 ng/µL, whereas samples with lower concentrations were used undiluted. Honey and pollen extracts provided by AGES (H1–H16, P1–P16) were analyzed using DNA metabarcoding by colleagues at AGES. The metabarcoding analysis identified the predominant pollen types present in each honey sample. These results were subsequently used as a reference to evaluate and validate the PCR-HRM method, allowing a direct comparison between the high-throughput sequencing data and the HRM-based pollen identification. The PCR-HRM assays PL1, PL2_1, and PL3_1 target specific DNA barcode regions commonly used for plant species identification: rbcL (PL1, PL3_1), and ITS2 (PL2_1). These barcode regions served as target sequence for evaluating HRM-based discrimination, allowing a direct comparison.

5.2.1 PL1 PCR-HRM assay

The primer pair PL1 was taken from literature (29), tested *in silico* and used in PCR-HRM analysis. The PL1 assay targets the rbcL gene region. According to Borkowska *et al.* the quantity and quality of DNA extracts from honey varies greatly and depends on the "degree of pollination"; how rich the honey is in pollen grains. This means that the efficiency of PCR is highly dependent on how much pollen is present and how its DNA is preserved in the honey. The plastid gene rbcL was chosen as the most suitable target marker for distinguishing plant species in honey compared to some nuclear markers. In addition, sequencing of the rbcL region confirmed the interpretation of the HRM curve, meaning that the HRM profile can reliably reflect genetic differences. Real-time PCR-HRM successfully classified different types of honey (acacia, linden, buckwheat, rapeseed, heather) according to their botanical origin (29).

The PCR-HRM analysis of rbcL region was conducted on DNA extracts obtained from honey samples (HP1–HP56, H1–H16, P1–P16) and selected plants. Selected plants showed successful amplification of rbcL fragment with PL1 assay (Figure 31). The selected honey samples shown in Figure 32 demonstrate that the amplification occurred later and the Ct values were higher compared to plants. As shown in Figure 33, six groups of plants which served as positive controls were identified based on their melting curves. Groups A–E comprise positive controls whose PCR products exhibit the same melting temperature and highly similar melting curve profiles. Group F includes positive controls whose PCR products did not show similarity in melting curves compared to the other groups. Ct values calculated using Rotorgene software are presented in Table S4.

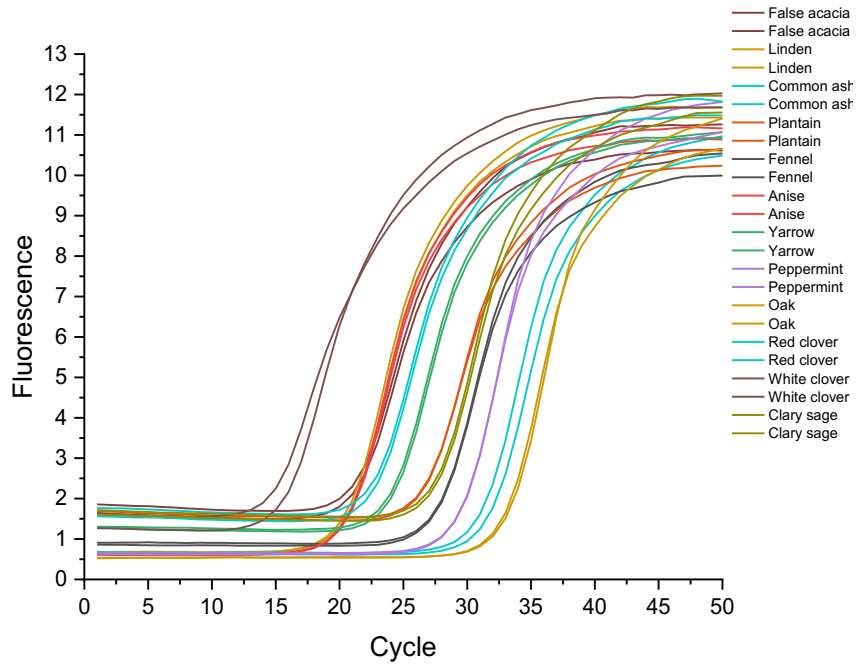

Figure 31 Amplification curves of PCR products of selected positive controls (false acacia, linden, common ash, plantain, fennel, anise, yarrow, peppermint, oak, red clover, white clover and clary sage) obtained with the primer pair PL1. Repeatability was satisfactory.

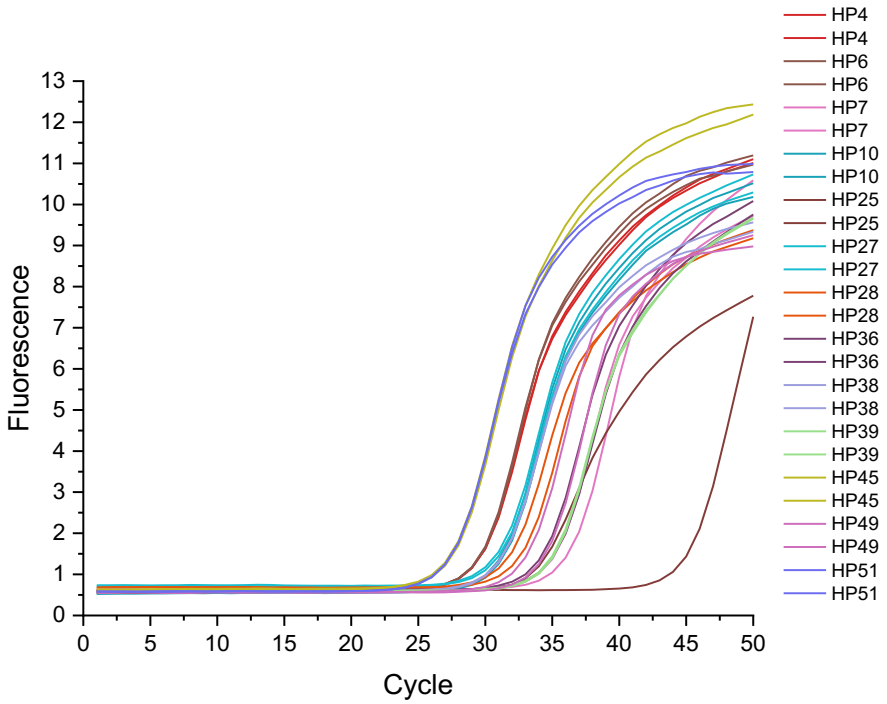

Figure 32 Amplification curves of PCR products of selected honey samples: forest honey (HP4, HP6, HP7, HP10, HP25, HP27, HP28); acacia honey (HP39, HP44, HP49), linden honey (HP38, HP45, HP51) and fennel honey (HP36) obtained with the primer pair PL1. Repeatability was satisfactory in most cases. Ct values were generally above 25.

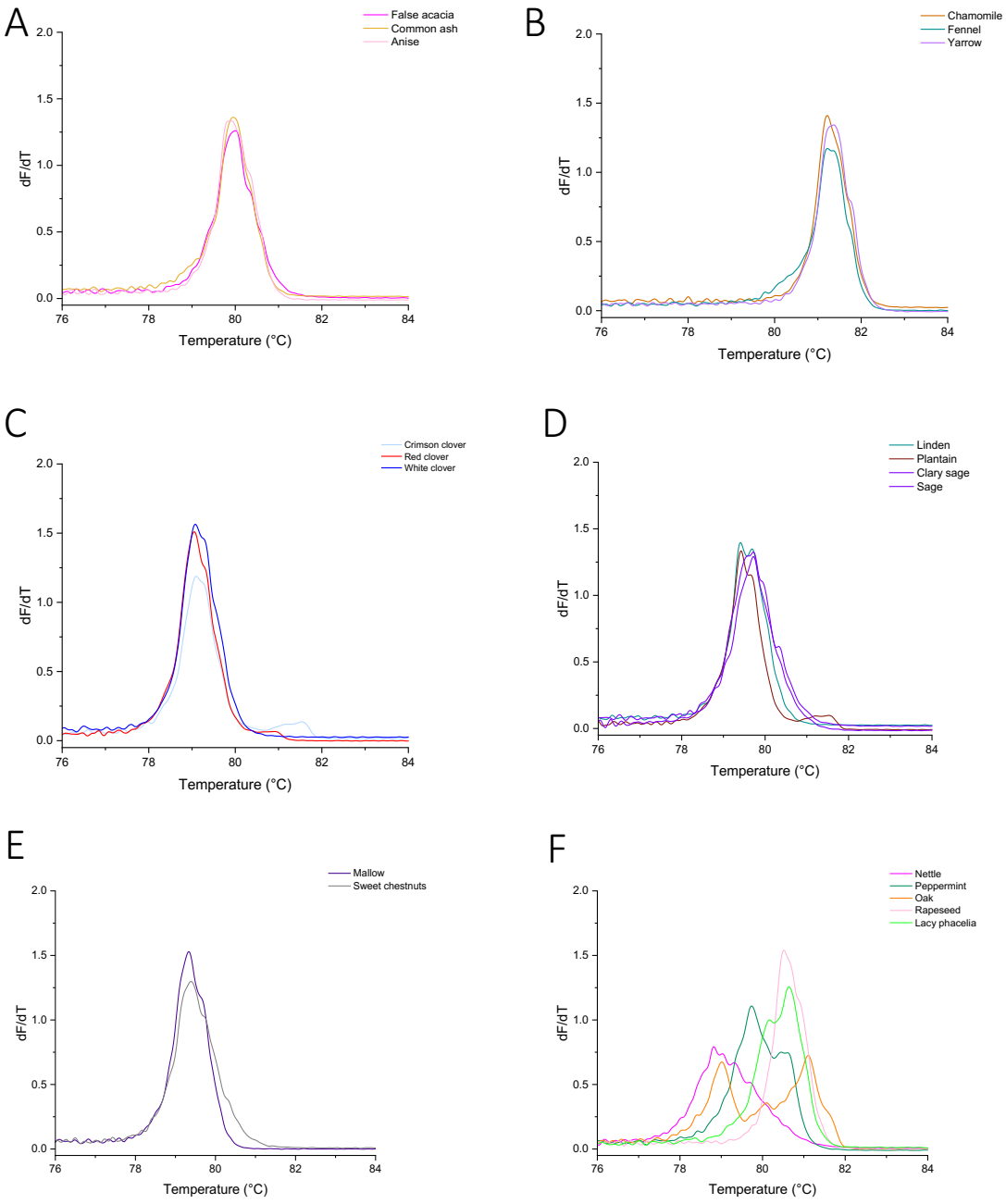

Figure 33 Melting curves of PCR products obtained from positive controls using primer pair PL1. Based on melting curve profiles, six groups (A–F) were distinguished: Group A includes false acacia, common ash, and anise; Group B includes chamomile, fennel, and yarrow; Group C includes crimson, red, and white clover; Group D includes linden, plantain, and different sage samples; Group E includes mallow bloom and sweet chestnut; and Group F includes nettle, peppermint, oak, and lacy phacelia. For improved clarity and visualization, only one representative replicate per sample is shown; all measurements were performed in duplicate and showed good reproducibility.

The following figures (Figure 34–Figure 39) present the comparative analysis of melting curves of PCR products obtained from honey (H) and corresponding pollen (P) samples from AGES, using primer pair PL1. Positive controls are shown as dashed curves, while honey (red) and pollen (black) are shown as solid curves. According to the results provided by AGES, where botanical composition was determined using DNA metabarcoding, predominant plant families od plant species were identified for each sample. Our melt curve analysis largely confirmed the presence of the predominant taxa reported by metabarcoding, as several honey-pollen pairs (H2/P2, H3/P3, H14/P14, H16/P16) exhibited melting profiles like the corresponding positive controls DNA extracts. In certain cases (H8/P8 and H10/P10), although the melt peaks were slightly shifted or did not fully correspond to the expected positive control profile, they remained within a comparable melting temperature range, suggesting genetic similarity but not complete identity. Overall, the results indicate partial concordance between DNA metabarcoding data and melt curve analysis.

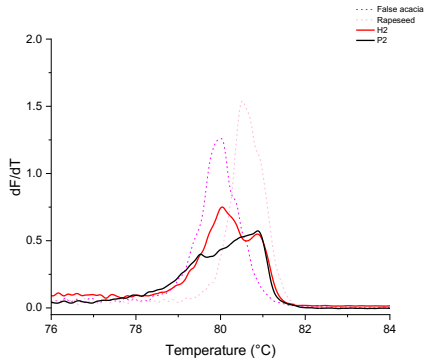

Figure 34 The melting curves of PCR products obtained using assay PL1 indicate the presence of both false acacia and rape profiles in the acacia honey and corresponding pollen samples (H2/P2).

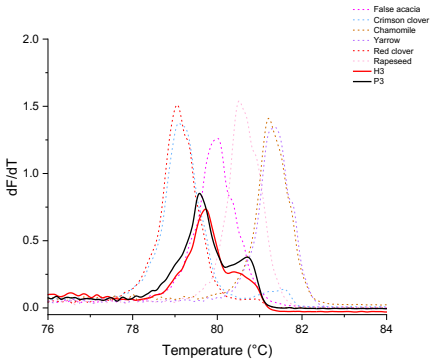

Figure 35 The melting curves of PCR products obtained using PL1 show similarity between herbal honey/pollen (H3/P3) and false acacia, crimson and red clover, while PCR products of chamomile and yarrow melt in a different region.

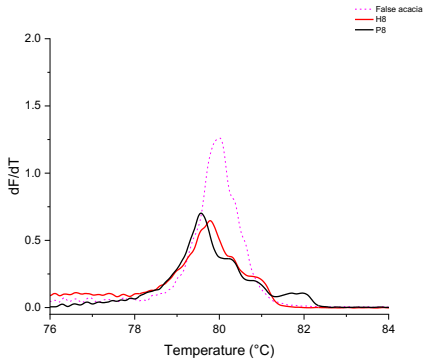

Figure 36 Melting curve analysis of PCR products generated with assay PL1 from blossom honey and pollen (H8/P8) revealed identical profiles, which are shifted to lower melting temperatures relative to the false acacia.

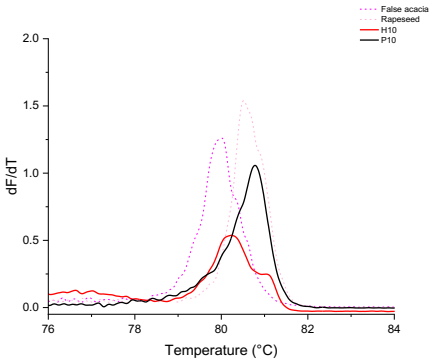

Figure 37 The melting curves of PCR products of rape honey and pollen (H10/P10) obtained with PL1 are not same as expected, but they melt in the same range as the positive controls (false acacia and rapeseed).

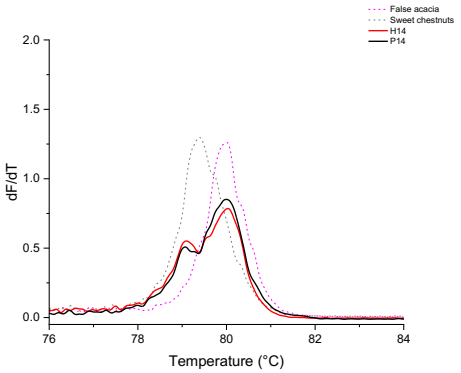

Figure 38 The melting curves of PCR products obtained with PL1 from chestnut honey and the corresponding pollen sample (H14/P14) are highly similar and closely match the positive control profile.

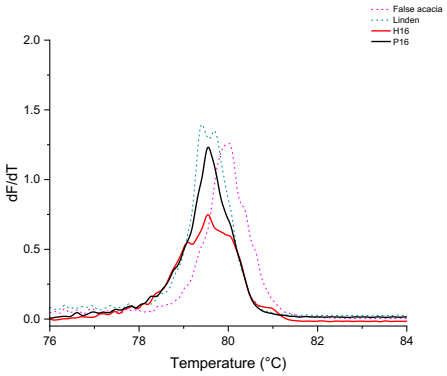

Figure 39 Melting curve analysis of PCR products from linden blossom honey and pollen (H16/P16) using PL1 assay revealed melting profiles corresponding to both false acacia and linden patterns.

In addition, honey samples (HP1–HP56) showed similar melting curves between the honey samples and positive controls. Since there were many mixed honey types such as forest honey (e.g. HP1, HP4, HP6, HP10) or blossom honey (e.g. HP39, HP48, HP55), it was challenging to obtain a comprehensive insight into the plant profile, as the melting profiles were relatively complex and the melt peaks could not always be clearly assigned to specific plant species. It should also be noted that many plant species that could theoretically be present in honey samples were not included as positive controls. Therefore, a clear taxonomic assignment of all detected melting peaks was not always possible.

Due to the very low concentration of DNA (≤ 0.1 ng/µL, Table S1) in the extracts of acacia honey, PCR amplification was not consistently repeatable (Figure 40). This low DNA yield likely limited the detection of plant species whose DNA may theoretically be present in honey samples.

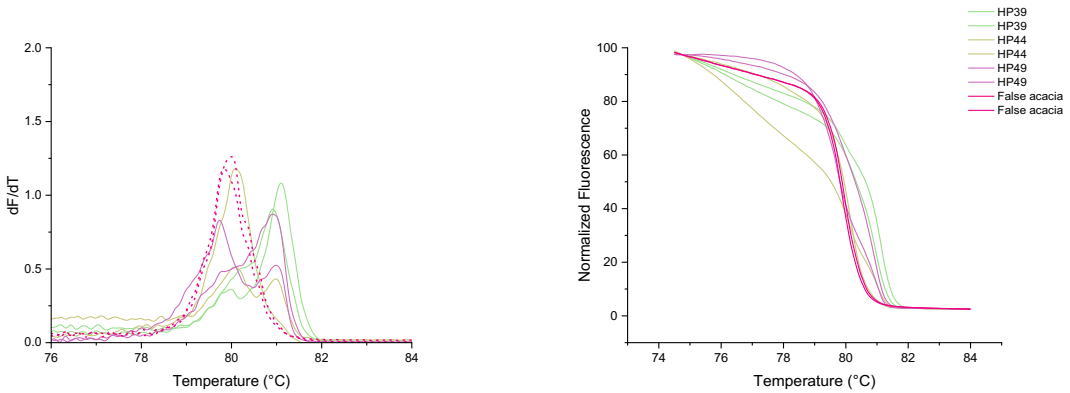

Figure 40 The melting curves (left) and normalized melting curve (right) of PCR products generated with assay PL1 from acacia honey and false acacia.

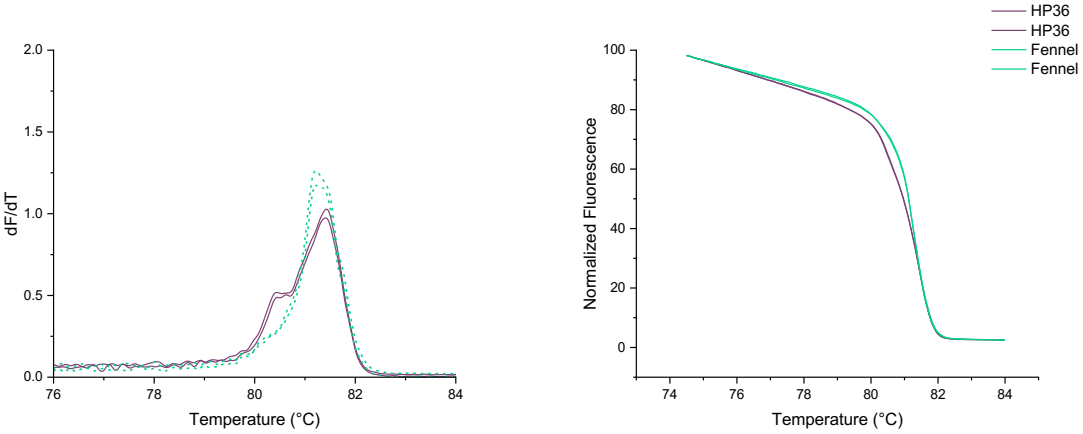

Figure 41 The melting curves (left) and normalized melting curves (right) of the honey sample containing fennel (HP36) show a main peak that overlaps with the fennel peak, indicating the presence of fennel DNA. in melting profile. An additional peak is also observed, suggesting the presence of DNA from other plant sources detected by the PL1 method.

Melting peaks of the PCR products obtained with the PL1 assay suggest the presence of plants such as common ash, oak, and sweet chestnut, which are typically found in forest honey (Figure 42). All honey samples showed double peaks at different temperatures, suggesting the presence of more than one plant species in the forest honey. The results obtained with assay PL1 suggest that the honey sample HP4 (forest honey) contains common ash. The two melting peaks obtained for sample HP6 (forest honey) hint at the presence of sweet chestnut and common ash. For sample HP7 (forest honey), the melting peaks of the PCR products are consistent with oak, while HP10 (pine honey) shows peaks suggesting the presence of sweet chestnut and oak. As many potential plant species that could be present in forest honey were not analyzed, these results cannot be considered fully reliable.

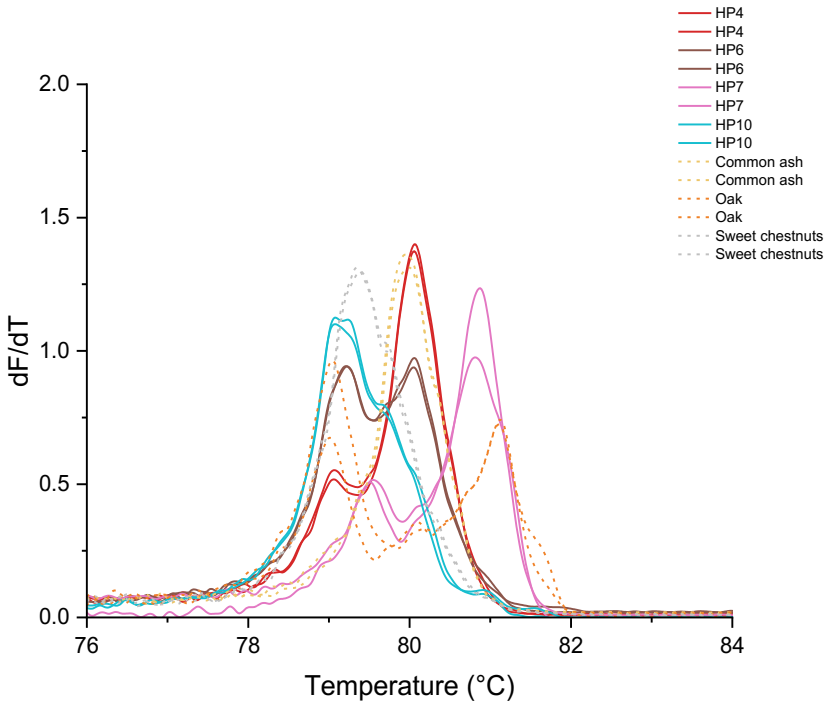

Figure 42 Comparison of melting curves of PCR products generated with the primer pair PL1 from different forest honey samples (HP4, HP6, HP7, HP10) and selected positive controls (common ash, oak, sweet chestnut).

Several linden honey samples exhibited melting curves closely matching those obtained from the linden as it can be seen in Figure 43. The similarity in curve shape and melting temperature suggests the presence of a dominant botanical source consistent with the declared floral origin. Samples HP45 and HP51 resulted in similar melting profiles, although the melting temperature of HP45 is slightly shifted to the right. PCR product of sample HP38 had a melting temperature close to that of the positive control, but its curve shape differs from the control, displaying an additional peak that suggests the presence of DNA from another plant species.

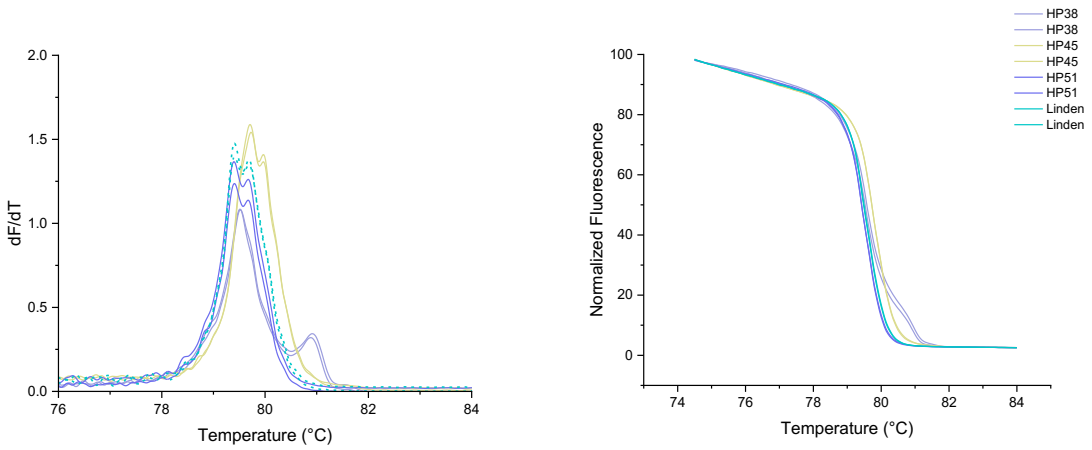

Figure 43 The melting curves (left) and normalized melting curves (right) of PCR products from linden honey (HP38, HP45, HP51) and linden generated with the primer pair PL1.

Compared to the melt curve of the PCR product generated with PL1 from sage, forest honey containing sage (HP28) and the sage honey samples (HP56) showed different melting profiles: the peaks were shifted to higher temperatures. For example, samples HP56 and the sage, although both from the same geographic origin (Krk, Croatia) exhibited different melting temperatures. Sample HP28 showed a small peak near the positive control, while the main peak was shifted to the right, consistent with its declaration as forest honey containing sage. Peak shifts and additional peaks suggest that the honey matrix affects the analysis, likely due to interactions with other compounds, or the presence of multiple plant DNAs.

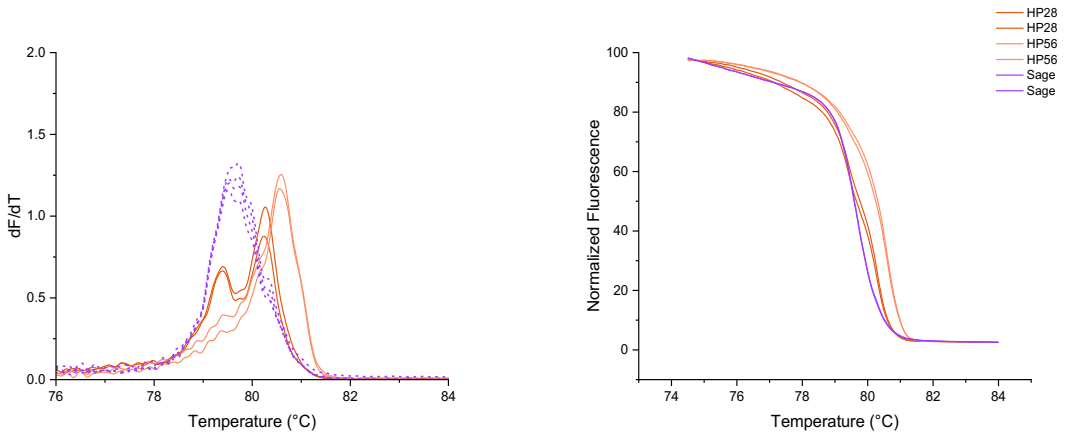

Figure 44 Melting curves (left) and normalized fluorescence (right) of PCR products from forest honey with sage (HP28), sage honey (HP56) and sage, obtained with PL1 assay.

Based on the results, the rbcL DNA fragment is a suitable barcode for differentiating plant sources in honey samples. These findings are consistent with those of Borkowska *et al.,* showing that the PL1 assay can distinguish plants such as acacia and linden (29). However, the study has limitations, as some positive controls exhibited similar melt curves of their PCR products. Incorporating sequencing could further improve the method, potentially allowing PL1 to serve as a rapid and reliable approach for assessing honey authenticity.

5.2.2 PL2_1 PCR-HRM assay

The primer pair PL2 was taken from literature, tested *in silico* and used in further PCR-HRM analysis (78). The primer pair PL2 targets the ITS2 gene. In silico analyses revealed a substantial difference of 5.2 °C in the annealing temperatures between the forward and reverse primers (Table 10). To address this issue, the reverse primer sequence was modified by removing certain nucleotides (Table 5), thereby correcting the annealing temperature. Subsequently, all honey samples were analyzed using the newly designed PL2_1 assay.

Table 10 *In silico* characteristics of primer pair PL2; fwd: forward primer, rev: reverse primer, primer sequence and length (bp), GC content (%), melting temperature (Tm).

Amplicon length: 226 bp	Sequence	Length (bp)	GC (%)	Tm (°C)
fwd	ATGCGATACTTGGTGTGAAT	20	40	54.3
rev	GACGCTTCTCCAGACTACAAT	21	48	59.5

Figure 45 presents the amplification curves obtained from plant species. In comparison to the PL1 assay, lower Ct values were observed (Table S5) indicating earlier amplification and more efficient PCR product formation when using the PL2_1 primer pair. In contrast, the honey samples exhibited higher Ct values, selected honey samples are shown in Figure 46.

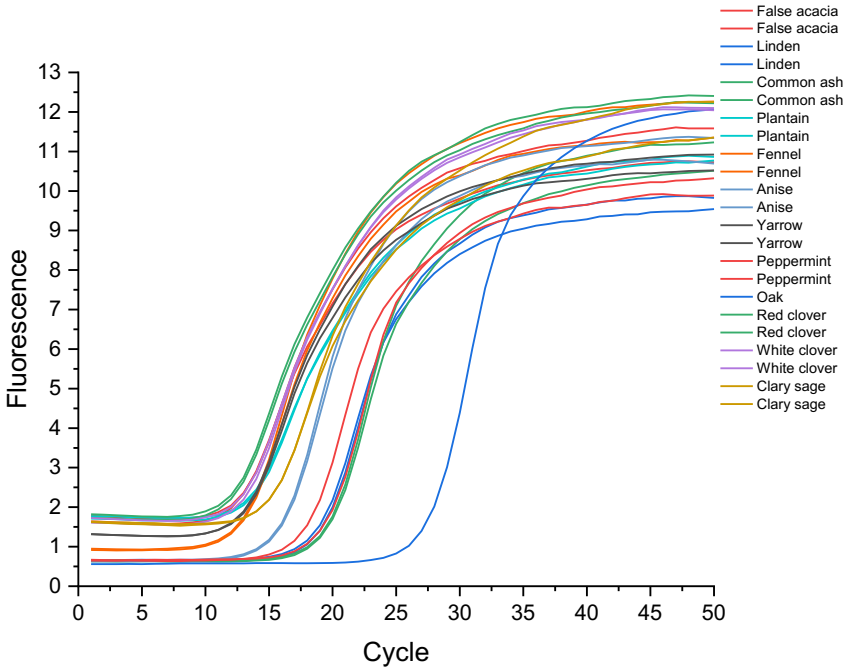

Figure 45 The amplification curves of PCR products of positive controls (false acacia, linden, common ash, plantain, fennel, anise, yarrow, peppermint, oak, red clover, white clover and clary sage) generated with the primer pair PL2_1.

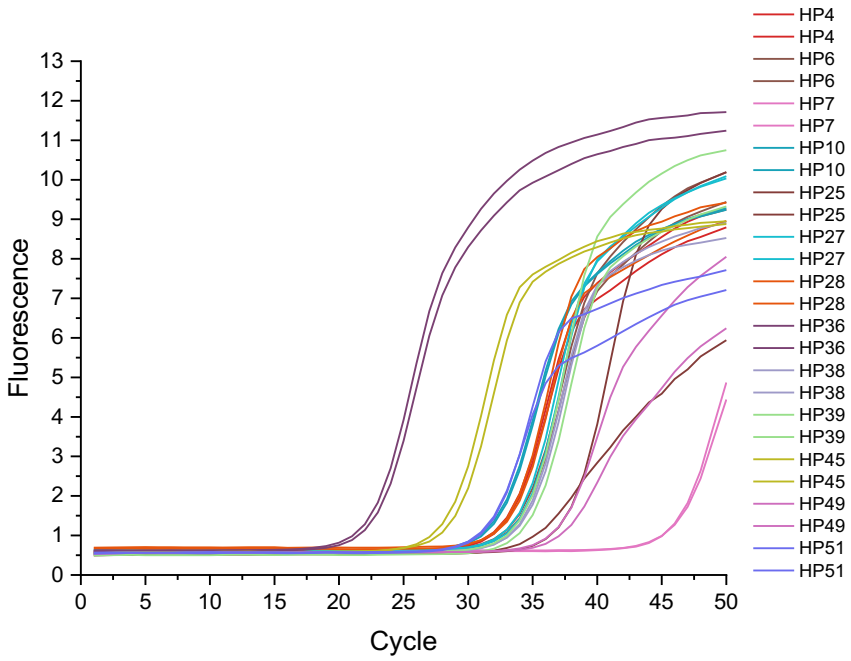

Figure 46 The amplification curves of PCR products generated with the primer pair PL2_1 from honey samples: forest honey (HP4, HP6, HP7, HP10, HP25, HP27, HP28); acacia honey (HP39, HP44, HP49), linden honey (HP38, HP45, HP51) and fennel honey (HP36).

For consistency and direct comparability with assay PL1, the same honey and pollen samples (H2/P2, H3/P3, H14/P14, H16/P16, H8/P8 and H10/P10; Table 4), provided by colleagues from AGES, were selected for performing melting curve analysis. In several cases, the target barcode region could not be amplified, and in others, honey and the corresponding pollen sample showed divergent melting profiles (Figure 47). Compared to the positive controls, many honey and pollen samples exhibited melting peaks in different temperature ranges. These findings indicate that this assay has methodological limitations for the tested sample types. In some cases, honey samples were not amplified at all and in others, honey and pollen did not show the same melting profile. It should also be noted that the DNA extracts were provided by our cooperation partner, who had not determined the DNA concentrations prior to analysis. Therefore, low template concentration may have contributed to the lack of amplification observed in some samples (H3, H8).

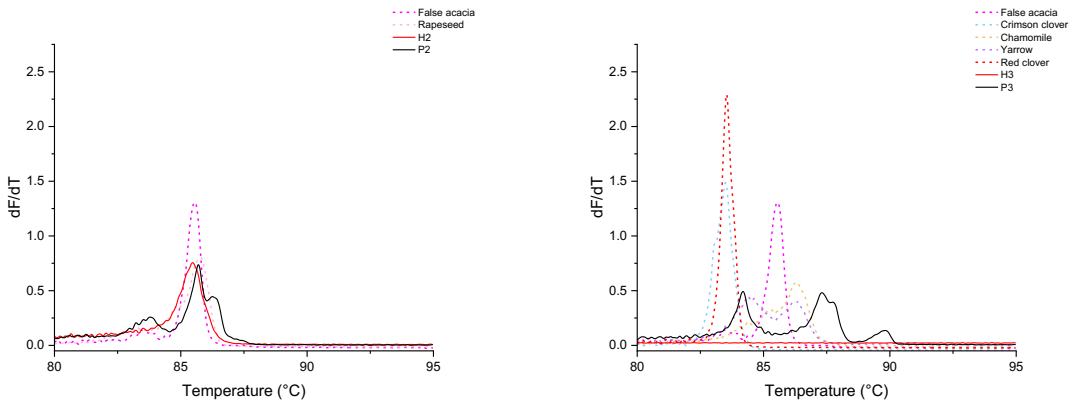

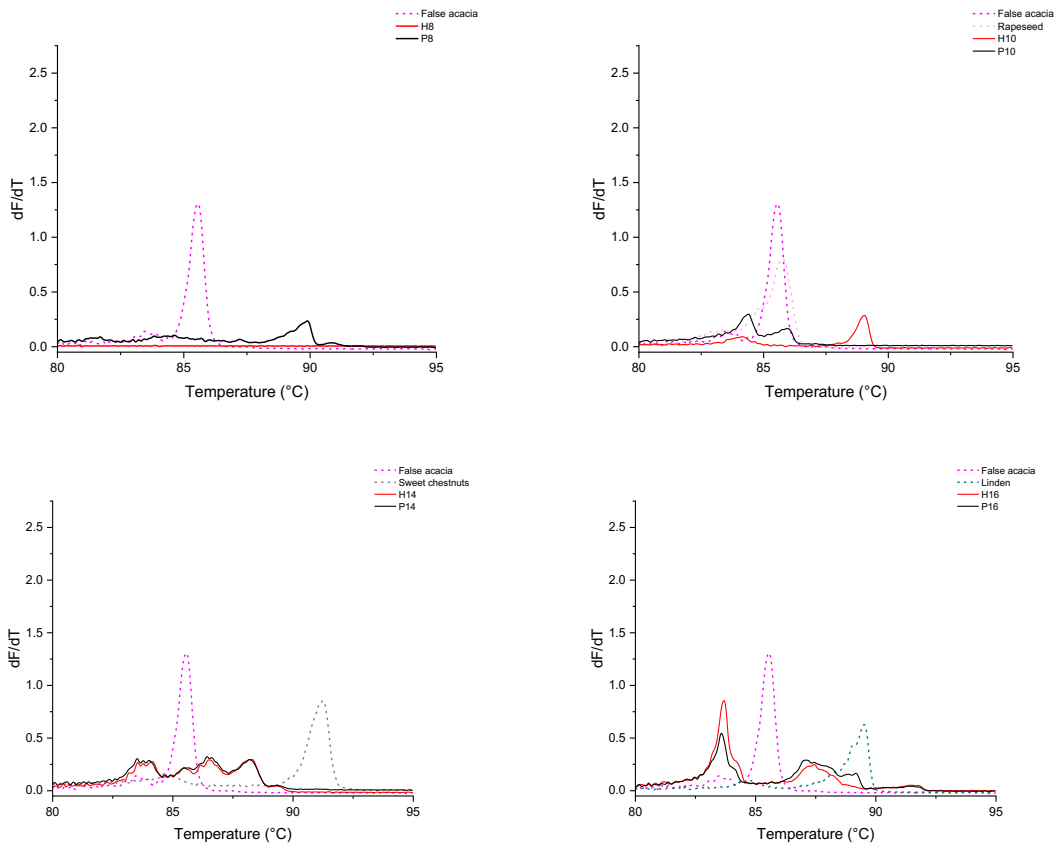

Figure 47 Melting curves of PCR products obtained with primer pair PL2_1 from selected honey samples and pollen (H2/P2, H3/P3, H14/P14, H16/P16, H8/P8 and H10/P10).

The following figures show the comparison of selected honey samples (HP1–HP56) and the positive controls. Figure 48 shows the melting curves of PCR products of acacia honey (HP39, HP38, HP49) and false acacia. Although amplification was successful, the low DNA concentration (<0.1 ng/µL) in honey samples resulted in reduced repeatability of the melting curves. This indicates that template limitations may compromise HRM reliability when analyzing honey-derived DNA. The HRM analysis demonstrated that sample HP36 (fennel in honey) exhibited a melting profile comparable to that of the fennel plant DNA (Figure 49). The concordance in melting temperature and curve shape indicates the presence of fennel DNA in the honey sample HP36, which contains added fennel, resulting in a clear HRM signal. These results are consistent with the specificity of the assay. The linden exhibited a distinct melting peak (Figure 50). Among the three honey samples labelled as linden honey (HP38, HP45, HP51), only one honey sample (HP45) showed a melting peak within the same temperature region as the positive control, indicating the presence of linden DNA and suggesting linden as the dominant botanical source. The remaining samples displayed different melting shapes, including shifted peaks. Multiple melt peaks observed in melting shapes suggest the presence of DNA from more than one plant species.

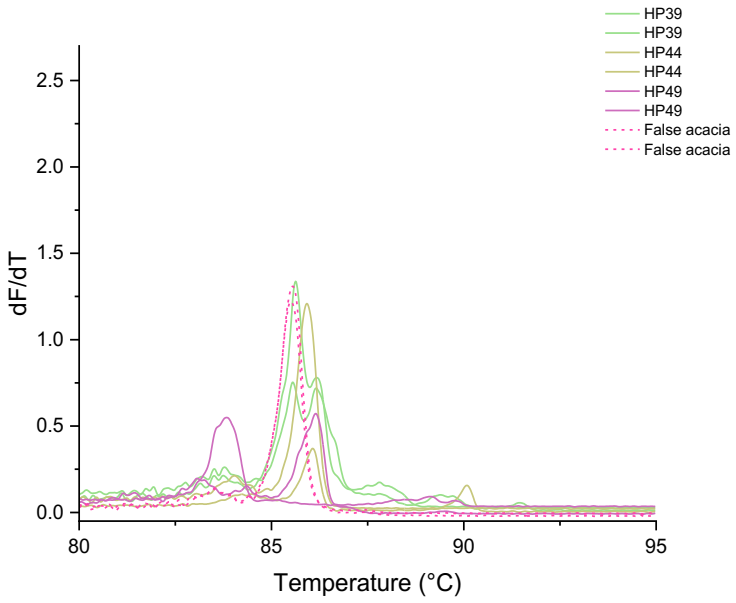

Figure 48 Melting curves of PCR products of acacia honey and false acacia, amplified with the primer pair PL2_1.

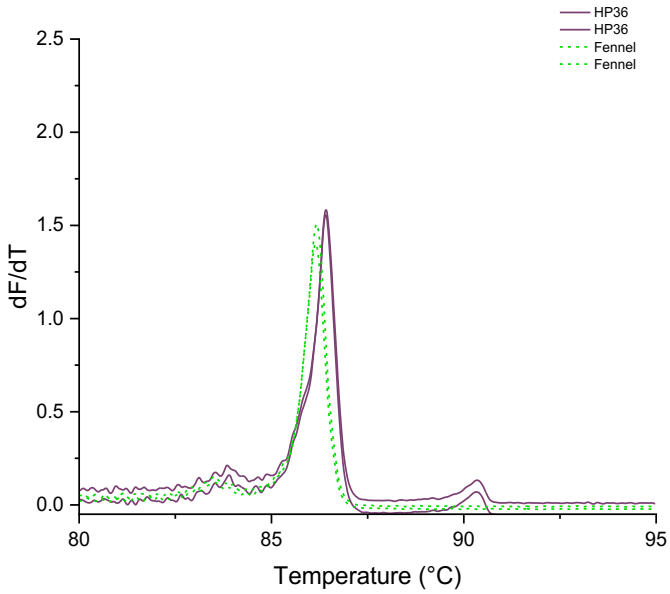

Figure 49 Melting curves of PCR products of sample fennel in honey (HP36) and fennel as the positive control, obtained with the primer pair PL2_1.

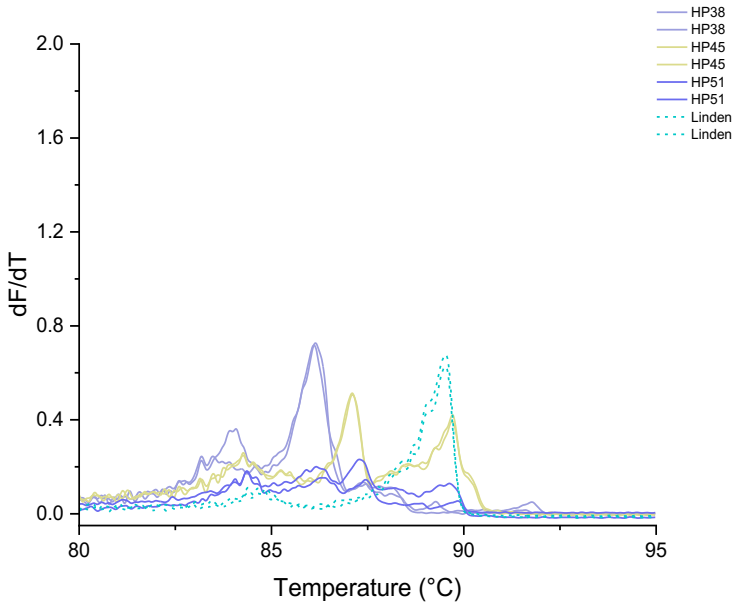

Figure 50 Melting curves of PCR products of linden and linden honey samples (HP38, HP45, HP51), obtained with the primer pair PL2_1.

HRM analysis of the ITS2 DNA region demonstrated variable reliability depending on DNA concentration and sample composition. The use of the ITS2 region in the present study aligns with previous research demonstrating its effectiveness in identifying plant taxa in bee-collected pollen. ITS2 metabarcoding has been shown to detect a wide diversity of botanical sources, highlighting the complex foraging behavior of honeybees (82).

Low DNA yield (<0.1 ng/µL) of honey samples reduced repeatability of melting profiles, indicating that template limitations can compromise HRM performance when analyzing honey-derived DNA. The assay successfully confirmed botanical origin in selected cases. Additional or shifted peaks observed in other samples indicate mixed botanical origin or a low proportion of target pollen. Furthermore, additional melting peaks detected with the PL2_1 assay suggest the presence of secondary botanical sources, demonstrating that this assay provides enhanced insight into honey composition. Overall, HRM analysis proved to be a useful tool for assessing botanical origin and detecting compositional complexity in honey, although sensitivity to DNA quality and assay-specific limitations must be considered.

5.2.3 PL3_1 PCR-HRM assay

Primer pair PL3 targets the *rbcL* gene. The primer sequences were initially adopted from the literature (79) and subsequently tested *in silico.* During this analysis, a difference of 6.2 °C in the predicted melting temperatures (Tm) between the forward and reverse primers was observed (Table 11). To optimize primer performance, the reverse primer was shortened, resulting in comparable annealing temperatures for both primers (Table 5). The primer pair PL3_1 was then tested *in silico* and applied in further PCR-HRM analyses.

Table 11 *In silico* characteristics of primer pair PL3; fwd: forward primer, rev: reverse primer, primer sequence and length (bp), GC content (%), melting temperature (Tm).

PL3	Sequence	Length (bp)	GC (%)	Tm (°C)
fwd	ATGTCACCACAAACAGAAAC	20	40	54.3
rev	TCGCATGTACCTGCAGTAGC	20	55	60.5

The PL3_1 assay was applied to plants DNA, served as positive controls and selected honey samples. Comparison of amplification curves revealed substantially higher Ct values in honey samples than in the plants, calculated at a threshold of 0.05. The elevated Ct values indicate a markedly lower concentration or quality of plant DNA in honey, which is consistent with DNA degradation, filtration processes, and the limited amount of pollen-derived material typically present in honey.

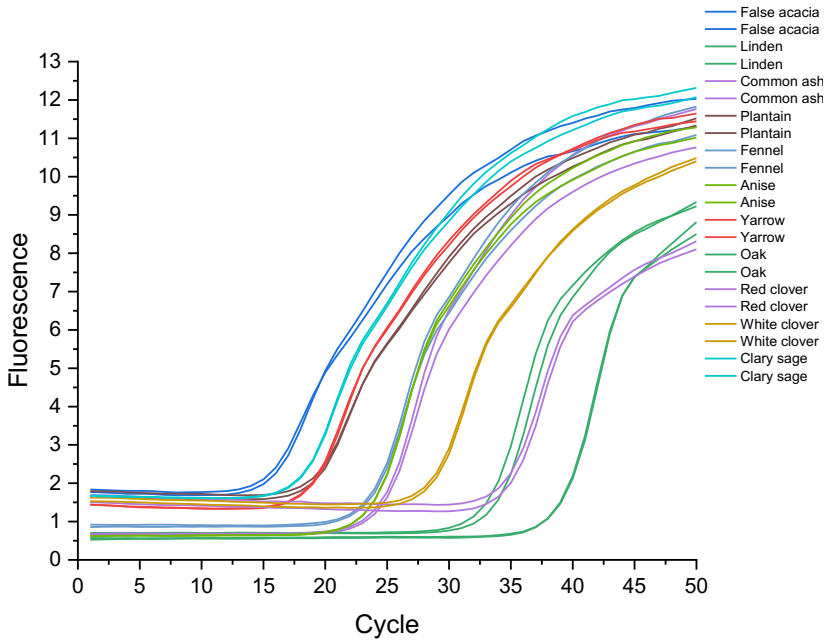

Figure 51 Amplification curves of PCR products of positive controls amplified with the primer pair PL3_1. Ct values are between 14.04 and 35.19 with threshold 0.05.

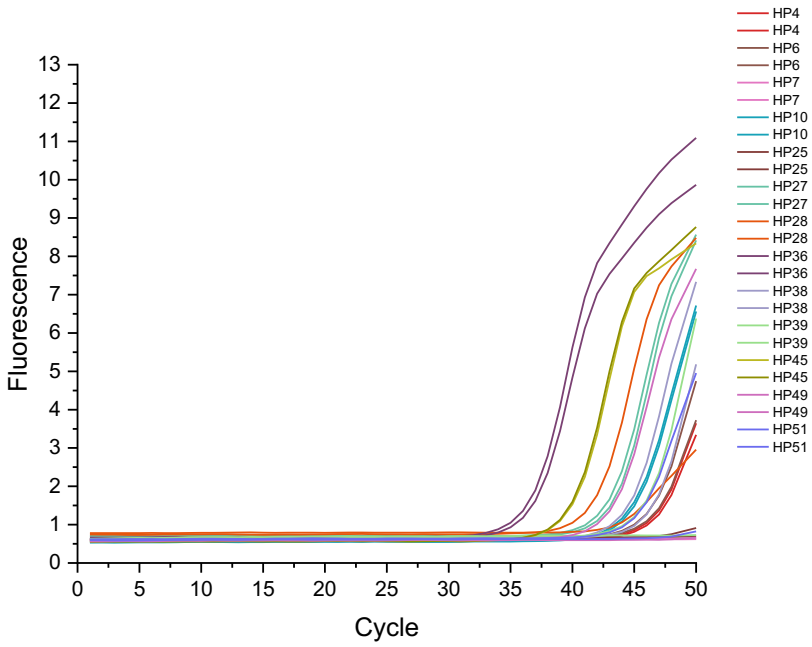

Figure 52 Amplification curves of honey samples (HP25–HP47) with the primer PL3_1. Ct values were very high (>35) in this case, and many honey samples were not amplified at all.

The following figure presents melting curves of PCR products obtained from selected honey and corresponding pollen samples provided by AGES. Amplification was performed using the PL3_1 assay targeting the rbcL region. Only sample H13/P13, H14/P14, H15/P15, and H16/P16 (Table 4) that yielded successful amplification are shown and compared with the corresponding positive controls assignments derived from DNA metabarcoding data supplied by AGES. All other samples failed to amplify with this assay. Samples H13 and P13 exhibited the most similar melt curves in the region of rape and false acacia. However, additional minor peaks were observed, indicating that other botanical sources cannot be excluded (Figure 53). The melt curves in honey and pollen samples (H14/P14) are shifted compared to the positive controls Such peak shifts may result from matrix effects, or low DNA concentration in the DNA extracts (Figure 54). The selected positive controls (false acacia and linden) showed one melted peak within a similar temperature region, which limits these observations and complicates precise taxonomic assignment. Additionally, the honey and pollen samples (H15/P15) melt at identical temperatures and displayed different curve shapes, indicating that matrix effects or low DNA concentration in the samples could be the reason (Figure 55). The melting profiles obtained for samples H16/P16 revealed multiple melting domains, indicating the presence of more than one botanical source (Figure 56). Peaks corresponding to the temperature regions characteristic of linden and false acacia were observed, which is consistent with DNA metabarcoding results identifying linden and false acacia as predominant pollen sources. Minor peak variations suggest the presence of additional trace plant DNA.

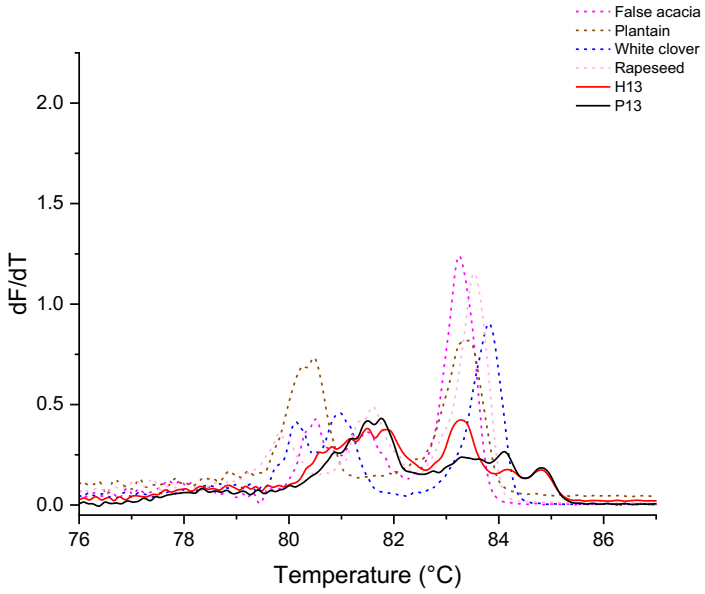

Figure 53 Melting curves of PCR products, generated with PL3_1 assay from honey and pollen samples (H13/P13) and positive controls (false acacia, plantain, white clover, rapeseed) identified in the samples by DNA metabarcoding at AGES.

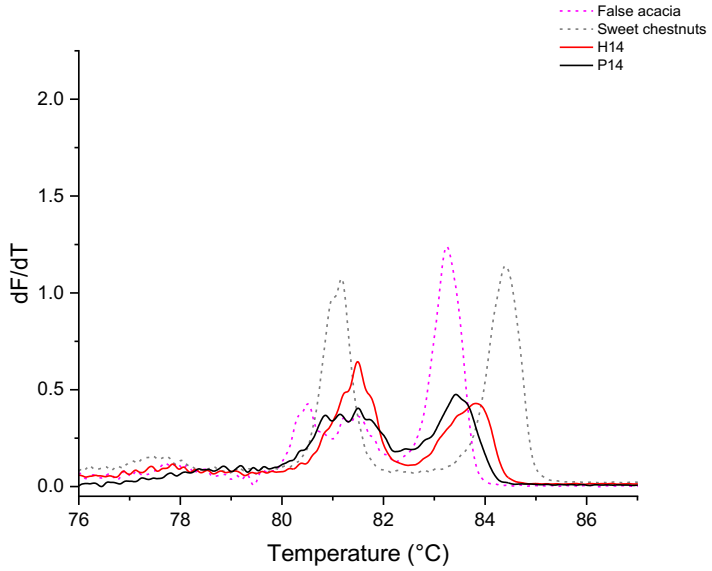

Figure 54 Melting curves of PCR products, obtained with primer pair PL3_1 from honey and pollen samples (H14/P14) and false acacia and sweet chestnut.

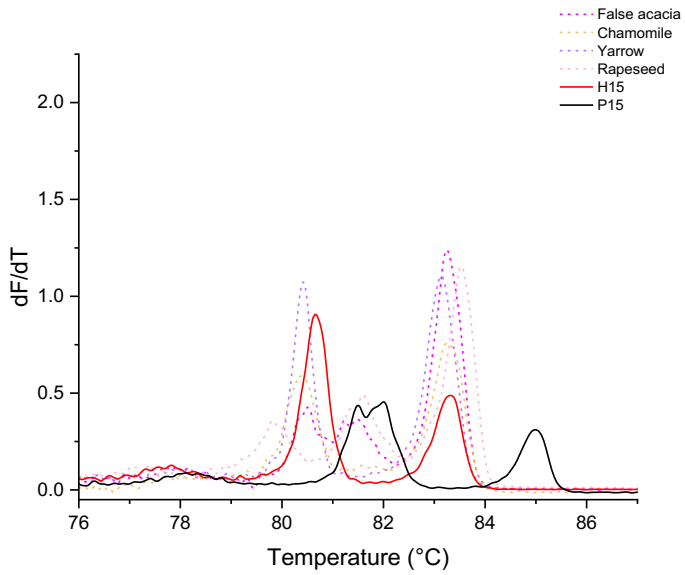

Figure 55 Melting curves of PCR products, generated with the primer pair PL3_1 from honey and pollen samples (H15/P15) and positive controls (false acacia, chamomile, yarrow, rapeseed) confirmed by DNA metabarcoding at AGES.

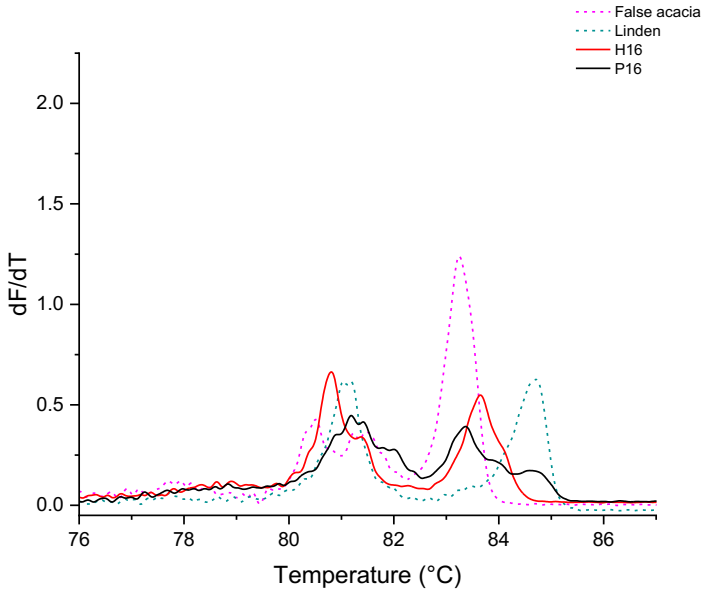

Figure 56 Melting curves of PCR products from honey and pollen samples (H16/P16) and positive controls (false acacia and linden), obtained with primer pair PL3_1.

Acacia honey showed the weakest amplification and poor repeatability between duplicates (Figure 57). The melting profiles were inconsistent, indicating low DNA. These results suggest that primer PL3_1 is not suitable for reliable HRM analysis of acacia honey. Most forest honey samples displayed similar melting behavior in the first peak region but differed in the second peak (Figure 58). Sample HP10 matched the oak control profile, while HP38 and HP51 showed similarity to the positive control with slight peak shifts, likely due to matrix effects or low DNA concentration. HP45 matched only one peak of the control, suggesting a mixed botanical origin. Because forest honey contains multiple plant sources and some of them are missing as positive controls, interpretation remains limited.

Samples showed partially overlapping melting profiles with controls but also distinct peak shifts and additional peaks. This indicates the presence of multiple plant DNA sources.

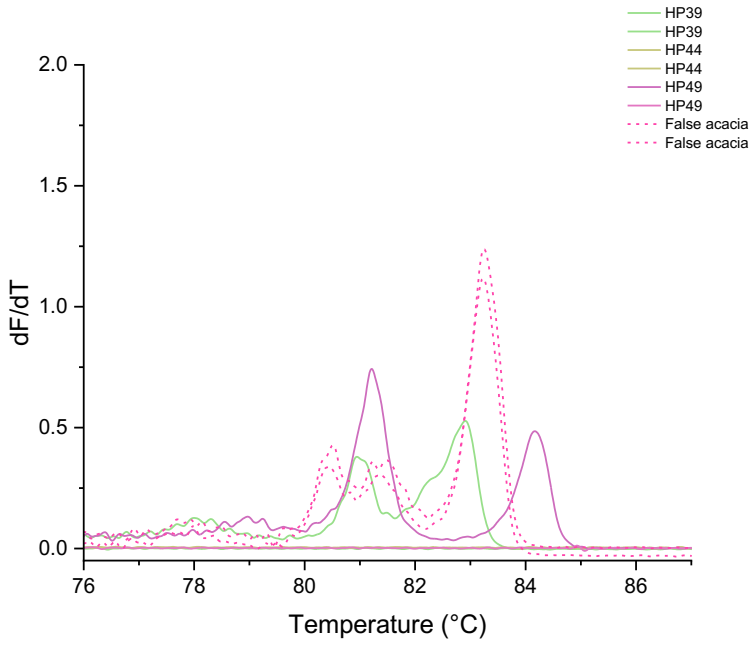

Figure 57 Melting curves of PCR products obtained with PL3_1 assay from acacia honey samples (HP39, HP44, HP49) compared with the positive control false acacia.

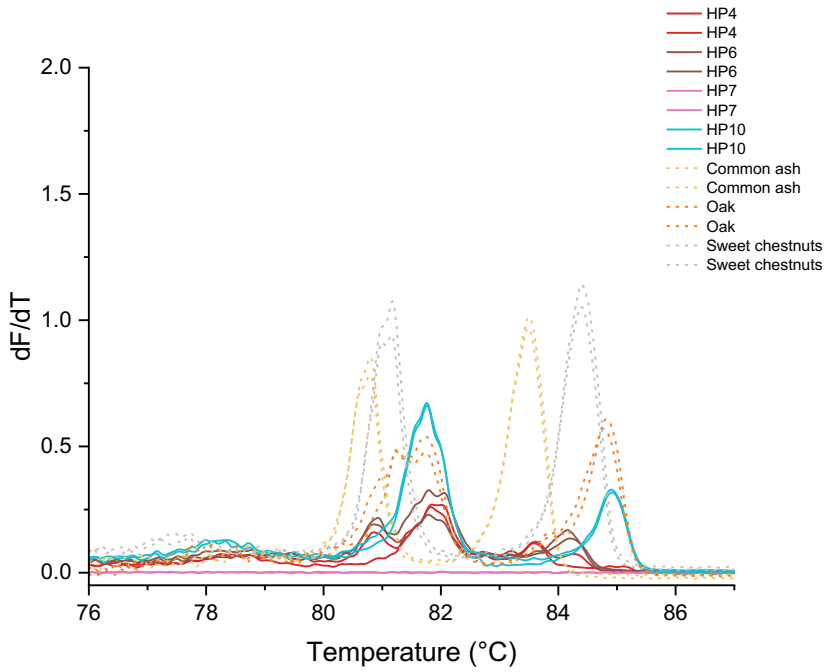

Figure 58 Melting curves of PCR products of selected forest honey samples (HP4, HP6, HP7, HP19) and positive controls that are typically part of forest honey (common ash, oak, sweet chestnut).

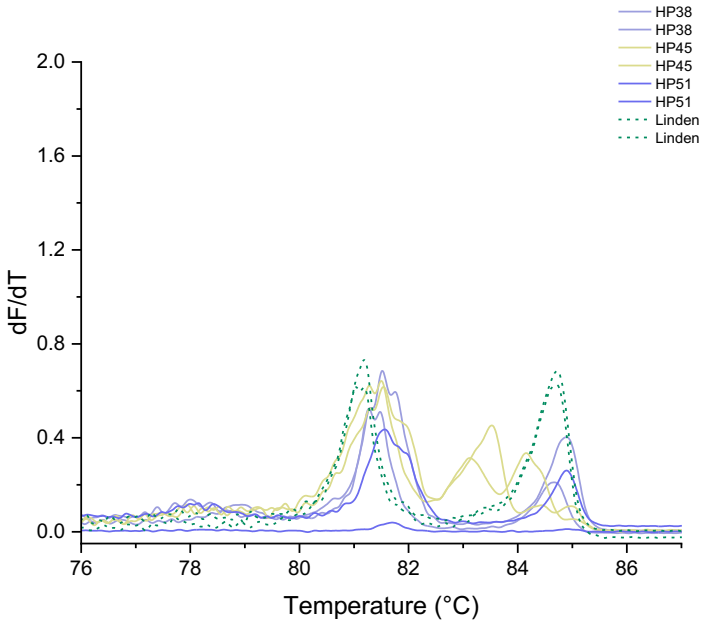

Figure 59 Melting curves of PCR products of linden honey (HP38, HP45, HP51) and linden obtained with the primer pair PL3_1.

Among the tested assays, PL3_1 produced the highest Ct values overall. Consequently, several honey samples failed to generate detectable melting peaks, suggesting that the amplification yield was insufficient for reliable HRM analysis. This reduced sensitivity may be attributed to the low copy number of plant DNA in honey extracts and the relatively conserved nature of the rbcL marker, which can limit amplification efficiency in highly degraded samples.

The positive controls belonging to the same family were grouped, and their melting peaks were compared across all three plant assays (Figure 60) The legume family (*Fabaceae*) consists of false acacia and different types of clover, where all clover types showed similar melting curves and temperatures with assays PL1 and PL3_1, while false acacia melted at a different temperature. Assay PL2_1, however, showed different melting profiles and temperatures within this family. In the mint family (*Lamiacea*), according to the results from assays PL1 and PL3_1, peppermint melted at the same temperature as sage, while PL2_1 showed different melting peaks. The carrot family (*Apiaceae*), consisting of fennel and anise, and the beech family (*Fagaceae*), consisting of sweet chestnut and oak, did not show the same melting curves across all assays. In contrast, plants in the aster family (*Asteraceae*), consisting of chamomile and yarrow, and in the mallow family (*Malvaceae*), consisting of linden and mallow bloom, melted at the same temperature with a similar melting curve profile in assays PL1 and PL3_1, while assay PL2_1 showed differences. The results lead to the conclusion that the PL2_1 assay has the highest ability to distinguish between different plant species.

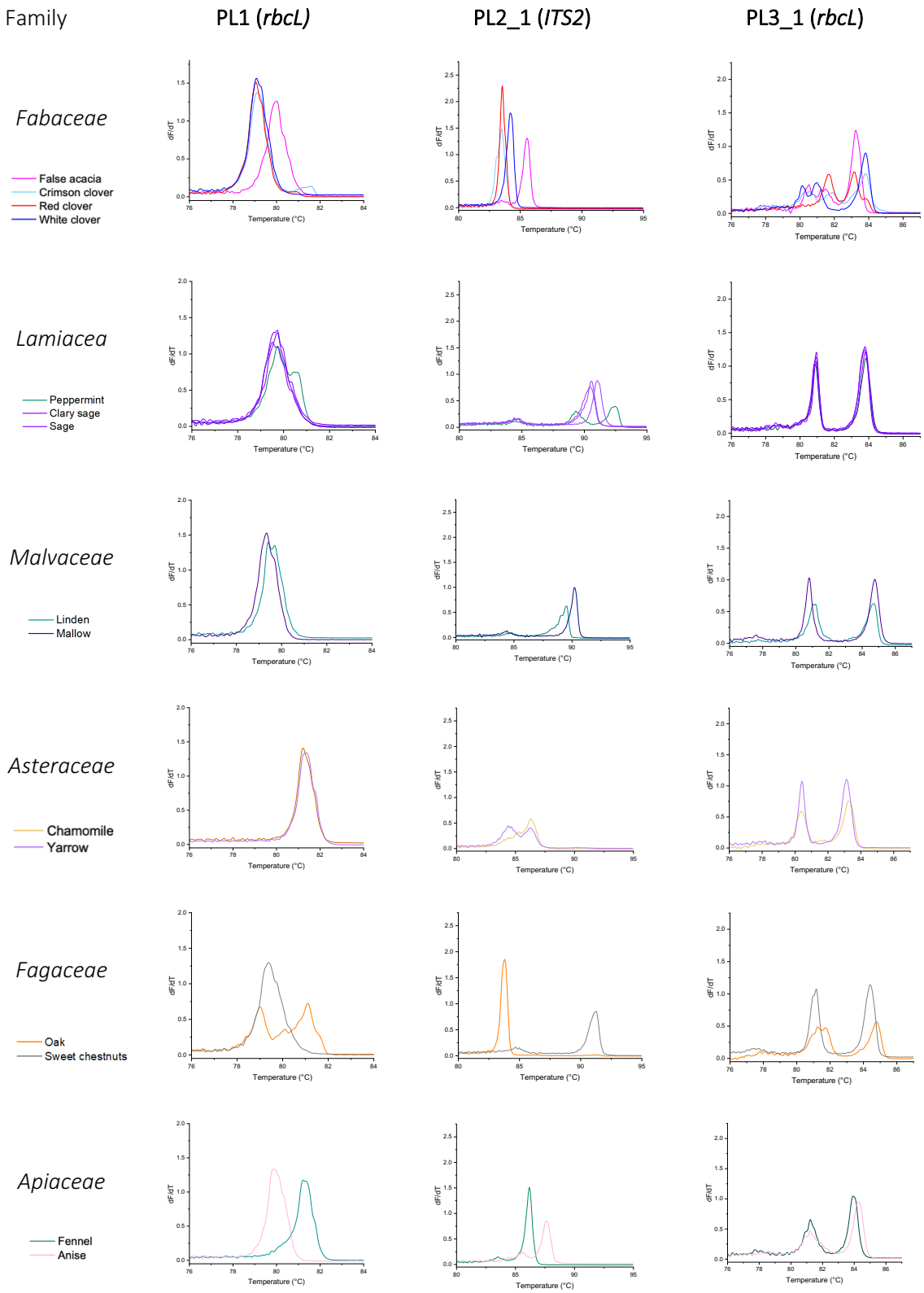

Figure 60 Comparison of melting curves of PCR products from plants, between rbcL2 and ITS2 DNA fragment across 20 plant species grouped by plant family. The rbcL2 assays (assays: PL1 and PL3_1) show limited sequence divergence within families, whereas ITS2 (assay PL2_1) reveals clear interspecific differentiation.

Analysis of the melting curves of different plant families showed that the results depend heavily on the assay selected. While assays PL1 and PL3_1 yielded similar melting temperatures and curve profiles for some families (e.g. *Asteraceae* and *Malvaceae*), other families such as *Fabaceae, Apiaceae* and *Fagaceae* showed significant differences. Assay PL2_1 showed the greatest ability to distinguish between individual plant species, but differences also occurred between different plants that served as positive control of the same species, such as sage or clover. Overall, it can be concluded that none of the assays used are reliably suitable for verifying the authenticity of honey. The melting curves of PCR products were too complex, and there were shifts compared to the positive controls, meaning that it was not possible to clearly classify or confirm individual plant species.

5.3 Water content and electrical conductivity

To assess the physicochemical quality and characteristics of the honey samples, water content and electrical conductivity were determined. Water content of honey samples (HP1–HP51) ranged from 14.5% to 20.4%. Electrical conductivity values varied between 112.6 to 1478 µS/cm (Table S7). Following the guideline summarized in Table 12 (83) some honey samples have electrical conductivity values below the guideline limits and are marked in red. As it can be seen in Figure 61, forest honey, pine honey and honeydew honey samples show higher electrical conductivity values, as expected, compared to blossom or acacia honey. The mixture of blossom and forest honey also exhibited higher electrical conductivity compared to pure blossom honey. Since some honey samples were crystallized in the meantime or were already purchased in a solid state, this can make the measurement of water content challenging and altogether, lead to inaccurate electrical conductivity results. Based on the results, it can be concluded that the sample HP47 consisting of a mixture of honey (10%) and syrup (90%) has a very low electrical conductivity value. This is followed by acacia honey samples, which show lower electrical conductivity values compared to other types of honey.

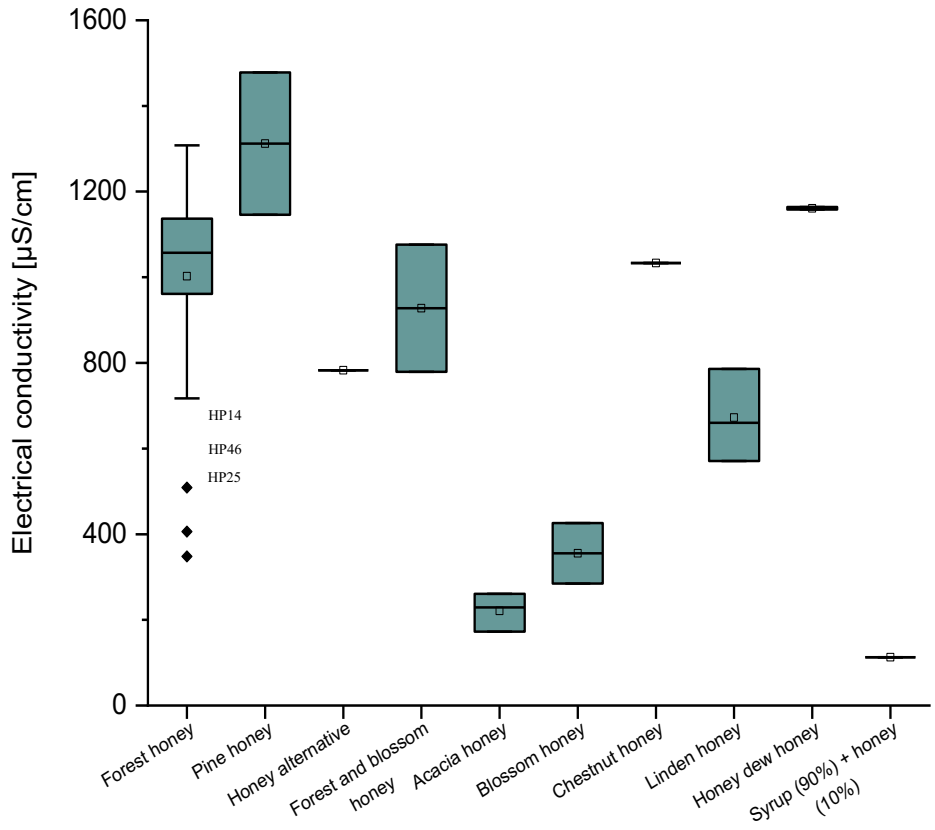

Figure 61 Electrical conductivity (µS/cm) of different honey types determined on dry matter basis. The boxes represent the interquartile range (25–75th percentile), the horizontal line indicates the median, whiskers denote minimum and maximum values excluding outliers, and points represent outliers.

The low electrical conductivity value in sample HP14 can be justified because it is the only sample that had been open for a long time and was not purchased like the other samples. HP25 shows a very low value for forest honey, which was not expected because there was no crystallization over time, therefore, the refractometric measurement of water in the sample was not disturbed.

Sample HP46 has a lower value than forest honey should have, the cause may be that it is raw honey, and therefore the refractometer reading during the water content measurement was not completely clear.

Table 12 Electrical conductivity guideline values for different types of honey (µS/cm) (83)

Guideline	Electrical conductivity × 100 = µS/cm
Blossom honey	< 4
Forest honey	min. 8
Linden honey	4–10
Acacia honey	1–3
Sweet chestnut honey	7–21
Pine honey	min. 10

5.4 NMR

To round off our results and better understand the honey profile, in collaboration with Univ.-Prof. Mag. Dr. Mathea Sophia Galanski, NMR analysis of selected honey samples (n=20) was performed. The selected honey samples were grouped into four clusters (Table 13): forest honey, linden honey, acacia honey (n=3) and blossom honey with acacia, and chestnut honey. To compare the NMR profile of honey with products potentially used for adulteration, the NMR profiles of vegan honey alternatives and a syrup-honey mixture (90% syrup + 10% honey) were also analyzed. It should be noted that within each cluster there are 3–9 different honey samples, which is certainly a small number for drawing conclusions, nevertheless, the following results are based on the obtained data. The processing of the results was carried out by Univ.-Prof. Mag. Dr. Mathea Sophia Galanski, and the preparation of the samples is explained in Section 4.8. As it can be seen in Table 13 honey typically exhibits a relatively narrow pH range (approximately 3.95–5.41). Since no evident impact on spectral characteristics was observed, pH was not determined for the remaining samples prepared for NMR analysis.

Table 13 Honey samples ID and type analyzed by NMR and their pH values

Sample ID	Honey type	pH
HP1	Forest honey	4.91
HP6	Forest honey	4.31
HP8	Organic forest honey	4.46
HP9	Forest honey	4.51
HP10	Organic pine honey	n.d.*
HP12	Honey alternative	4.12
HP15	Forest honey	n.d.*
HP25	Forest honey	5.18
HP27	Forest honey with heather	4.36
HP28	Forest honey with sage	4.52
HP32	Acacia honey	4.08
HP37	Sweet chestnut honey	n.d.*
HP38	Linden honey	n.d.*
HP39	Blossom with acacia	n.d.*
HP44	Organic acacia honey	3.98
HP45	Organic linden honey	n.d.
HP47	Syrup (90%) + honey (10%)	4.19
HP49	Acacia honey	3.95
HP51	Linden honey	n.d.*

*n.d. – not determined

As shown in Figure 62, this NMR method allows the differentiation of various honey samples. In the following figures, three distinct clusters are presented: chestnut honey, linden honey, and acacia honey. In panel A, three different linden honey samples exhibit the same characteristic NMR signals (marked in red) in the region between 1.0 and 2.5 ppm. In panel B, similar NMR signals are also observed for three linden honey samples in the region between 6 and 7.5 ppm. In this spectral region, the NMR spectra of chestnut honey are also visible and differ clearly from those of linden honey. It can be observed that the three acacia honey samples exhibit similar NMR profiles, with no distinct peaks, except for sample HP39, which shows a clear peak (Figure 62A); this difference is consistent with the fact that HP39 is a blossom honey containing acacia, and the peak most likely reflects the presence of DNA or metabolites from another plant species. In conclusion, the different honey types can be distinguished using this NMR approach, indicating that this method can be useful as an additional analytical tool for honey characterization and authenticity.

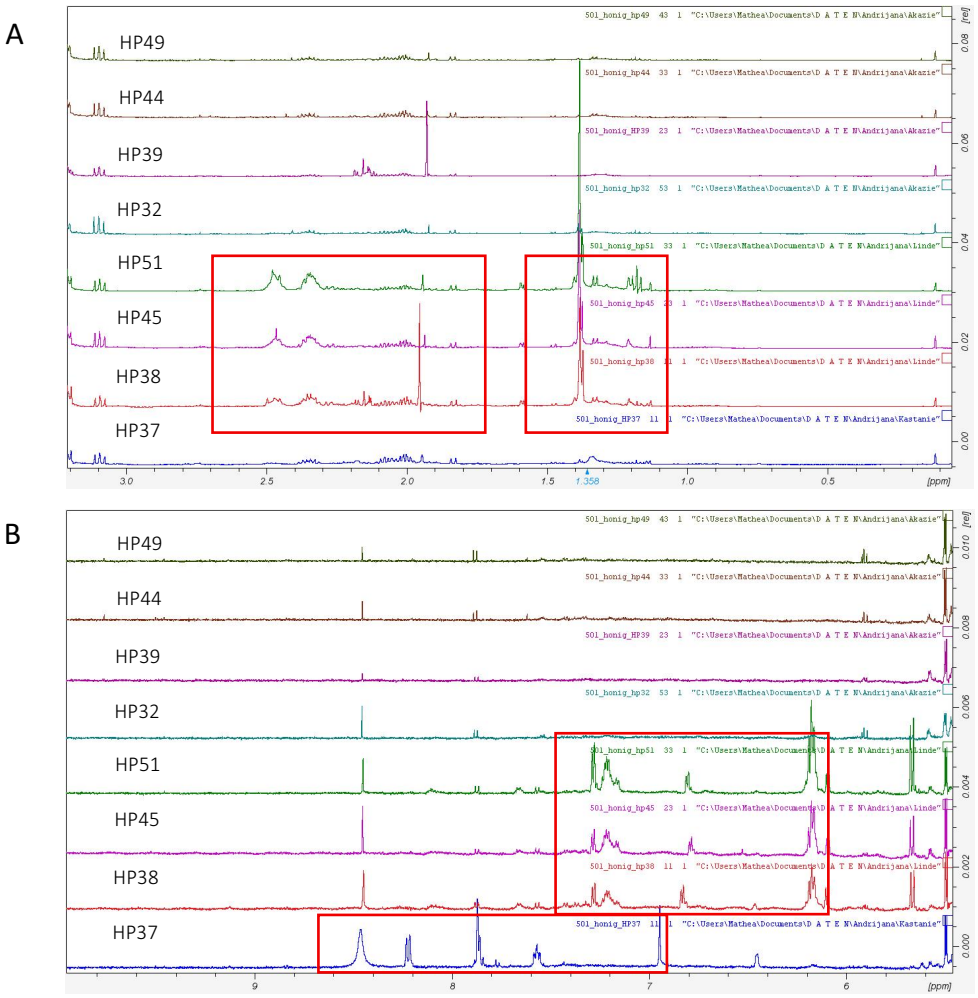

Figure 62 Fingerprint region of honey samples showing three clusters: chestnut (HP37), linden (HP38, HP45, HP51), and acacia (HP32, HP39, HP44, HP49), with characteristic peaks for each honey type. Characteristic peaks for each honey type are observed in two regions: A (0–3.2 ppm) and B (5.7–10 ppm).

Figure 63 additionally shows the NMR spectra of two more forest honey samples (HP1 and HP10). Sample HP10 is organic pine honey, and differences between these two samples can also be observed in the NMR spectra, particularly in panel B, in the spectral region between 6.5 and 7.5 ppm.

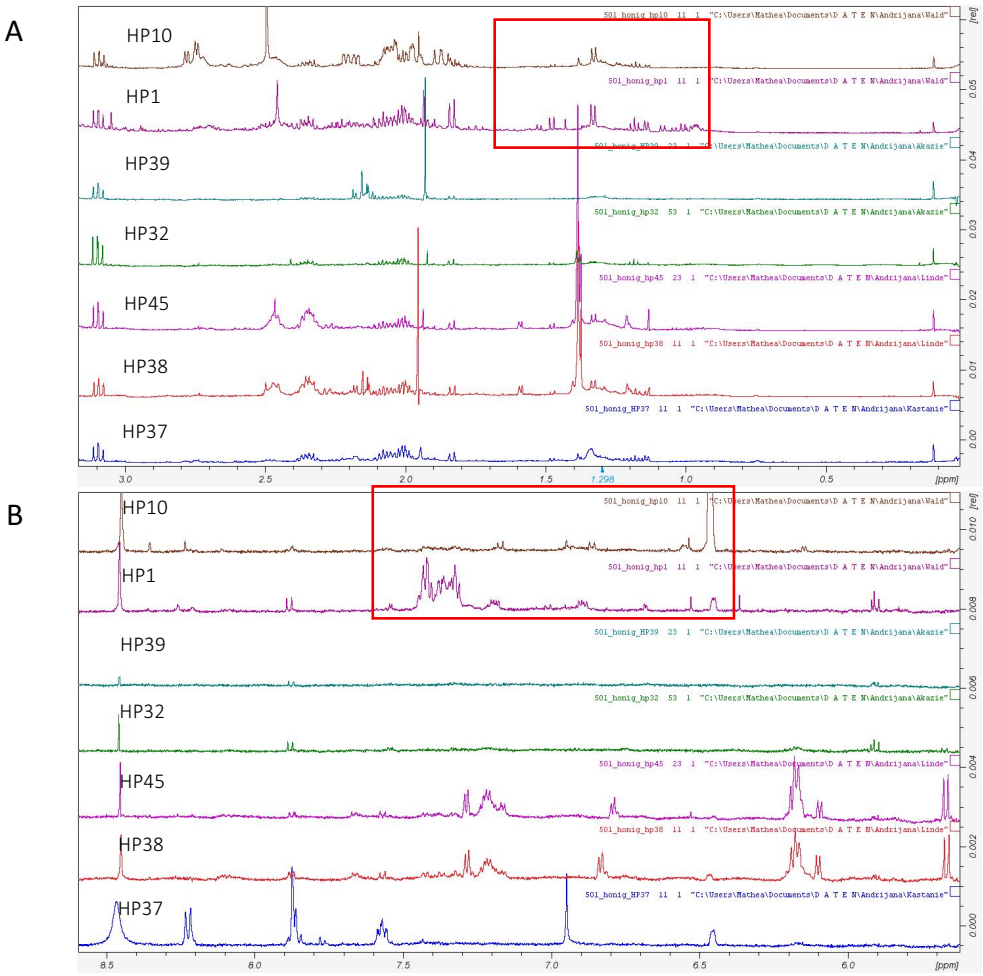

Figure 63 Comparison of the NMR fingerprint regions of four different honey types: chestnut (HP37), linden (HP38, HP45), acacia (HP32, HP39), and forest honey (HP1, HP10). Characteristic peaks for each honey type are observed in two regions: A (0–3.2 ppm) and B (5.6–8.5 ppm).

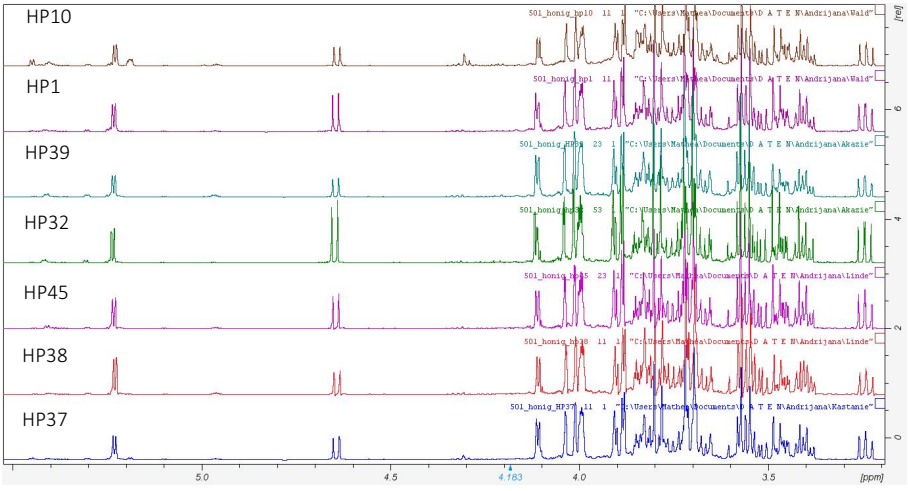

Figure 64 NMR spectra of sugar profiles of different honey sample types: chestnut (HP37), linden (HP38, HP45), acacia (HP32, HP39), and forest honey (HP1, HP10) showing similarities in same NMR spectral regions.

There were a total of 9 honey samples belonging to forest honey cluster. It was observed that the HP25 honey deviates from the other honey samples. In HP25, it is also possible to observe a distinct signal (Figure 65) that does not occur in the other forest honey samples, and particular attention was drawn to the fact that this same signal is also present in the sample of alternative honey HP12 (consisting of rice syrup), also in the region between 1.0 and 1.4 ppm, as it can be seen in Figure 66.

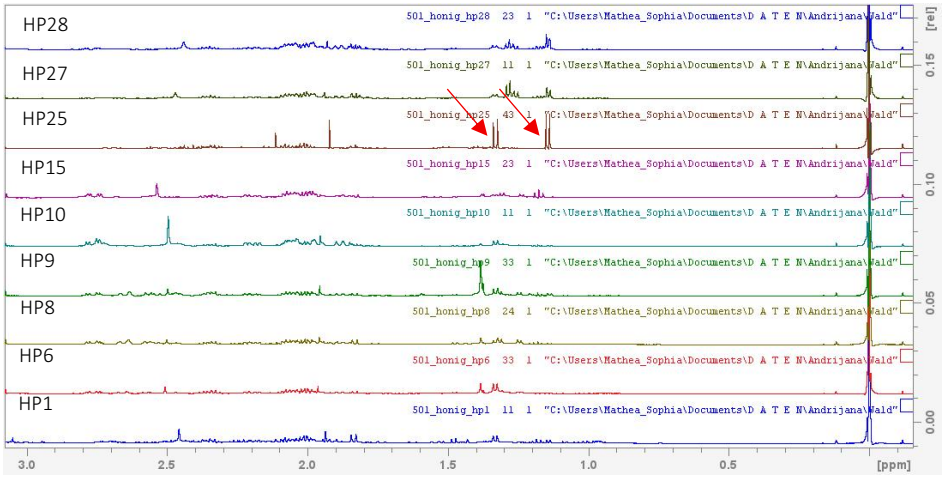

Figure 65 NMR spectra of selected forest honey samples (HP1, HP6, HP8, HP9, HP10, HP15, HP25, HP27, HP28). Sample HP25 exhibits two signals that are absent in the NMR spectra of the other forest honey samples.

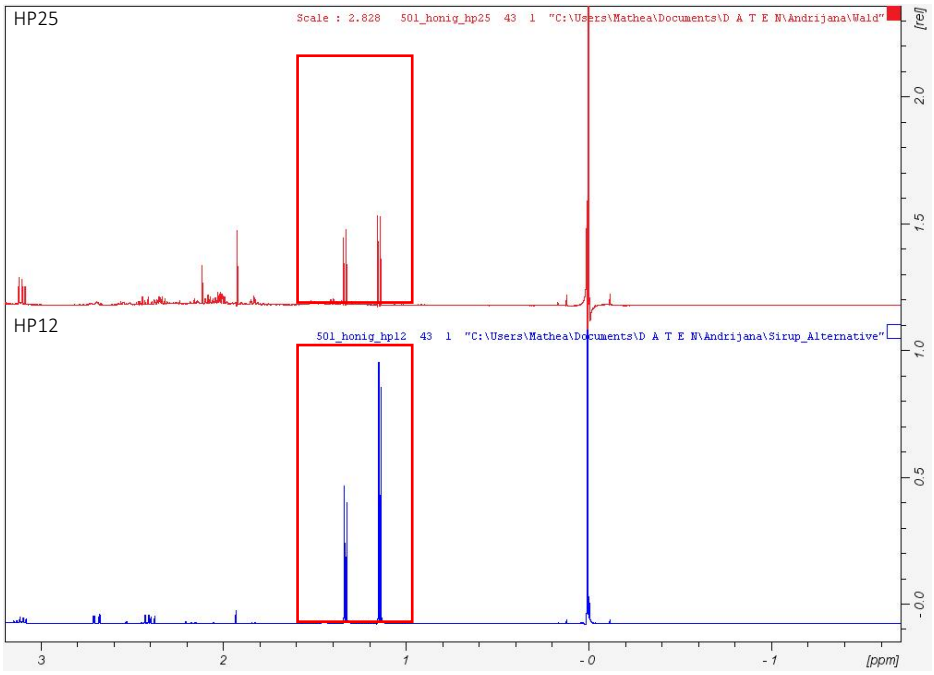

Figure 66 NMR spectra of the honey alternative sample HP12 and forest honey sample HP25 showing identical signals in corresponding spectral regions.

Figure 67 shows that all forest honey samples have distinct signals in the regions between 4.95 and 5.1 and 6.45 and 6.5 ppm, while HP25 does not.

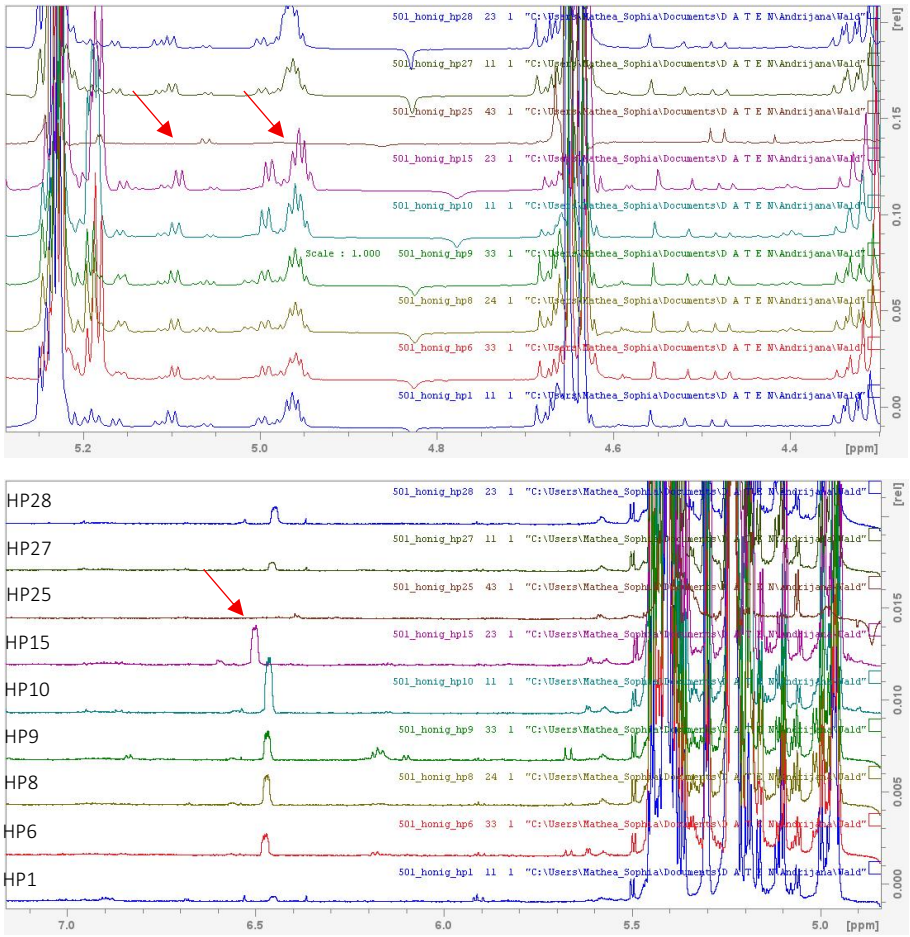

Figure 67 NMR spectra of nine selected forest honey samples (HP1, HP6, HP8, HP9, HP10, HP15, HP25, HP27, HP28). The red arrows indicate regions where signals are absent in sample HP25, whereas distinct peaks are observed in the same spectral regions in the other samples.

6 Conclusion

The findings of this study demonstrate that PCR-HRM analysis represents a promising and efficient screening tool for honey authentication. The primer pair BEE2_1, developed for DNA barcoding of a 132 bp fragment of the mitochondrial COI region, proved to be highly suitable for the development of a PCR-HRM assay capable of distinguishing honeybee subspecies of *A. mellifera*. The assay enabled detection of subspecies-specific variation directly in honey samples, a complex biological matrix composed primarily of sugars, proteins, enzymes and small particles. The presence of four SNPs within the amplified fragment additionally allows confirmation by PSQ. However, identical sequence patterns within the COI region prevented discrimination between certain subspecies (e.g. *A. m. carnica* (Alpine type) and *A. m. macedonica*), indicating that additional DNA barcoding markers are required to improve resolution and reliability in honey authentication.

The complex HRM profiles of multifloral honeys (e.g. forest honey, blossom honey) indicate a heterogeneous botanical origin, which complicates precise plant identification even when plant species DNA were used. Three plant primer pairs adapted from literature were evaluated for PCR-HRM analysis of botanical origin. Two assays targeted the rbcL region (PL1 and PL3_1), while PL2_1 targeted the ITS2 region. Among them, the PL1 assay showed the most consistent amplification efficiency and repeatable melting profiles. Although overlap among plant species limited species-level discrimination, several taxa could be differentiated, and similarities between plant species and corresponding monofloral honey samples (e.g. linden and linden honey) were observed. The comparative analysis confirmed the conserved nature of the rbcL region, which supports reliable amplification but offers limited discrimination within plant families. In contrast, ITS2 displayed higher sequence variability and improved resolution at the species level. These findings are consistent with previous research indicating that rbcL is suitable for higher-level taxonomic identification, whereas ITS2 provides enhanced species-level differentiation (79,84).

Physicochemical measurements, including water content and electrical conductivity, showed that most samples were within acceptable quality limits. While these parameters alone cannot confirm adulteration, they provide useful supplementary information due to their simplicity, low cost, and rapid execution.

NMR analysis, performed on 20 honey samples, demonstrated the potential of spectral fingerprinting to differentiate honey types such as chestnut, forest, acacia, and linden honey. Moreover, deviations in NMR profiles enabled identification of atypical samples within the same honey category. For instance, sample HP25, labelled as forest honey, showed spectral deviations and lower electrical conductivity values compared to typical forest honey samples, and inconsistent amplification in several PCR-HRM assays. These observations highlight the value of combining analytical approaches for detecting anomalies.

Overall, this study demonstrates that PCR-HRM analysis, particularly using the BEE2_1 and PL1 assays, represents a rapid and effective screening approach for assessing the entomological and botanical origin of honey. When complemented by physicochemical measurements and NMR profiling, a more comprehensive assessment of honey authenticity can be achieved.

This study represents the first master's thesis in our research group focusing on honey authentication using DNA barcoding. The initial results are very promising, demonstrating that the PCR-HRM approach can discriminate honeybee subspecies and detect plant-derived DNA in honey samples. Future studies including additional genetic markers and a larger sample set will be necessary to further improve the robustness and applicability of this multi-method approach, enabling more comprehensive identification of both honeybee subspecies and plant species.

7 Materials

7.0.1 Laboratory Equipment

Table 14 Name and manufacturer of laboratory equipment used in this research

Name	Manufacturer
Analytical balance TE214S	Sartorius
Thermomixer C Eppendorf	Eppendorf
Vortex Vortex-Genie 2	Scientific Industries
Centrifuge 5425	Eppendorf
Centrifuge 5910 Ri	Eppendorf
PCR Workstation Pro	VWR International
Pipette Xplorer, 0.5–10 µL	Eppendorf
Pipette Xplorer, 1–20 µL	Eppendorf
Pipette Xplorer, 10–200 µL	Eppendorf
Pipette Xplorer, 50–1000 µL	Eppendorf
Pyromark Q48 Autoprep	Qiagen
Quantstudio 5 Thermocycler	Thermo Fisher
Qubit 4 Fluorometer	Invitrogen Thermo Fischer
Rotor Gene Q Thermocycler	Qiagen
FastPrep-24 5G Instrument	MP Biomedicals
pH meter 691	Metrohm
Ultrashield 500 Plus	Bruker
Beekeeper Refractometer Honey 12–30%	HHTEC
Water Moist Hand Refractometer	
pH meter with conductivity electrode	
MP Biomedicals FastPrep-24 5G Bead Beating Grinder and Lysis System	Fisher Scientific

7.0.2 Solutions

Table 15 Name and manufacturer of solutions used in this research

Name	Manufacturer
DNA/RNA-ExitusPlus IF	ITW Reagents
ELGA water	Department of Analytical Chemistry, University of Vienna
2x Type-it HRM PCR Kit	Qiagen
Ethanol (abs.)	Merck
Oligonucleotides (primer)	Sigma Aldrich
PyroMark PCR Kit	Qiagen
PyroMark Q48 Advanced CpG Reagents	Qiagen
PyroMark Q48 Magnetic Beads	Qiagen
RNase-free water	Qiagen
Qubit ds DNA HS Assay Kit	Invitrogen Thermo Fisher Scientific

Qubit ds DNA BR Assay Kit	Invitrogen Thermo Fisher Scientific
DNeasy maricon Food Kit	Qiagen
Formaldehyde	Merck
Electrical conductivity calibration solution (1413 µS/cm)	Roth

7.0.3 Software

Table 16 Name and manufacturer of software, that were used during the research

Name	Manufacturer
PyroMark Assay Design Software 2.0	Qiagen
PyroMark Q24 Advanced 3.0.1	Qiagen
PyroMark Q48 Autoprep	Qiagen
QuantStudio Design & Analysis Software	Thermo Fisher Scientific
Rotor-Gene Q Series Software 2.3.1	Qiagen
Microsoft Office 365 (Excel, Word)	Microsoft
Origin Pro 2024 10.1.0.170	OriginLab
ChatGPT was used to check and improve the grammar and style of the own-written text	OpenAI
DeepL Translator	DeepL GmbH

7.0.4 Other

Table 17 Other materials that were used during this research

Name	Manufacturer
Biosphere Filter Tips (0.5–20 µL)	Sarstedt
Biosphere Filter Tips (100–1000 µL)	Sarstedt
Safe Lock Tubes (1.5, 2, and 5 mL)	Eppendorf
duoSHIELD, PFT Nitrile 240 Gloves	Shield Scientific
Strip Tubes and Caps, 0.1 mL	Qiagen

8 Bibliography

1. FAO/WHO Codex Alimentarius Commission. CODEX STAN 12-1981, Rev.1 (1987), Rev.2 (2001)1. <https://www.fao.org/fao-who-codexalimentarius/sh-proxy/es/?lnk=1&url=https%253A%252F%252Fworkspace.fao.org%252Fsites%252Fcodex%252FStandards%252FCXS%2B12-1981%252FCXS_012e.pdf> Accessed 26.02.17.
2. European Union. *Council Directive 2001/110/EC of 20 December 2001 Relating to Honey*; 2001; pp 47–52. <https://eur-lex.europa.eu/eli/dir/2001/110/oj> Accessed 25.11.12.
3. AGES. Kennzeichnung von Honig, 2020. <https://www.ages.at/download/sdl-eyJ0eXAiOiJKV1QiLCJhbGciOiJIUzI1NiJ9.eyJpYXQiOjE2MDk0NTkyMDAsImV4cCI6NDA3MDkwODgwMCwidXNlciI6MCwiZ3JvdXBzIjpbMCwtMV0sImZpbGUiOiJmaWxlYWRtaW4vQUdFU18yMDIyLzJfTUVOU0NIL0Vyblx1MDBlNGhydW5nX0xlYmVuc21pdHRlbC9MZWJlbnNtaXR0ZWxpbmZvcm1hdGlvbmVuL0hvbmlnL0hvbmlnX0tlbm56ZWljaG51bmcucGRmIiwicGFnZSI6MTQzMH0.kc6Q0WLG9NhSC2Nb5q7kzdTRQ0saRQlChQ7sKFYLKSU/Honig_Kennzeichnung.pdf> Accessed 25.12.01.
4. Tlak Gajger, I.; Dar, S. A.; Ahmed, M. M. M.; Aly, M. M.; Vlainić, J. Antioxidant Capacity and Therapeutic Applications of Honey: Health Benefits, Antimicrobial Activity and Food Processing Roles. *Antioxidants* 2025, *14*(8), 959. doi:10.3390/antiox14080959.
5. Bezerra, A.; Fonseca, H.; Rodrigues, F.; Delerue-Matos, C.; Gouvinhas, I.; Garcia, J. Honey Therapy in Diabetic Foot Ulcers: A Promising Strategy for Effective Wound Healing. *Applied Sciences* 2023, *13*(23), 12820. doi:10.3390/app132312820.
6. FAOSTAT – Countries by Commodity (Rankings). *FAOSTAT – Countries by Commodity (Rankings)*. <https://www.fao.org/faostat/en/#rankings/countries_by_commodity> Accessed 25.12.01.
7. Bundesministerium für Soziales, Gesundheit, Pflege und Konsumentenschutz. *Honigkontrolle Verbrauchergesundheit – Lebensmittelkontrolle*. <https://www.verbrauchergesundheit.gv.at/lebensmittel/lebensmittelkontrolle/Honigkontrolle.html> Accessed 25.11.28.
8. Geana, E.-I.; Ciucure, C. T. Establishing authenticity of honey via comprehensive Romanian honey analysis. *Food Chemistry* 2020, *306*, 125595. doi:10.1016/j.foodchem.2019.125595.
9. U.S. Food and Drug Administration (FDA). Economically Motivated Adulteration of Food (Food Fraud). <https://www.fda.gov/food/compliance-enforcement-food/economically-motivated-adulteration-food-fraud> Accessed 25.11.21.
10. European Commission / Knowledge4Policy. *Adulteration of Honey – Food Fraud & Quality*. <https://knowledge4policy.ec.europa.eu/food-fraud-quality_en/adulteration-honey_en)> Accessed 25.11.11.
11. Zhang, X.-H.; Gu, H.-W.; Liu, R.-J.; Qing, X.-D.; Nie, J.-F. A comprehensive review of the current trends and recent advancements on the authenticity of honey. *Food Chemistry: X* 2023, *19*, 100850. doi:10.1016/j.fochx.2023.100850.
12. Honrado, M.; Lopes, A. R.; Pinto, M. A.; Amaral, J. S. A novel real-time PCR coupled with high resolution melting analysis as a simple and fast tool for the entomological authentication of honey by targeting Apis mellifera mitochondrial DNA. *Food Research International* 2022, *161*, 111761. doi:10.1016/j.foodres.2022.111761.

13. Jusline. *K-BiWG - Kärntner Bienenwirtschaftsgesetz IV. Abschnitt Bienenzucht § 11*. <https://www.ris.bka.gv.at/NormDokument.wxe?Abfrage=LrK&Gesetzesnummer=20000208&Artikel=&Paragraf=11&Anlage=&Uebergangsrecht=&ShowPrintPreview=True> Accessed 26.02.17.
14. Das Rechtsinformationssystem des Bundes (RIS). *Steiermärkisches Bienenzuchtgesetz*; LGBl. Nr. 18/1998 § 22. <https://www.ris.bka.gv.at/NormDokument.wxe?Abfrage=LrStmk&Gesetzesnummer=20000846&Artikel=&Paragraf=22&Anlage=&Uebergangsrecht=> Accessed 26.02.16.
15. Tennakoon, S.; Apan, A.; Maraseni, T. Unravelling the impact of climate change on honey bees: An ensemble modelling approach to predict shifts in habitat suitability in Queensland, Australia. *Ecology and Evolution* 2024, *14*(4), e11300. doi:10.1002/ece3.11300.
16. European Union. *Richtlinie (EU) 2024/1438*; 2024; pp 1–19. <https://eur-lex.europa.eu/legal-content/DE/TXT/PDF/?uri=OJ:L_202401438> Accessed 26.02.17.
17. Kaškonienė, V.; Venskutonis, P. R. Floral Markers in Honey of Various Botanical and Geographic Origins: A Review. *Comprehensive Reviews in Food Science and Food Safety* 2010, *9*(6), 620–634. doi:10.1111/j.1541-4337.2010.00130.x.
18. Von Der Ohe, W.; Persano Oddo, L.; Piana, M. L.; Morlot, M.; Martin, P. Harmonized methods of melissopalynology. *Apidologie* 2004, *35*(Suppl. 1), S18–S25. doi:10.1051/apido:2004050.
19. Sobrino-Gregorio, L.; Vargas, M.; Chiralt, A.; Escriche, I. Thermal properties of honey as affected by the addition of sugar syrup. *Journal of Food Engineering* 2017, *213*, 69–75. doi:10.1016/j.jfoodeng.2017.02.014.
20. Won, S.-R.; Lee, D.-C.; Ko, S. H.; Kim, J.-W.; Rhee, H.-I. Honey major protein characterization and its application to adulteration detection. *Food Research International* 2008, *41*(10), 952–956. doi:10.1016/j.foodres.2008.07.014.
21. AOAC International. *AOAC Official Method 998.12*; 998.12. <https://brooksapplied.com/wp-content/uploads/AOAC_Method998-12_Honey_Adulteration.pdf> Accessed 26.02.17.
22. Novais, L. M. R. D.; Santos, M. D. F. C.; Marques, A. C. Q.; Mascarenhas, R. D. O.; Freitas, J. M. D.; Andrade, M. V. D. O.; et al. Combining analytical techniques to detect honey adulteration in Brazil – A case study. *Journal of Food Composition and Analysis* 2025, *144*, 107716. doi:10.1016/j.jfca.2025.107716.
23. Kuballa, T.; Brunner, T. S.; Thongpanchang, T.; Walch, S. G.; Lachenmeier, D. W. Application of NMR for authentication of honey, beer and spices. *Current Opinion in Food Science* 2018, *19*, 57–62. doi:10.1016/j.cofs.2018.01.007.
24. Zhang, G.; Abdulla, W. On honey authentication and adulterant detection techniques. *Food Control* 2022, *138*, 108992. doi:10.1016/j.foodcont.2022.108992.
25. Donarski, J. A.; Jones, S. A.; Harrison, M.; Driffield, M.; Charlton, A. J. Identification of botanical biomarkers found in Corsican honey. *Food Chemistry* 2010, *118*(4), 987–994. doi:10.1016/j.foodchem.2008.10.033.
26. Liu, M.; Clarke, L. J.; Baker, S. C.; Jordan, G. J.; Burridge, C. P. A practical guide to DNA metabarcoding for entomological ecologists. *Ecological Entomology* 2020, *45*(3), 373–385. doi:10.1111/een.12831.
27. Hebert, P. D. N.; Cywinska, A.; Ball, S. L.; deWaard, J. R. Biological identifications through DNA barcodes. *Proceedings of the Royal Society of London. Series B: Biological Sciences* 2003, *270*(1512), 313–321. doi:10.1098/rspb.2002.2218.

28. Wirta, H.; Abrego, N.; Miller, K.; Roslin, T.; Vesterinen, E. DNA traces the origin of honey by identifying plants, bacteria and fungi. *Scientific Reports* 2021, *11*(1), 4798. doi:10.1038/s41598-021-84174-0.
29. Borkowska, M.; Burzyńska, M.; Piasecka-Kwiatkowska, D.; Celińska, E. Tracking adulteration of nectar honey varieties using a high-resolution melting qPCR technique validated with melissopalinology. *Food Control* 2024, *155*, 110086. doi:10.1016/j.foodcont.2023.110086.
30. Al-Kahtani, H. A.; Ismail, E. A.; Asif Ahmed, M. Pork detection in binary meat mixtures and some commercial food products using conventional and real-time PCR techniques. *Food Chemistry* 2017, *219*, 54–60. doi:10.1016/j.foodchem.2016.09.108.
31. Sobrino-Gregorio, L.; Vilanova, S.; Prohens, J.; Escriche, I. Detection of honey adulteration by conventional and real-time PCR. *Food Control* 2019, *95*, 57–62. doi:10.1016/j.foodcont.2018.07.037.
32. Ruttner, F. Chapter 1: The Genus Apis. In *Biogeography and Taxonomy of Honeybees*; Springer Berlin Heidelberg: Berlin, Heidelberg, 1988; pp 3–13. doi:10.1007/978-3-642-72649-1.
33. Van Nest, B. N.; Moore, D. Energetically optimal foraging strategy is emergent property of time-keeping behavior in honey bees. *Behavioral Ecology* 2012, *23*(3), 649–658. doi:10.1093/beheco/ars010.
34. Engel, M. S. The Taxonomy of Recent and Fossil Honey Bees (Hymenoptera: Apidae; Apis). 1999. doi:10.5281/ZENODO.16256755.
35. Ruttner, F.; Lindauer, M. Die Westliche Honigbiene, Apis mellifera Linnaeus, 1758 in systematischer Übersicht. In *Naturgeschichte der Honigbienen: Biologie, Sozialleben, Arten und Verbreitung, 2. Auflage*; Franckh-Kosmos Verlag: Stuttgart, 2003; pp 188–236.
36. De La Rúa, P.; Jaffé, R.; Dall'Olio, R.; Muñoz, I.; Serrano, J. Biodiversity, conservation and current threats to European honeybees. *Apidologie* 2009, *40*(3), 263–284. doi:10.1051/apido/2009027.
37. Ellis, J. S.; Soland-Reckeweg, G.; Buswell, V. G.; Huml, J. V.; Brown, A.; Knight, M. E. Introgression in native populations of Apis mellifera mellifera L: implications for conservation. *Journal of Insect Conservation* 2018, *22*(3–4), 377–390. doi:10.1007/s10841-018-0067-7.
38. Zhang, Y.-Z.; Chen, Y.-F.; Wu, Y.-Q.; Si, J.-J.; Zhang, C.-P.; Zheng, H.-Q.; et al. Discrimination of the entomological origin of honey according to the secretions of the bee (Apis cerana or Apis mellifera). *Food Research International* 2019, *116*, 362–369. doi:10.1016/j.foodres.2018.08.049.
39. Soares, S.; Grazina, L.; Mafra, I.; Costa, J.; Pinto, M. A.; Duc, H. P.; et al. Novel diagnostic tools for Asian (Apis cerana) and European (Apis mellifera) honey authentication. *Food Research International* 2018, *105*, 686–693. doi:10.1016/j.foodres.2017.11.081.
40. Moškrič, A.; Mole, K.; Prešern, J. EPIC markers of the genus Apis as diagnostic tools for detection of honey fraud. *Food Control* 2021, *121*, 107634. doi:10.1016/j.foodcont.2020.107634.
41. Utzeri, V. J.; Ribani, A.; Fontanesi, L. Authentication of honey based on a DNA method to differentiate Apis mellifera subspecies: Application to Sicilian honey bee (A. m. siciliana) and Iberian honey bee (A. m. iberiensis) honeys. *Food Control* 2018, *91*, 294–301. doi:10.1016/j.foodcont.2018.04.010.

42. Utzeri, V. J.; Ribani, A.; Taurisano, V.; Fontanesi, L. Entomological authentication of honey based on a DNA method that distinguishes Apis mellifera mitochondrial C mitotypes: Application to honey produced by A. m. ligustica and A. m. carnica. *Food Control* 2022, *134*, 108713. doi:10.1016/j.foodcont.2021.108713.
43. Mackay, I. M. Real-time PCR in virology. *Nucleic Acids Research* 2002, *30*(6), 1292–1305. doi:10.1093/nar/30.6.1292.
44. Everman, S.; Wang, S. Y. Distinguishing Anuran species by high-resolution melting analysis of the COI barcode (COI-HRM). *Ecology and Evolution* 2019, *9*(23), 13515–13520. doi:10.1002/ece3.5808.
45. Pathiraja, D.; Cho, J.; Kim, J.; Choi, I.-G. Metabarcoding of eDNA for tracking the floral and geographical origins of bee honey. *Food Research International* 2023, *164*, 112413. doi:10.1016/j.foodres.2022.112413.
46. Dodd, S.; Kevei, Z.; Karimi, Z.; Kumar, J. J. S.; Koidis, A.; Anastasiadi, M. Tracing the botanical origins of UK heather honey by relative quantification of plant DNA. *npj Science of Food* 2025, *9*(1), 196. doi:10.1038/s41538-025-00561-1.
47. Fahner, N. A.; Shokralla, S.; Baird, D. J.; Hajibabaei, M. Harmonised methods of the international honey commission. *PLOS ONE* 2016, *11*(6), e0157505. doi:10.1371/journal.pone.0157505.
48. Ullah, S.; Huyop, F.; Wahab, R. A.; Sujana, I. G. A.; Antara, N. S.; Gunam, I. B. W. Using pollen DNA metabarcoding to trace the geographical and botanical origin of honey from Karangasem, Indonesia. *Heliyon* 2024, *10*(12), e33094. doi:10.1016/j.heliyon.2024.e33094.
49. Matissek, R.; Fischer, M. DNA-Isolierungsverfahren. In *Lebensmittelanalytik, 7. Auflage*; Springer Berlin Heidelberg: Berlin, Heidelberg, 2021; pp 291–293. doi:10.1007/978-3-662-63409-7.
50. Qiagen. DNeasy mericon Food Handbook, 2020. <https://www.qiagen.com/us/resources/resourcedetail?id=bd9cc2a8-aa71-4cb5-b6f7-97b3d7fc306d&lang=en> Accessed 26.02.17.
51. Schenk, J. J.; Becklund, L. E.; Carey, S. J.; Fabre, P. P. What is the “modified” CTAB protocol? Characterizing modifications to the CTAB DNA extraction protocol. *Applications in Plant Sciences* 2023, *11*(3), e11517. doi:10.1002/aps3.11517.
52. Thermo Fisher Scientific Inc. *Invitrogen™ Qubit™ 4 Fluorometer*. <https://www.fishersci.de/shop/products/qubit-4-fluorometer/15723679?change_lang=true> Accessed 25.12.03.
53. Müller, H.-J.; Prange, D. R. In *PCR - Polymerase-Kettenreaktion, 2. Auflage*; Springer Berlin Heidelberg: Berlin, Heidelberg, 2016; pp 2–9. doi:10.1007/978-3-662-48236-0.
54. Kubista, M.; Andrade, J. M.; Bengtsson, M.; Forootan, A.; Jonák, J.; Lind, K.; et al. The real-time polymerase chain reaction. *Molecular Aspects of Medicine* 2006, *27*(2–3), 95–125. doi:10.1016/j.mam.2005.12.007.
55. Schmidt, O. G. In *Genetik und Molekularbiologie, 2. Auflage*; Kompaktwissen Biologie; Springer Berlin Heidelberg: Berlin, Heidelberg, 2023; pp 379–385. doi:10.1007/978-3-662-66947-1.
56. Matissek, R.; Hahn, A. Aminosäuren, Peptide, Proteine und Nucleinsäuren. In *Lebensmittelchemie, 10., neu bearbeitete und aktualisierte Auflage*; Springer Berlin Heidelberg: Berlin, Heidelberg, 2023; pp 321–326. doi:10.1007/978-3-662-66925-9.
57. Metzker, M. L.; Caskey, T. C. Polymerase Chain Reaction (PCR). In *Encyclopedia of Life Sciences*; Wiley, 2003. doi:10.1038/npg.els.0000998.

58. Dorak, M. In *Real-Time PCR*; Advanced Methods Series; CRC Press LLC: Milton, 2006; pp 3–145.
59. Integrated DNA Technologies, Inc. OligoAnalyzer™: Primer analysis tool. <https://eu.idtdna.com/pages/tools/oligoanalyzer> Accessed 25.11.11.
60. Oligonucleotide Properties Calculator. <https://oligocalc.eu> Accessed 25.04.12.
61. Institute for Theoretical Chemistry | University of Vienna. RNAfold WebServer. <http://rna.tbi.univie.ac.at/cgi-bin/RNAWebSuite/RNAfold.cgi> Accessed 25.12.04.
62. National Library of Medicine. Basic Local Alignment Search Tool. <https://blast.ncbi.nlm.nih.gov/Blast.cgi> Accessed 25.12.04.
63. Ableitner, O. Molekularbiologische Methoden. In *Einführung in die Molekularbiologie, 2. Auflage*; essentials; Springer Fachmedien Wiesbaden: Wiesbaden, 2018; pp 33–52. doi:10.1007/978-3-658-20624-6.
64. *A Guide to Forensic DNA Profiling*; Jamieson, A., Bader, S., Eds.; John Wiley & Sons: Chichester, West Sussex, UK, 2016.
65. Mülhardt, C. *Der Experimentator: Molekularbiologie / Genomics*; 6. Aufl. 2009.; Experimentator; Spektrum Akademischer Verlag: Heidelberg, 2009. doi:10.1007/978-3-8274-2158-6.
66. Hawkins, J.; De Vere, N.; Griffith, A.; Ford, C. R.; Allainguillaume, J.; Hegarty, M. J.; et al. Using DNA Metabarcoding to Identify the Floral Composition of Honey: A New Tool for Investigating Honey Bee Foraging Preferences. *PLOS ONE* 2015, *10*(8), e0134735. doi:10.1371/journal.pone.0134735.
67. Wallberg, A.; Han, F.; Wellhagen, G.; Dahle, B.; Kawata, M.; Haddad, N.; et al. A worldwide survey of genome sequence variation provides insight into the evolutionary history of the honeybee Apis mellifera. *Nature Genetics* 2014, *46*(10), 1081–1088. doi:10.1038/ng.3077.
68. Reed, G. H.; Kent, J. O.; Wittwer, C. T. High-Resolution DNA Melting Analysis for Simple and Efficient Molecular Diagnostics. *Pharmacogenomics* 2007, *8*(6), 597–608. doi:10.2217/14622416.8.6.597.
69. Druml, B.; Cichna-Markl, M. High resolution melting (HRM) analysis of DNA – Its role and potential in food analysis. *Food Chemistry* 2014, *158*, 245–254. doi:10.1016/j.foodchem.2014.02.111.
70. Słomka, M.; Sobalska-Kwapis, M.; Wachulec, M.; Bartosz, G.; Strapagiel, D. High Resolution Melting (HRM) for High-Throughput Genotyping—Limitations and Caveats in Practical Case Studies. *International Journal of Molecular Sciences* 2017, *18*(11), 2316. doi:10.3390/ijms18112316.
71. Ronaghi, M. Pyrosequencing Sheds Light on DNA Sequencing. *Genome Research* 2001, *11*(1), 3–11. doi:10.1101/gr.11.1.3.
72. Ahmadian, A.; Ehn, M.; Hober, S. Pyrosequencing: History, biochemistry and future. *Clinica Chimica Acta* 2006, *363*(1–2), 83–94. doi:10.1016/j.cccn.2005.04.038.
73. Metzker, M. L. Sequencing technologies — the next generation. *Nature Reviews Genetics* 2010, *11*(1), 31–46. doi:10.1038/nrg2626.
74. Stefan Bogdanov, Bee Product Science. Harmonised methods of the international honey commission, 2009. <https://www.ihc-platform.net/ihcmethods2009.pdf> Accessed 26.02.17.
75. Vorwohl, G. Die beziehungen zwischen der elektrischen leitfähigkeit der honige und ihrer trachtmäßigen herkunft. *Annales de l'Abeille* 1964, *7*(4), 301–309. doi:10.1051/apido:19640403.

76. Soares, S.; Amaral, J. S.; Oliveira, M. B. P. P.; Mafra, I. Improving DNA isolation from honey for the botanical origin identification. *Food Control* 2015, *48*, 130–136. doi:10.1016/j.foodcont.2014.02.035.
77. Hillinger, S.; Saeckler, J.; Domig, K. J.; Dobrovolny, S.; Hochegger, R. Development of a DNA Metabarcoding Method for the Identification of Insects in Food. *Foods* 2023, *12*(5), 1086. doi:10.3390/foods12051086.
78. Chen, S.; Yao, H.; Han, J.; Liu, C.; Song, J.; Shi, L.; et al. Validation of the ITS2 Region as a Novel DNA Barcode for Identifying Medicinal Plant Species. *PLoS ONE* 2010, *5*(1), e8613. doi:10.1371/journal.pone.0008613.
79. Bruni, I.; Galimberti, A.; Caridi, L.; Scaccabarozzi, D.; De Mattia, F.; Casiraghi, M.; et al. A DNA barcoding approach to identify plant species in multiflower honey. *Food Chemistry* 2015, *170*, 308–315. doi:10.1016/j.foodchem.2014.08.060.
80. QIAGEN GmbH, QIAGEN Strasse 1, 40724 Hilden, GERMANY. PyroMark® Q48 Autoprep User Manual, Version 1.0, 2025. <https://www.qiagen.com/us/resources/resourcedetail?id=650a0c13-3b8e-4a77-b433-6b1e50b9525a&lang=en> Accessed 26.02.18.
81. Wildbacher, M.; Andronache, J.; Pühringer, K.; Dobrovolny, S.; Hochegger, R.; Cichna-Markl, M. Authentication of EU-Authorized Edible Insect Species in Food Products by DNA Barcoding and High-Resolution Melting (HRM) Analysis. *Foods* 2025, *14*(5), 751. doi:10.3390/foods14050751.
82. Richardson, R. T.; Lin, C.; Sponsler, D. B.; Quijia, J. O.; Goodell, K.; Johnson, R. M. Application of ITS2 metabarcoding to determine the provenance of pollen collected by honey bees in an agroecosystem. *Applications in Plant Sciences* 2015, *3*(1), 1400066. doi:10.3732/apps.1400066.
83. *Leitfähigkeitsmessung von Honig*. <https://imkerverein-buchen.de/wp-content/uploads/2018/11/Leitfaehigkeitsmessung_Honig.pdf> Accessed 26.01.02.
84. Qin, Y.; Li, M.; Cao, Y.; Gao, Y.; Zhang, W. Molecular thresholds of ITS2 and their implications for molecular evolution and species identification in seed plants. *Scientific Reports* 2017, *7*(1), 17316. doi:10.1038/s41598-017-17695-2.

9 Appendix

9.1 List of abbreviations

A- adenine
AGES- Austrian Agency for Health and Food Safety
AOAC- Association of Official Analytical Chemists
bp- basepair
BLAST- Basic Local Alignment Search Tool
C- cytosine
COI- cytochrome c oxidase subunit I
Ct- cycle threshold
dATP- deoxyadenosine triphosphate
dCTP- deoxycytidine triphosphate
dGTP- deoxyguanosine triphosphate
dH_2O- distilled water
dTTP- thymidine triphosphate
DNA- deoxyribonucleic acid
EB- elution buffer
EtOH- ethanol
Fwd- forward
G- guanine
GC- guanine-cytosine
HRM- high resolution melting analysis
H_2O- water
ITS2- internal transcribed spacer
mg- milligram
min- minute
mL- milliliter
lab- laboratory
NCBI- National Center for Biotechnology Information
NGS- next-generation sequencing
NMR- nuclear magnetic resonance
ng- nanogram
NTC- no template control
PCR- polymerase chain reaction
PSQ- pyrosequencing

rbcL- ribulose bisphosphate carboxylase large chain

rev- reverse

RNA- ribonucleic acid

rpm- rounds per minute

s- second

SNP- single nucleotide polymorphism

Seq- sequencing

T- thymidine

T_A- annealing temperature

T_E- elongation temperature

Tg- the glass transition temperature

Tm- melting temperature

TSP- trimethylsilyl propanoic acid

µg- microgram

µL- microliter

µM- micromolar

%- percent

°C- degree Celsius

UV- ultraviolet

9.2 List of figures

9.3 List of tables

9.4 Raw data

Table S1 Overview of honey samples (HP1–HP56) including sample ID, honey type, and DNA concentration in ng/µL.

Sample ID	Sample	Concentration [ng/µL]
HP1	Forest honey	2.16
HP2	Forest honey	2.96
HP3	Forest honey	2.64
HP4	Forest honey	2.14
HP5	Forest honey	6.26
HP6	Forest honey	3.00
HP7	Organic forest honey	1.46
HP8	Organic forest honey	1.09
HP9	Forest honey	2.26
HP10	Organic pine honey	0.51
HP11	Organic forest honey	1.44
HP12	Vegan honey-honey alternative	0.02
HP13	Organic forest honey	2.14
HP14	Forest honey	0.03
HP15	Forest honey	0.44
HP16	Organic forest honey	2.18
HP17	Organic forest honey	3.70
HP18	Organic forest honey with blossom honey	2.52
HP19	Organic forest honey	2.94
HP20	Forest honey	1.23
HP21	Forest honey	1.28
HP22	Forest honey	2.38
HP23	Forest honey	2.96
HP24	Forest honey	3.48
HP25	Forest honey	0.05
HP26	Forest honey with pine thyme	2.16
HP27	Forest honey with heather	2.38
HP28	Forest honey with sage	2.40
HP29	Mountain honey with white thyme	1.14
HP30	Forest honey	0.72
HP31	Blueberry honey	2.62
HP32	Acacia honey	0.07
HP33	Cornflower honey	0.12
HP34	Honey with turmeric	0.58
HP35	North German early bloom honey	0.75
HP36	Fennel in honey	4.46
HP37	Chestnut honey	1.91
HP38	Linden blossom	0.60
HP39	Blossom honey with acacia	0.08

HP40	Pine honey	0.38
HP41	Forest and blossom honey	4.18
HP42	Honey dew honey	5.34
HP43	Organic honey dew honey	5.78
HP44	Organic acacia honey	0.10
HP45	Organic linden honey	1.15
HP46	Raw forest honey	3.06
HP47	Syrup (90%) + honey (10%)	0.02
HP48	Blossom honey	1.44
HP49	Acacia honey	0.37
HP50	Goldenrod honey	3.96
HP51	Linden honey	0.80
HP52	Forest honey	7.62
HP53	Forest honey	8.5
HP54	Field honey	0.32
HP55	Mixed blossom honey	0.64
HP56	Sage honey	2.06

Table S2 Sample ID, plant as positive control, concentration of DNA extract in ng/µL

Sample ID	Sample	Concentration [ng/µL]
RK	Red clover	7.54
WK	White clover	6.52
MSA	Clary sage	9.76
RA	Black locust	9.46
LB	Linden	5.22
GE	Common ash	4.44
BM	Bee magnet	10.80
IK	Crimson clover	7.86
SWB	Plantain	7.84
KA	Chamomile	6.58
BN	Nettle	6.10
FE	Fennel	5.24
ANIS	Anise	89.10
MM	Mallow bloom	141.00
SFG	Yarrow	33.10
PF	Peppermint	29.00
QR	Oak	580.00
SLB1	Sage (leaves)	9.22
SLB2	Sage (seed)	7.74
Raps	Rape	7.42
EK	Sweet chestnut	7.44
PT	Lacy phacelia	6.38

Table S3 Sample ID, honeybee subspecies and DNA concentration of extract in ng/µL

Sample ID	Honeybee subspecies	Origin	Concentration [ng/µL]
HPBF1.1	*A. m. carnica*	Styria, Austria	7.66
HPBF1.2	*A. m. carnica*	Styria, Austria	8.42
HPBF2.1	*A. m. carnica*	Bosnia & Hercegovina	9.04
HPBF2.2	*A. m. carnica*	Bosnia & Hercegovina	8.42
HPBF3.1	*A. m. carnica*	Bosnia & Hercegovina	8.08
HPBF3.2	*A. m. carnica*	Bosnia & Hercegovina	8.04
HPBF4	*A. m. carnica*	Croatia	9.29
HPBF5.1	*A. m. carnica*	Salzburg Austria	10,.2
HPBF5.1.1	*A. m. carnica*	Salzburg Austria	9.0
HPBF5.2	*A. m. carnica*	Salzburg Austria	8.04
PBF1.1	*A. m. carnica*	Lower Austria	10.8
PBF1.2	*A. m. carnica*	Lower Austria	9.52
PBF2.1	*A. m. carnica*	Lower Austria	8.82
PBF2.2	*A. m. carnica*	Lower Austria	8.32
PBF3.1	*A. m. carnica*	Vienna, Austria	6.48
PBF3.2	*A. m. carnica*	Vienna, Austria	10.8
PBF4.1	*A. m. carnica*	Lower Austria	8.76
PBF4.2	*A. m. carnica*	Lower Austria	10.6
PBF5.1	*A. m. carnica*	Lower Austria	9.52
PBF5.2	*A. m. carnica*	Lower Austria	9.66
PBF6.1	*A. m. carnica*	Lower Austria	9.32
PBF6.2	*A. m. carnica*	Lower Austria	8.4
PBF7.1	*A. m. macedonica*	North Macedonia	9.3
PBF7.2	*A. m. macedonica*	North Macedonia	9.92

Table S4 Ct values for all positive controls amplified with assay PL1.

PL1 (Threshold=0.04)	
Sample	Ct
False acacia	18.91
False acacia	18.75
Linden	16.71
Linden	16.51
Common ash	26.99
Common ash	27.56
Bee magnet	13.62
Bee magnet	13.55
Crimson clover	21.02
Crimson clover	21.15
Plantain	24.12
Plantain	23.97
Chamomile	17.62
Chamomile	17.77
Nettle	19.64
Nettle	19.33
Fennel	24.04
Fennel	24.01
Anise	16.64
Anise	16.55
Mallow bloom	21.78
Mallow bloom	21.91
Yarrow	20.83
Yarrow	21.02
Peppermint	25.28
Peppermint	25.23
Oak	28.53
Oak	28.79
Red clover	20.11
Red clover	20
White clover	12.66
White clover	12.42
Clary sage	24.76
Clary sage	24.73
Rape	10.54
Rape	10.62
Sage	23.37
Sage	23.52
Sage	24.83
Sage	24.74
Sweet chestnut	24.78
Sweet chestnut	24.95
Lacy phacelia	27.1
Lacy phacelia	27.13

Table S5 Ct values for all positive controls amplified with assay PL2_1.

PL2_1 (Threshold=0.025)	
Sample	Ct
False acacia	9.93
False acacia	9.61
Linden	14.25
Linden	14.43
Common ash	14.94
Common ash	14.98
Bee magnet	8.73
Bee magnet	8.61
Crimson clover	9.83
Crimson clover	9.87
Plantain	10.71
Plantain	10.63
Chamomile	9.51
Chamomile	9.6
Nettle	16.25
Nettle	15.95
Fennel	8.78
Fennel	8.86
Anise	11.29
Anise	11.1
Mallow bloom	9.82
Mallow bloom	9.9
Yarrow	9.75
Yarrow	9.66
Peppermint	14.62
Peppermint	13.13
Oak	22.16
Oak	-
Red clover	9.24
Red clover	9.26
White clover	9.82
White clover	9.82
Clary sage	11.91
Clary sage	11.77
Rape	7.72
Rape	7.71
Sage	9.44
Sage	9.34
Sage	10.2
Sage	9.85
Sweet chestnut	13.98
Sweet chestnut	12.99
Lacy phacelia	11.91
Lacy phacelia	11.71

Table S6 Ct values for all positive controls amplified with assay PL3_1.

PL3_1 (Threshold=0.05)	
Sample	Ct
False acacia	14.2
False acacia	14.04
Linden	29.64
Linden	30.43
Common ash	21.03
Common ash	21.21
Bee magnet	18.17
Bee magnet	18.24
Crimson clover	32.95
Crimson clover	32.65
Plantain	17.71
Plantain	17.51
Chamomile	23.1
Chamomile	22.44
Nettle	19.15
Nettle	18.87
Fennel	20.5
Fennel	20.54
Anise	20.25
Anise	20.23
Mallow bloom	20.23
Mallow bloom	20.41
Yarrow	16.78
Yarrow	16.65
Peppermint	17.78
Peppermint	17.62
Oak	35.19
Oak	35.06
Red clover	32.81
Red clover	32.88
White clover	26.65
White clover	26.63
Clary sage	16.1
Clary sage	16.24
Rape	16.08
Rape	16.17
Sage	15.36
Sage	15.51
Sage	16.54
Sage	16.64
Sweet chestnut	16.64
Sweet chestnut	16.7
Lacy phacelia	24.16
Lacy phacelia	24.56

Table S7 Values of water content and electrical conductivity of 51 honey samples (HP1–HP51)

Sample	Honey type	Water content (%)	Electrical conductivity (µS/cm)
HP1	Forest honey	16.2	1057
HP2	Forest honey	16	1137
HP3	Forest honey	16.2	868
HP4	Forest honey	15	1199
HP5	Forest honey	15.8	961
HP6	Forest honey	15.4	993
HP7	Organic forest honey	15.6	1113
HP8	Organic forest honey	15.8	1056
HP9	Forest honey	16.7	1073
HP10	Organic pine honey	15.4	1478
HP11	Organic forest honey	15	1303
HP12	Vegan honey-honey alternative	17.2	783
HP13	Organic forest honey	15.3	1206
HP14	Forest honey	17.4	509
HP15	Forest honey	15.2	1090
HP16	Organic forest honey	15	1003
HP17	Organic forest honey	16.5	1280
HP18	Organic forest honey with blossom honey	16.6	779
HP19	Organic forest honey	15.4	1137
HP20	Forest honey	14.5	1228
HP21	Forest honey	15	1308
HP22	Forest honey	16.2	1101
HP23	Forest honey	16.5	1118
HP24	Forest honey	16.5	997
HP25	Forest honey	15.5	348
HP26	Forest honey with pine thyme	16.3	1026
HP27	Forest honey with heather	16.8	835
HP28	Forest Honey with sage	16.2	994
HP29	Mountain honey with white thyme	16.8	818
HP30	Forest honey	16.8	717
HP31	Blueberry honey	17	444
HP32	Acacia honey	16	229
HP33	Cornflower honey	19.4	559
HP34	Honey with turmeric	18	788
HP35	North German early bloom honey	20.4	285
HP36	Fennel in honey	19	522
HP37	Chestnut honey	17.6	1033
HP38	Linden blossom	17.2	660
HP39	Blossom honey with acacia	15.6	136.4
HP40	Pine honey	15.4	1146
HP41	Forest and blossom honey	16.3	1076
HP42	Honey dew honey	16.8	1158
HP43	Organic honey dew honey	16.7	1164

HP44	Organic acacia honey	16.8	261
HP45	Organic linden honey	14.6	571
HP46	Raw forest honey	16	406
HP47	Syrup (90%) + honey (10%)	17	112.6
HP48	Blossom honey	16	426
HP49	Acacia honey	15.8	172.3
HP50	Goldenrod honey	16.3	735
HP51	Linden honey	17	786